

Dissertation

zur Erlangung des Grades

Doktor der Naturwissenschaften im Promotionsfach Chemie

Am Fachbereich Chemie, Pharmazie und Geowissenschaften

der Johannes Gutenberg-Universität in Mainz

Functional Poly(phosphoester)s The Olefin Metathesis Route

vorgelegt von

Filippo Marsico

geboren in Acquaviva, Bari. Italien

Mainz, 2014



Tag der mündlichen Prüfung: 02/07/2014



MAX-PLANCK-GESELLSCHAFT

“Wie stellst du dir das Ende vor?” fragte der Geistliche. “Früher dachte ich, es müsse gut enden”, sagte K., “jetzt zweifle ich daran manchmal selbst. Ich weiß nicht, wie es enden wird. Weißt du es?” “Nein”, sagte der Geistliche, “aber ich fürchte, es wird schlecht enden. Man hält dich für schuldig. Dein Prozeß wird vielleicht über ein niedriges Gericht gar nicht hinauskommen. Man hält wenigstens vorläufig deine Schuld für erwiesen.” “Ich bin aber nicht schuldig”, sagte K., “es ist ein Irrtum. Wie kann denn ein Mensch überhaupt schuldig sein. Wir sind hier doch alle Menschen, einer wie der andere.” “Das ist richtig”, sagte der Geistliche, “aber so pflegen die Schuldigen zu reden.”

Der Prozess. Franz Kafka, 1925.

[“Come t’immagini che andrà a finire?” chiese il sacerdote. “Prima pensavo che sarebbe finita bene,” disse K., “adesso ho io stesso qualche dubbio”. “Come finirà non lo so. Tu lo sai?” “No,” disse il sacerdote, “ma temo che finirà male. Sei ritenuto colpevole. Forse il tuo processo non andrà neppure oltre un tribunale di grado inferiore. Almeno per il momento, la tua colpevolezza si dà per dimostrata.” “Ma io non sono colpevole,” disse K., “è un errore. E poi, in generale, come può un uomo essere colpevole? E qui siamo pure tutti uomini, gli uni quanto gli altri.” “È giusto” disse il sacerdote, “ma è proprio così che parlano i colpevoli.”]

Abstract

This thesis presents the first report on a metathesis approach to synthetic saturated and unsaturated poly(phosphoester)s allowing easy variation of the polymer backbone and side chains through precise placement of functional and/or solubilizing groups.

Combining the advantages of olefin metathesis with the versatility of the phosphorus chemistry, this variable approach allows one to synthesize a new class of unsaturated polyphosphates by tailoring the architecture and the microstructure of the polymers. Linear, hyperbranched, labeled and telechelic poly(phosphoester)s can be obtained and scaled-up with a high degree of functionalization.

One major advantage of this approach is the possible variation of the polymer backbone which is not possible by ring-opening polymerization or classical polycondensations where structurally limited monomers are available.

The phosphorous properties are reflected into novel polymeric architectures with advantages in term of performances for flame retardancy and tissue engineering applications. This thesis work also present unique poly(phosphoester)s that can be used as oxygen scavengers in the field of optoelectronics. The procedures described can be easily scaled up and is very promising even for industrial application as unsaturated polyesters represent a very important market.

Zusammenfassung

Diese Dissertation zeigt zum ersten Mal den Ansatz gesättigte und ungesättigte Poly(Phosphorester) herzustellen, deren Polymergerüst und Seitenketten durch präzises Anbringen von funktionellen und/oder solubilisierenden Gruppen modifiziert werden können.

Durch Kombinieren der Vorteile der Olefinmetathese mit der Vielseitigkeit der Phosphorchemie, eröffnet dieser variable Ansatz den Zugang zu einer neuen Klasse ungesättigter Polyphosphate. Die zu Grunde liegende Idee ist das maßgeschneiderte Anpassen der Architektur und der Mikrostruktur dieser Polymere. Lineare, verzweigte, markierte und telechelle Poly(Phosphorester) können in großem Maßstab mit hohem Funktionalisierungsgrad hergestellt werden.

Einer der größten Vorteile dieses Ansatzes ist es, das Polymerrückgrat modifizieren zu können, was weder bei der Ringöffnungs- noch bei klassischen Polymerisationen möglich ist, bei denen nur eine limitierte Anzahl an Monomeren existieren.

Die Eigenschaften des Phosphors werden in neue Polymerarchitekturen übertragen, was von Nutzen für flammenhemmenden Materialien und Anwendung bei Gewebetherapeutika ist. Diese Doktorarbeit führt auch einzigartige Poly(Phosphorester) ein, welche im Feld der Optoelektronik als Sauerstofffänger eingesetzt werden können. Die beschriebenen Syntheseprozesse können einfach in größerem Maßstab durchgeführt werden und sind vielversprechend für industrielle Anwendungen, da ungesättigte Polyester einen sehr wichtigen Markt repräsentieren.

Content

Abstract	ix
Zusammenfassung	xi
Content	13
Chapter 1 Introduction	17
Outline	18
1.1 Organophosphates.....	19
1.2 Synthetic Poly(phosphoester)s.....	21
1.2.1 Polyphosphoesters via Ring Opening Polymerization and Polycondensation	22
1.3 Metathesis Polymerization	23
1.3.1 Acyclic Diene Metathesis Polymerization	26
Chapter 2 Motivations	31
Chapter 3 Synthesis of Poly(Phosphoester)s	37
Outline	38
3.1 Linear Polyphosphoesters	39
3.1.1 Monomer Synthesis.....	40
3.1.2 ADMET Polymerization	40
3.1.3 Thermal Characterization	47

3.2	A metathesis Route for BODIPY Labeled Polyolefins.....	49
3.2.1	BODIPY Dyes: Synthesis.....	51
3.2.2	Photophysical Properties	52
3.2.3	BODIPY Labeled Polyolefins: Considerations.....	55
3.3	Telechelic Polyphosphoesters ^a	55
3.4	Hyperbranched Polyphosphoesters	57
3.4.1	Monomer Design	58
3.4.2	Kinetics of Polymerization and Structural Considerations	63
Chapter 4	Applications	65
	Outline	66
4.1	Optical Upconversion.....	67
4.1.1	Strategies for Designing TTA-UC in Polymeric Systems.....	69
4.1.2	Hyperbranched Poly(phosphoester)s for Active Oxygen Scavenging.....	73
4.1.3	Towards Solar Upconversion: Broadband Excitation.....	75
4.1.4	Oxygen-Scavenging Activity	76
4.1.5	Upconversion in Organophosphates : Considerations	82
4.2	Flame Retardants	83
4.2.1	Flame Retarding Mechanisms	84
4.2.2	Phosphorous-based Flame Retardants	85
4.3	Olefin Metathesis for the Preparation of Hollow Nanocapsules	88
4.4	Tissue Engineering.....	91
Chapter 5	Thiol-ene Addition, Alternative Routes	93
5.1	An Alternative Route for Synthetic Poly(phosphoester)s	95

5.1.1 Thiol-ene Addition.....	96
Chapter 6 Experimental Section	101
Outline	102
General Procedure (a) for the Synthesis of Phenyl-di-(alkenyl)-phosphate.....	103
General Procedure (b) for the Synthesis of Tri-(alkenyl)-phosphate	104
Representative Procedures for Metathesis Polymerizations	105
Chapter 7 Spectroscopic Selection.....	119
Outline	120
Publications	133
Declaration	138
Bibliography.....	139

Chapter 1

Introduction

Outline

This introductory chapter will highlight the background and the motivation for the necessity of this thesis, to design novel phosphorous-containing polymers for the needs of modern materials science. A general overview about organophosphates and synthetic poly(phosphoester)s will be given since their similarities to nucleic acids like DNA recently make them appealing for several applications. Afterwards the novel synthetic strategy based on olefin metathesis will be introduced, and its major advantages compared to classical routes that up to now have been developed for the preparation of these polymers.

1.1 Organophosphates

Phosphorus plays a central role in living organism; it is sufficient to mention photosynthesis, metabolism, saccharide synthesis, nucleic acid helices, involvement in coenzyme systems, etc. If reduction and oxidation reactions between carbon and oxygen taking place in the organism are regarded in simplified terms as being responsible for gain and expenditure of energy then, disregarding their structural function, the phosphorus-oxygen compounds serve predominantly for the transport and storage of energy.^{1a} Two factors are decisive: firstly the condensed phosphates, anhydrides or esters are thermodynamically stable under such redox conditions, and secondly compounds of this type hydrolyze in most of the biochemical reactions taking place in aqueous solution or at aqueous interfaces.^{1b} Depending upon their structure and the type of enzyme involved, these compounds hydrolyze over many kinetic stages and under very mild conditions. Expressed in more general terms, this means that phosphorus compounds can exert a phosphorylating action on nucleophilic molecules.^{1b} The best known example is the interplay between adenosine triphosphate (ATP) forms (Figure 1).

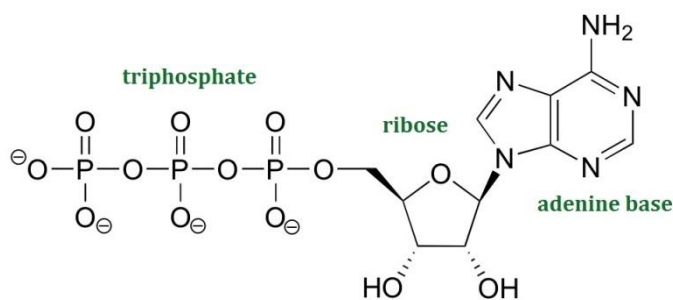


Figure 1. Adenosine triphosphate (ATP).

Organophosphorus compounds are characterized by an unusually large variety of structures and a wide range of uses (Figure 2). The reason is that phosphorus is able to form stable compounds with a coordination number of 1 to 6, and an oxidation state of -III to + V. On the basis of its position in the periodic system, phosphorus in its fundamental state possesses the external configuration $3s^2 3p^3$. In accordance with the structure $3s^2 3p^3$ of the neutral phosphorus atom, primarily

compounds with the co-ordination number 3 are to the expected. In contrast to the elements of the second period, $3d$ orbitals may participate during the formation of phosphorus compounds. However, the transfer from $3s^2 3p^3$ to $3s^2 3p^s 3d$ requires a relatively high promotion energy of about 200 kcal/mol.

Based on value, organophosphorus products are all value-added and specialized products. However, for reasons of industrial secrecy, there is very little information available from the manufacturers concerning production quantities and values, so that some of the figures given here are only estimates. The organophosphorus product with by far the largest sales value is still phosphonomethyl glycine (Glyphosate, Monsanto). From 2004 to 2008, the average growth rate of global glyphosate reached 27%, much higher than the global economic growth rate, and the total consumption volume has reached about 600,000 tonnes. Halogen-free phosphonic and phosphinic acid derivatives are of increasing importance in the production of nonflammable textiles.^{1c}

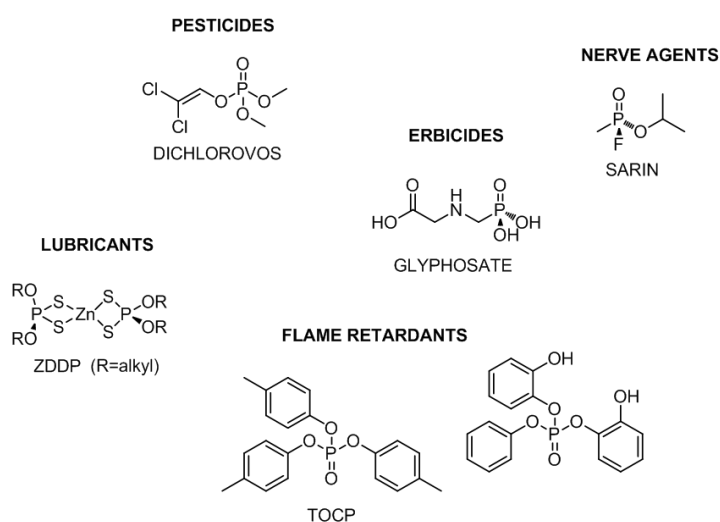


Figure 2. Widely used organophosphates.

The market for plastics additives (flame retardants, plasticizers and antioxidants) expressed as PCl_3 in the USA for 1990 is estimated at 30 000 tonnes of phosphorus trichloride.^{1c} The annual consumption of flame retardants is currently (2009) over 1.5 million tonnes per year, which

is the equivalent of a sales volume of approx. 1.9 billion Euro (2.4 billion USD). Apart from the esters of thiophosphoric acid used in plant protection, the most important compounds of this class are the zinc dithiophosphates used in lubricants, for which over 50% of phosphorus pentasulfide production is used. A wide range of possible compound, industrially relevant are available, and the chemistry of organophosphorous compounds is rapidly developing because of their importance in biochemical, medicinal, and synthetic applications.^{1c}

1.2 Synthetic Poly(phosphoester)s

Biodegradable polymers have received tremendous interest in recent decades.² Used for the development of novel materials in the medical field of modern biotechnology or tissue engineering, most of them are based on conventional polyesters such as polylactide or similar.³ However, a major drawback is the restriction to a few monomer systems that results often in the need of polymer modifications that are demanding multistep approaches. In contrast, poly(phosphoester)s (PPEs) which were earlier used as flame-retardant materials, are potentially degradable and biocompatible polymers with repeating phosphoester bonds along the backbone comparable to biomacromolecules such as nucleic and teichoic acids.^{4,5} Several structural modifications are known (Figure 3) such as poly(phosphate)s, poly(phosphonate)s, poly(phosphite)s and poly(phosphoramidate)s.

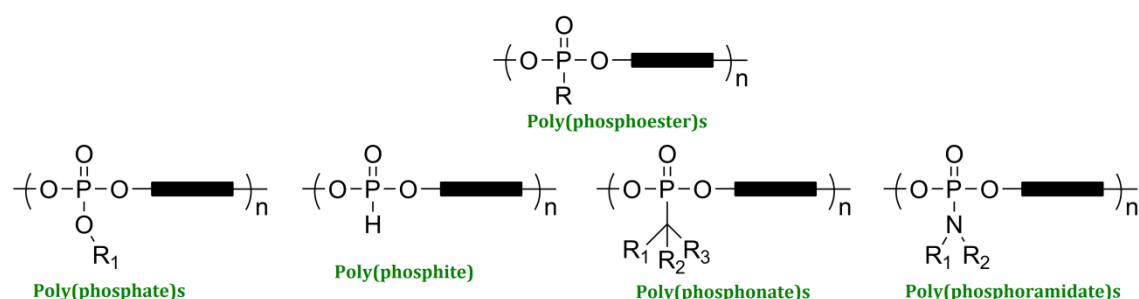
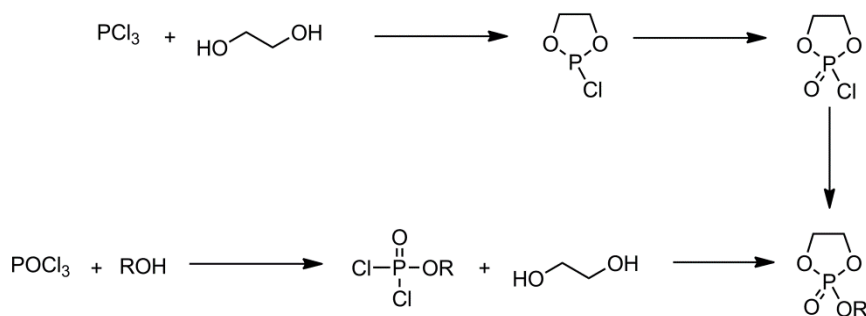


Figure 3. Schematic representation of several types of poly(phosphoester)s.

The chemical versatility of the monomeric phosphate allows the design of functional materials with tunable and complex architectures and many different properties for drug delivery,⁶ gene delivery,⁷ pH/thermoresponsive materials,⁸ and tissue engineering,⁹ of which are particularly appealing for biomedical applications. Regenerative medicine, for example, requires scaffolds with tunable properties for tissue engineering applications, and unsaturated polyphosphoesters (UPPEs) with the phosphates being capable of binding calcium phosphates are advantageous in terms of cytocompatibility and good tissue compatibility.^{10,11} The treatment of bone defects could benefit from biocompatible and degradable materials, which also assist in bone regeneration, and could be a valid substitute to the widely used poly(methylmethacrylate).¹² Aliphatic polyesters such as poly(ϵ -caprolactone) (PCL), poly-(lactic acid) (PLA), poly(glycolic acid) (PGA), and similar are generally considered useful for biomedical applications because of their favorable biocompatibility and biodegradability.¹³ Their hydrophobicity and slow degradation rate, however, may not be ideal for some applications, but could be tuned by copolymerization combining the advantages of aliphatic polyesters and PPEs.¹⁴

1.2.1 Polyphosphoesters via Ring Opening Polymerization and Polycondensation

In the early 1970s, seminal works carried out by Penczek and coworkers established the basis for the synthesis and the potential biological application for a series of PPEs.^{15,16} These polymers can be synthesized by polycondensation, transesterification, or ring opening polymerization (ROP) of strained cyclic phosphates. Polycondensation (Scheme 1) is probably the most used method for the preparation of PPEs due to readily available monomers.¹⁷ However, in an early work, Vogt and Balasubramanian have already reported that the conventional polycondensation route is plagued by side reactions that prevent the formation of polymers with molecular weights higher than ca. 1,000 g mol⁻¹.^{18,19} Penczek and coworkers have reported that the transesterification route yields polymers with molecular weights higher than 10,000 g mol⁻¹.^{20,21} The second approach to PPEs is ROP that has been studied extensively for cyclic phosphate monomers in bulk with enzymatic catalysis,²² or via cationic,²³ anionic or coordinative polymerization.²⁴



Scheme 1. Classical strategies for the synthesis of cyclic phosphoesters.

Typical problems in cationic polymerization is that it produces exclusively colored products with low molecular weights, while triisobutyl aluminum is very efficient for catalyzing ROP to obtain homo or random copolymers. Stannous octoate is a widely used catalyst for the polymerization of cyclic esters, also for the polymerization of five-membered phosphates.²⁵ In a typical synthesis, 2-chloro-2-oxo-1,3,2-dioxaphospholane (COP) is reacted with the alcohol of choice to produce the desired monomer. A second strategy introduces the side chain first by the reaction of the respective monofunctional alcohol with phosphoryl chloride and subsequent ringclosure with ethylene glycol for example. Both synthetic strategies have been applied for the synthesis of several monomers with R being an ethyl, isopropyl, methacryl or diethylene glycol, etc. The latter pathway omits the oxidation of the intermediate phosphine but the yields are usually lower compared to the alternative route starting from phosphorus trichloride. Typical problems here are low molecular weight materials, the need of high-purity monomers and the absence of water. Also, varying, but low monomer conversions can be problematic (usually ca. 70%) and the materials show polydispersities around 1.50 or lower in some cases.

1.3 Metathesis Polymerization

Olefin metathesis is one of the very few fundamentally novel organic reactions discovered in the last 40 years. Among others, it opens up new industrial routes to important petrochemicals, polymers, oleochemicals and specialty chemicals. At Phillips Petroleum Co. this reaction was dis-

covered serendipitously by Banks and Bailey 40 years ago, when they were seeking an effective heterogeneous catalyst to replace the HF acid catalyst for converting olefins into high-octane gasoline via olefin-isoparaffin alkylation.^{26a} When using a supported molybdenum catalyst, they found that, e.g. instead of alkylating the paraffin, the olefin molecules were split, and discovered that propene can be catalytically converted into ethene and butene. Olefin metathesis was then first commercialized in petroleum reformation for the synthesis of higher olefins from the products (α -olefins) from the Shell higher olefin process (SHOP) under high pressure and high temperatures.^{26b}

Since then, olefin metathesis enjoyed increasing interest, in particular in recent years it has quickly become one of the most widely used methods for mild carbon-carbon bond formation in organic synthesis.^{27,28} With the development of highly active, functional group-tolerant catalysts like Grubbs' second generation catalyst (Figure 4), metathesis has successfully applied across many areas of research.²⁹

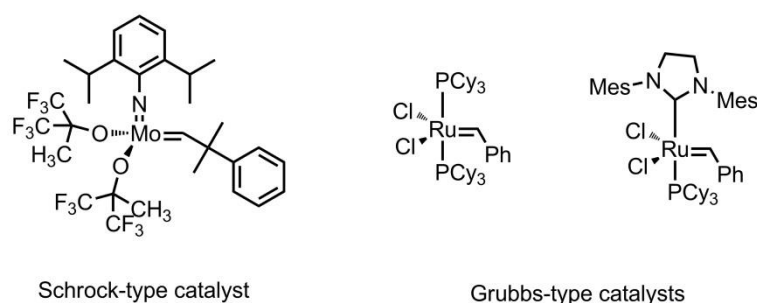
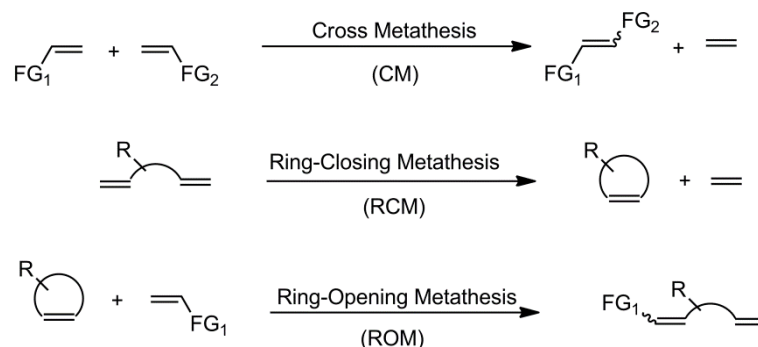


Figure 4. Common metathesis catalysts.

Macromolecular chemistry has embraced olefin metathesis, as it allows the preparation of functionalized hydrocarbon polymers. Ring-opening metathesis polymerization (ROMP) and acyclic diene metathesis (ADMET) are attractive processes for making linear polymers when based on cheap monomers or possessing special properties compensating for a high price. Several industrial processes involving homogeneously catalyzed ROMP have been developed and brought into practice (Scheme 2).^{30,31,32,33}



Scheme 2. Conventional olefin metathesis strategies.

With the right choice of catalyst and monomer, well-defined polymers can be obtained with good molecular weight control and a narrow polydispersity index (PDI). These functional group tolerant catalysts (Scheme 3) generally operate under mild conditions, such as room temperature, bench-top chemistry and short reaction times.³⁴

Titanium (Ti)	Tungsten (W)	Molybdenum (Mo)	Ruthenium (Ru)
Acids	Acids	Acids	<i>Olefins</i>
Alcohols, Water	Alcohols, Water	Alcohols, Water	Acids
Aldehydes	Aldehydes	Aldehydes	Alcohols, Water
Ketons	Ketons	<i>Olefins</i>	Aldehydes
Esters, Amides	<i>Olefins</i>	Ketons	Ketons
<i>Olefins</i>	Esters, Amides	Esters, Amides	Esters, Amides

Functional group tolerance

Increasing order of reactivity

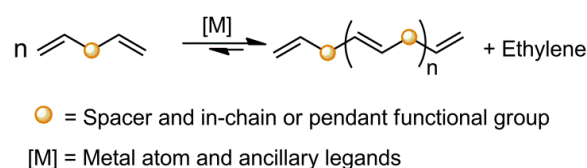
Scheme 3. Functional group tolerance of olefin metathesis catalysts.

While total synthesis creates synthetic issues for the design of exact chemical structures through RCM or ADMET, polymer chemists who only desire the incorporation of functionality into polymer systems through ROMP or ADMET are able to take advantage of the improved stability and reactivity of the [Ru] complex. In the chemical process industry, olefin metathesis has now become a

process with large-scale applications using heterogeneous as well as homogeneous catalysts systems. More commercial applications are to be expected, in particular considering the recent development of highly active ruthenium metathesis catalysts that are more tolerant to functional groups and resistant towards moisture and oxygen. Moreover, the metathesis reaction has also favorable perspectives for application in the oleochemical industry, and in this respect has good prospects as a contribution to a sustainable chemical industry.

1.3.1 Acyclic Diene Metathesis Polymerization

ADMET polymerization is performed on acyclic dienes to produce strictly linear polymers with unsaturated polyethylene-like backbones (Scheme 4).



Scheme 4. Acyclic diene metathesis polymerization.

As for all metathesis reactions, the development of ADMET polymerisations have been closely linked to the discovery and optimisation of metathesis catalysts of improved activity, selectivity and stability. The first metathesis reactions applied to α,ω -dienes were reported in the early 1970s using combinations of nitrosyl molybdenum and tungsten compounds with organoaluminum halides as catalytic systems.^{35a} However, only low yields of oligomers could be obtained in the reactions of 1,5-hexadiene and 1,7-octadiene. Subsequently, Schrock and coworkers developed a series of highly reactive neutral molybdenum and tungsten metathesis catalysts.^{35b} The use of these Lewis acid free catalysts by Wagener's group led to the first quantitative metathesis polymerisation¹⁵ and copolymerisation of 1,5-hexadiene and 1,9-decadiene.^{35c} The further development of the ADMET polymerizations then was influenced by the availability of metathesis catalysts being

compatible with different functional groups. Up to now, this step-growth polymerization is a thermally neutral process driven by the release of a small molecule condensate, ethylene. ADMET polymer products have been isolated up to 80 kg mol⁻¹ using [Mo] and up to 100 kg mol⁻¹ using [Ru].³⁶

1.3.1.1 The ADMET Polymerization Cycle

The acyclic diene metathesis polymerization cycle is illustrated in (Figure 5).³⁶

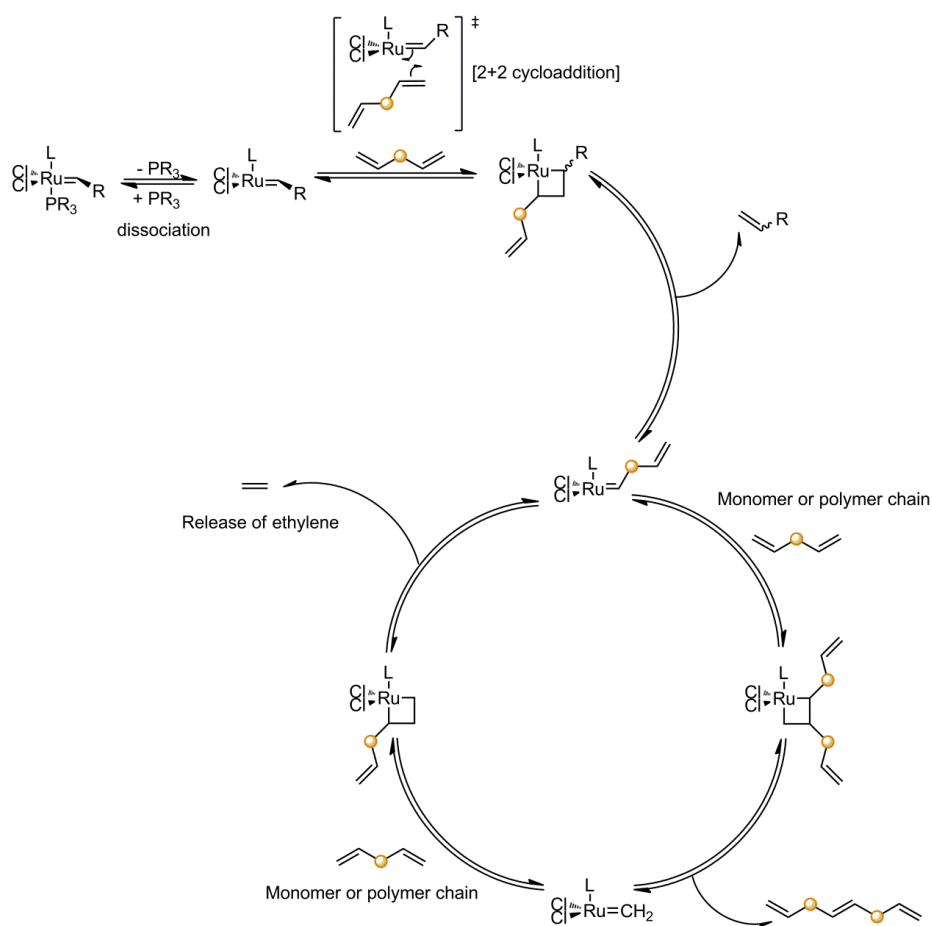


Figure 5. ADMET polymerization mechanism.

The principal reaction intermediate, a metallacyclobutane, is identical to that found in all other metathesis chemistry, including ring opening metathesis polymerization and the formation of small molecules through metathesis. The ADMET polymerization cycle itself, however, is distinct and quite different from any other reaction scheme found in metathesis chemistry. Acyclic diene metathesis is an equilibrium process, whereas ROMP typically propagates in an irreversible manner. First, the alkylidene forms a π complex with one of the olefins of the monomer, and then the complex undergoes an insertion to form the initial metallacyclobutane. This metallacycle can undergo productive metathesis to eliminate a catalyst fragment and form a new alkylidene at the terminus of a monomer molecule.

The polymerization cycle then precedes by complexing this metallized monomer with another monomer unit, forming a new metallacycle. Formation of this metallacycle is essential to propagation, and understanding the factors that lead to its formation is important in the elucidation of what type of monomers can be used in ADMET polymerization. This new metallacyclobutane collapses to form an ADMET "dimer" and a methylene alkylidene, the latter of which is the true catalyst for this system. The methylene alkylidene continues the cycle by reacting with another monomer (or polymer chain end) to form a metallacycle, which is the precursor to the formation of ethylene.

Thus the cycle is completely the consequence being the condensation of two monomer units. The cycle must operate many times in order to produce a high molecular weight polymer by ADMET chemistry. This mechanism has proven to be acceptable in explaining all experimental observations made for both pure hydrocarbon monomers, as well as those that possess functional groups.

1.3.1.2 Functional Groups in ADMET Chemistry

As almost quantitative conversion monomer is standard in these polymerizations, as few side reactions occur other than a small amount of cyclic formation common in all polycondensations.^{35,36}

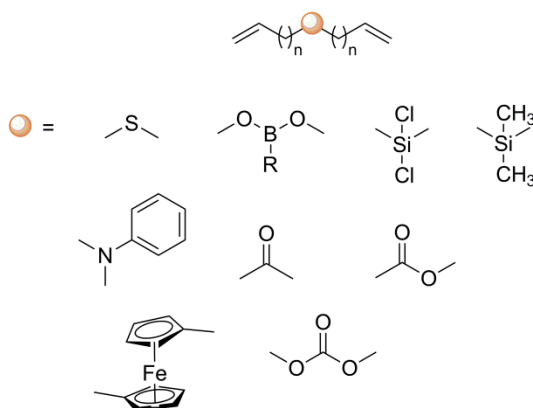


Figure 6. Functional groups that have been included in ADMET polymerization.

ADMET has proven to be a valuable tool for the production of novel polymer structures for material applications as well as model copolymer systems to help elucidate fundamental structure and property relationship. Due to the mild nature of the polymerization and the ease of monomer synthesis, ADMET polymers have been incorporated into various materials and functionalized hydrocarbon resins (Figure 6).

Wagner's group has explored the use of this polymerization technique to elegantly synthesize precision polyethylene containing functional groups such as halogens,³⁷ polyolefins targeted for biological applications,³⁸ or silicon containing materials.³⁹ More recently Meier and coworkers has broadened the applications of this technique by preparing functional hyperbranched materials through the metathesis of acyclic triene monomers.^{40, 41} This approach has led to a wide range of unsaturated and saturated polymers bearing different functionalities with the possibility to modify the polyolefin architectures by placing precise functional groups phosphorous containing throughout the backbone.^{42, 43, 44} ADMET as polymerization technique, generates a continuum of

high-molecular-weight functional polymers, which may be hydrogenated to yield analogous polyethylene (PE) copolymers, exactly linear with precise functional group placement.

Polyolefins is the collective description for plastics types that include polyethylene - low density polyethylene (LDPE), linear low density polyethylene (LLDPE) and high density polyethylene (HDPE) - and polypropylene (PP). Together they account for more than 47% (12 million tons) of western europe's total consumption of 25 million tons of plastics each year. The global market for Polyolefin resins is going reach \$187.5 Billion in 2016 (Source : BCC Research and Reuters). Polyolefins are the largest group of thermoplastics, often referred to as commodity thermoplastics, they are polymers of simple olefins such as ethylene, propylene, butenes, isoprenes, and pentenes, and copolymers and modifications thereof. The term "polyolefin" means "oil-like" and refers to the oily or waxy feel that these materials have. Polyolefins consist only of carbon and hydrogen atoms and they are non-aromatic. Polyolefins are usually processed by extrusion, injection molding, blow molding, and rotational molding methods. An inherent characteristic common to all polyolefins is a nonpolar, nonporous, low-energy surface that is not receptive to inks, and lacquers without special oxidative pretreatment. The two most important and common polyolefins are polyethylene and polypropylene and they are very popular due to their low cost and wide range of applications.

Chapter 2

Motivations



Olefin metathesis provides an efficient strategy for designing tailorable architectures after rationally drawing suitable monomers. ADMET should be a perfect approach for the synthesis of functional polyphosphoesters, in an efficient way from versatile starting materials, which is in the case of PPEs, POCl_3 (Figure 7a).

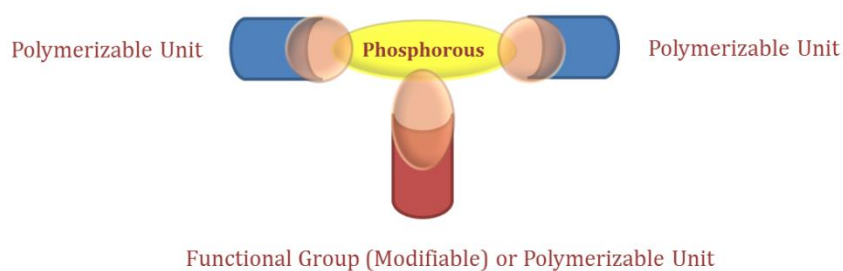


Figure 7a. Acyclic organophosphate diene: structural design from POCl_3

This thesis presents the first ADMET approach to functional synthetic polyphosphoesters allowing easy variation of the polymer backbone (Figure 7b) and side chains by combining the advantages of metathesis with the versatility of phosphorus chemistry.

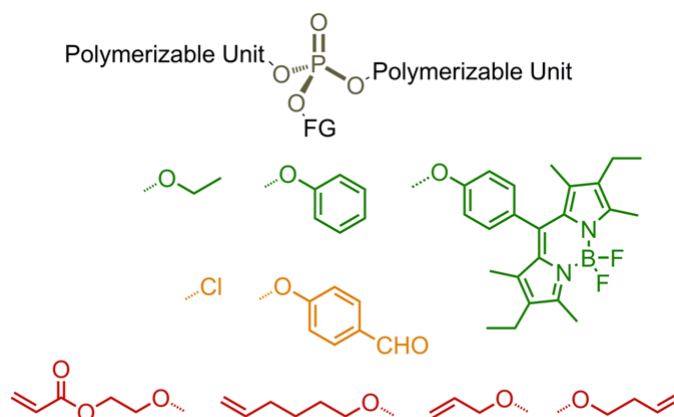


Figure 7b. Functional groups introduced over a polyphosphoester backbone.

We report a variable approach to functional unsaturated poly(phosphoester)s (UPPEs) which cannot be obtained via other synthetic method (Figure 8). The ADMET approach opens a great toolbox of a tremendous variety of substrates which are more stable and easily available. The molecular weights vary for the different monomers and catalysts applied but in all cases tunable molecular weight polymers were obtained and thus empirically the molecular adjusted.

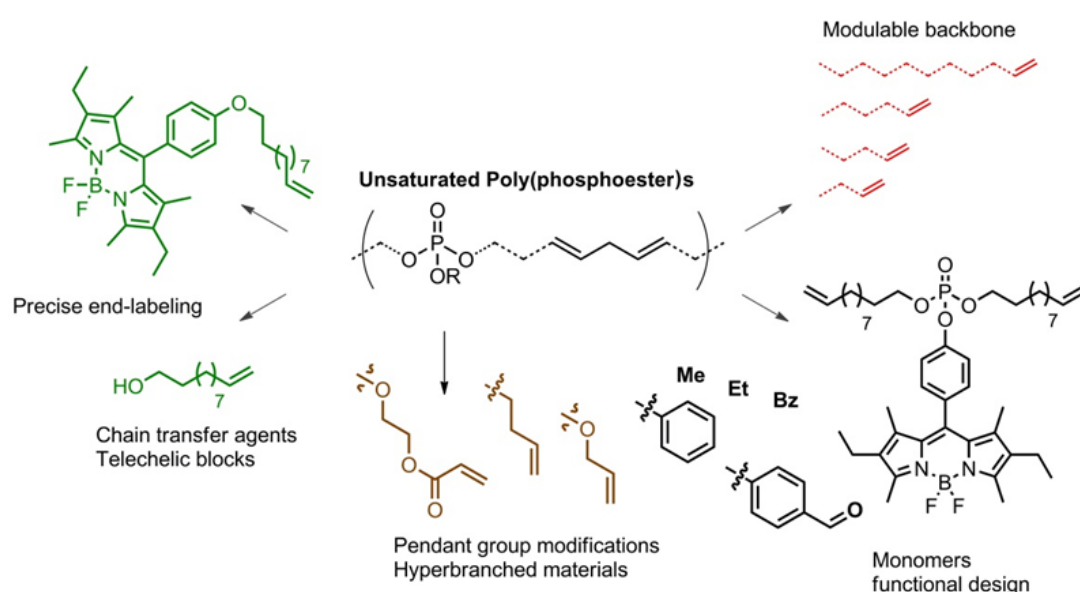


Figure 8. Thesis work, synthetic strategy developed.

Further, the molecular weights of the resulting PPEs are much higher compared to many literature protocols, confirming the advantages by using ADMET as an ideal synthetic strategy for UPPEs. Another major advantage of this approach is the possible variation of the PPE backbone, which is not possible by ring-opening polymerization where usually ethylene-bridged cyclic phosphates are applied. Olefin metathesis is a versatile polymerization technique which tolerates several functional groups. Olefins (electron rich) and acrylates (electron poor) functionalities ensure a control over molecular weights and polydispersities, but also over the molecular backbone, and consequently on the resulting thermal behaviour. We achieve a control over the polymer properties by precisely introducing the desired functionality (monomer).

-
- ✦ The material results then as a (i) combination of the introduced functionality, (ii) final architecture of the system, and (iii) phosphorous properties (Figure 9).

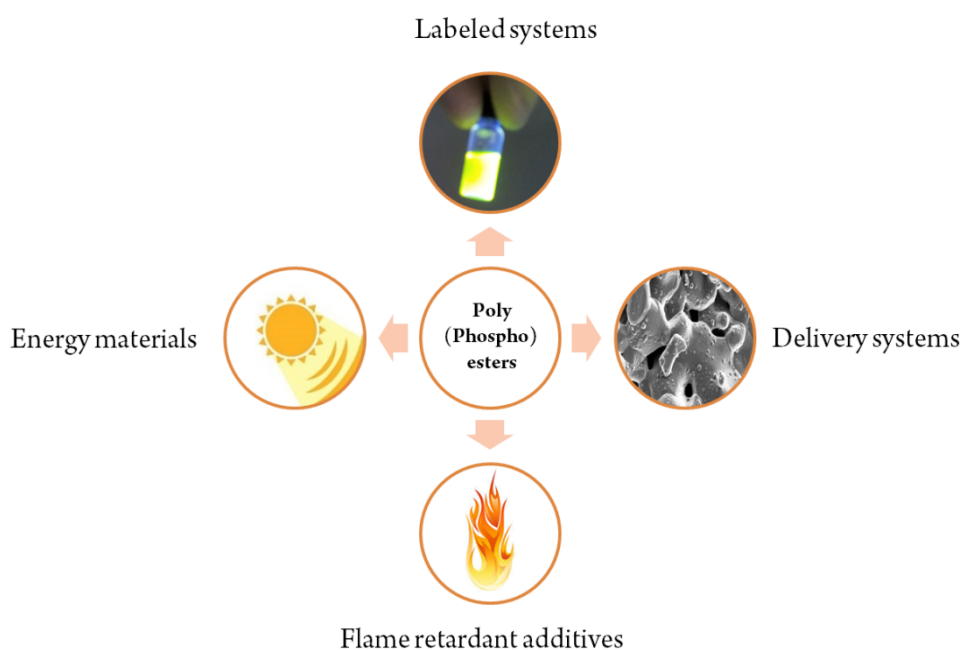


Figure 9. UPPEs, versatile materials for different applications.

This approach has led to a wide range of unsaturated and saturated polymers bearing different functionalities with the possibility to modify the polyolefin architectures by placing precise functional groups phosphorous containing throughout the backbone. The UPPEs presented in this thesis found novel biomedical applications as potential tissue engineering scaffold materials but also in materials science concerning their flame-retardant properties and activity against oxygen. We reasonably believe that this procedure can be easily scaled up and is very promising even for industrial application, in the business of high performance polymer materials.

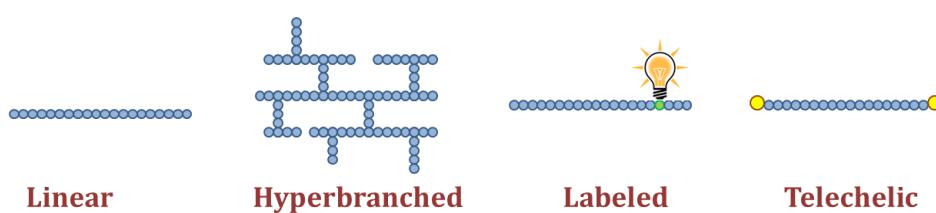


Chapter 3

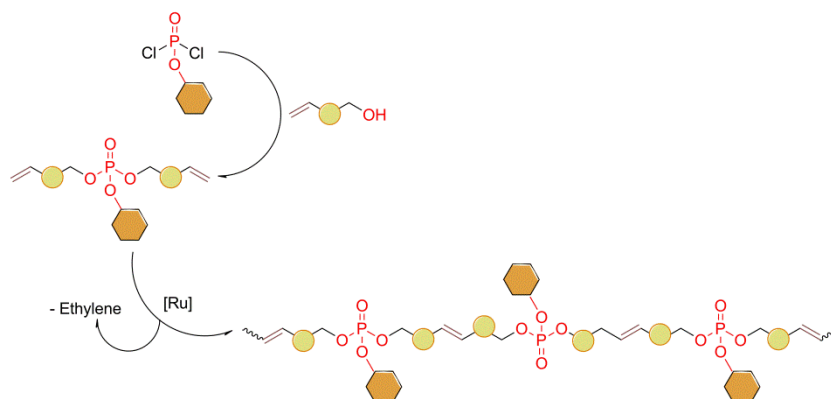
Synthesis of Poly(Phosphoester)s

Outline

This chapter will describe synthesis and characterization of the poly(phosphoester)s synthesized during this thesis. Linear, hyperbranched, labeled and telechelic systems can be prepared via olefin metathesis with a high degree of functionalization and control. Up to now the classical approach like ring opening polymerization or polycondensation limited the variability of this system and only the new, herein presented approach made the synthesis of these PPEs possible for a wide range of applications.

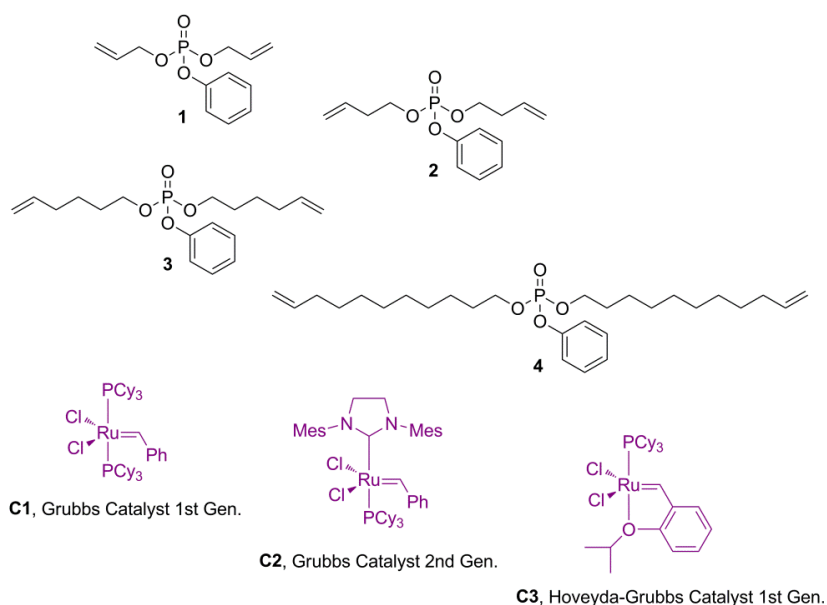


3.1 Linear Polyphosphoesters



Scheme 5a. Unsaturated Poly(Phosphoester)s : The olefin metathesis approach.

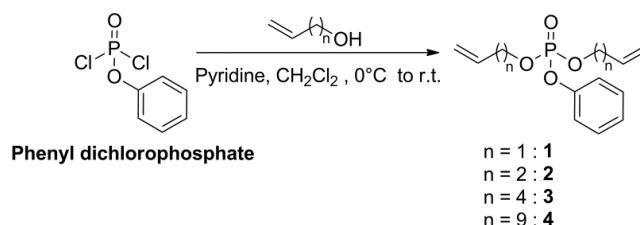
The acyclic diene metathesis polymerization is a quantitative reaction tolerating many functional groups and yields only the desired linear polymer and ethylene as a byproduct. First of all we have demonstrated how ADMET provides tools for accessing linear unsaturated and saturated polyphosphoester structures in an efficient way (Scheme 5a, 5b).⁴⁵



Scheme 5b. Ruthenium-based catalysts used and acyclic dyene organophosphate as model systems synthesized.

3.1.1 Monomer Synthesis

The monomers investigated were synthesized using commercially available phenyl dichlorophosphate which was esterified with the respective alcohol in the presence of a base, pyridine (or triethylamine), as described in the following representative procedure (Scheme 6) for the compounds **1-4**. The pure compounds are colorless liquids at room temperature and can be stored at room temperature over a period of (at least) several months. In contrast, the five and six membered cyclic phosphates which are used in ROP are sensitive monomers, and special precautions have to be followed in handling these monomers, during the preparation, the purification (generally by distillation) and especially while conducting the ROP. Their sensitivity easily quenches the polymerization or unwanted initiation by water can occur. For the liability of these cyclic compounds, most of the ROPs are carried out on rather simple five membered, ethylene glycol-bridged cyclic phosphates and subsequent post-polymerization modification reactions are carried out. The ADMET approach opens a great toolbox of a tremendous variety of substrates which are more stable and easily available from POCl_3 .



Scheme 6: General protocol for the synthesis of acyclic diene phosphate monomers for ADMET.

3.1.2 ADMET Polymerization

Motivated by the high functional group tolerance of the Grubbs-type catalysts, we investigated the influence of different catalysts on the molecular weight and the polydispersity for the ADMET polymerizations of the monomers **1-4** (Grubbs first generation (**C1**), Grubbs second generation (**C2**), and Grubbs-Hoveyda first generation (**C3**)) in bulk with stirring at different temperatures (see below). Since the monomers described herein are liquids, a bulk polymerization is feasi-

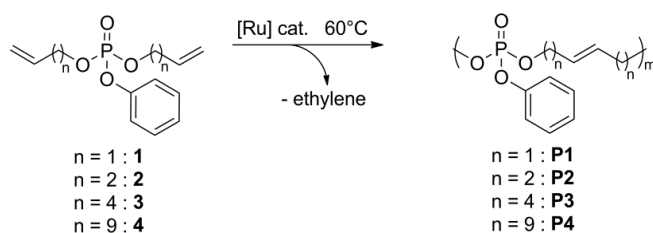
ble and maximizing of the molar concentration of the olefin and appropriate shifting of the reaction equilibrium can be obtained when solvent is omitted.

Table 1. Conditions for the ADMET polycondensation (general representative procedure) of **1-4** and molecular weight data of the resulting polymers.

run	monomer	catalyst	catalyst [mol%]	temperature [°C]	$M_w^{(a)}$ [g mol ⁻¹]	$M_n^{(a)}$ [g mol ⁻¹]	$M_w^{(a)}/M_n^{(a)}$
1	1	C1	1.3	60	-	-	-
2	1	C2	1.3	60	-	-	-
3	1	C3	1.3	60	-	-	-
4	1	C1	1.3	80	-	-	-
5	2	C1	1.3	60	14,500	7,700	1.88
6	2	C3	1.3	60	14,000	6,000	2.33
7	3	C1	1.3	60	19,300	10,000	1.93
8	3	C3	1.3	60	17,000	8,700	1.95
9	4	C1	1.3	60	57,300	38,000	1.50
10 ^(b)	4	C2	0.2	40	7,200	5,050	1.42
11	4	C2	1.3	60	43,200	26,800	1.83
12	4	C3	1.3	60	34,200	23,600	1.45
13	4	C1	0.6	60	54,700	32,400	1.68
14	4	C2	0.6	60	50,000	22,700	2.20
15	4	C1	0.3	60	33,000	20,200	1.63
16	4	C2	0.3	60	50,000	22,700	2.20
17 ^(c)	3,4	C1	0.6	60	13,000	6,100	2.13

(a) In g mol⁻¹, determined by gel permeation chromatography (GPC) in THF vs. polystyrene standards. (b) The monomer (100 mg) and Grubbs' first generation catalyst (0.2 mol%) were dissolved in CH₂Cl₂ (2 mL). (c) Random copolymer between **3** and **4** in ratio 1:1.

Table 1 lists the results of the polymerizations. The first reactions were carried out at 40 °C, however, it was observed that the temperature was not high enough to activate the reaction efficiently, and sometimes unreacted monomer was recovered (Scheme 7).



Scheme 7: ADMET polymerization of a phosphate monomer **1-4**.

Therefore, the polymerization temperature was raised to 60 °C, where upon a sudden color change from purple to red (using **C1** with monomer **4**), evolution of ethylene, and a quick increase in the viscosity of the reaction mixture was observed.

Polydispersities of the polymers are in agreement with the theory concerning the Carothers equation that predicts the most probable distribution of 2 for a linear polycondensation, as conversion reaches 100%.⁴⁶ Because of the increase in viscosity after one/two hours the reaction temperature was gradually raised to 80 °C to allow efficient mixing of the polymerization mixture. After ca. 10 h at 80 °C the evolution of ethylene ceased. The polymers were dissolved in dichloromethane and precipitated into methanol or hexane. For monomer **1**, no polymeric materials were obtained and the monomer was recovered in all the cases (runs 1-4). This is attributed to the so called "negative neighboring group effect" (Figure 10). Because of the proximity of the coordinating ester, metathesis under ruthenium catalysis is slow or even prevented due to complexation of the heteroatom lone pair with the metal center.⁴⁷

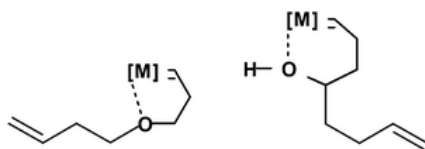


Figure 10. Negative neighboring group effect.

This lack of reactivity could alternatively be justified by the formation of particular resting state of the carbene formed with the allyl substrate possible via coordination to the phosphate.⁴⁸ This was also visible with the naked eye for polymerization attempts of **1**, as the reaction mixture turned brown immediately. As expected, when the distance of the coordinating oxygen atom to the reactive double bond was increased just by one methylene unit (monomer **2**), polycondensation results improved. After the catalyst, the mixture immediately turned red, with a gradual increase of the viscosity to give polymers with M_n 's of 8,000 g mol⁻¹ (runs 5,6). The polycondensation of **3** proceeded in a fashion similar to that of **2**. The polymeric materials isolated were in the range of 8,000-10,000 g mol⁻¹ (M_n) and were readily soluble in THF.

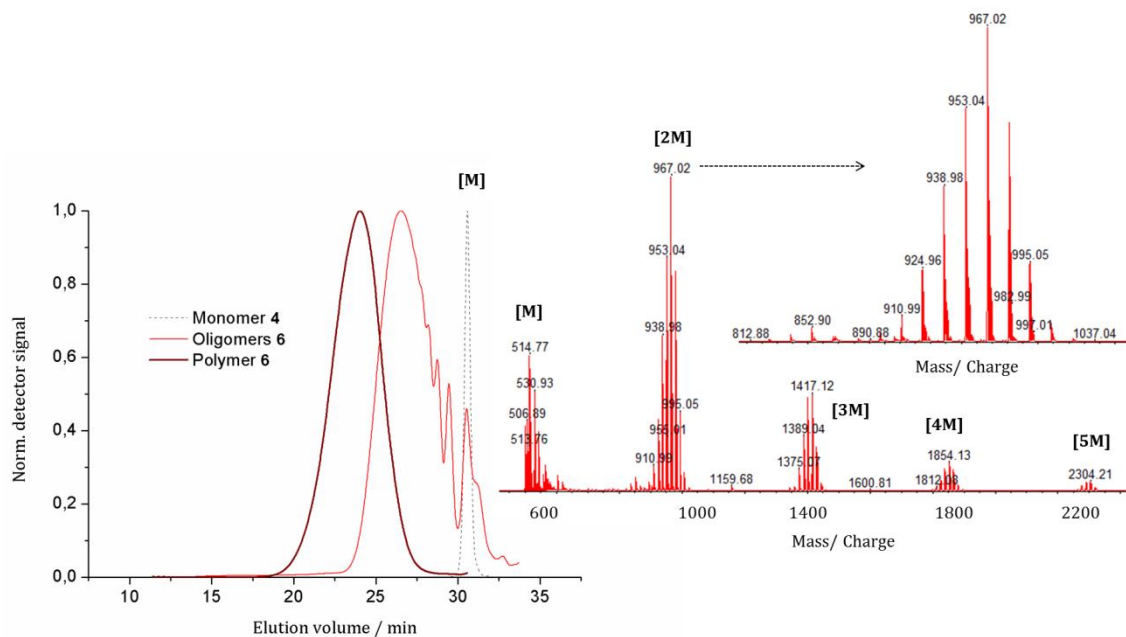


Figure 11: GPC-elugram of polymer P4 (runs 10 (solution) and 13 (bulk)) vs. polystyrene standards in THF (bottom). The dotted signal belongs to the monomer 4. The presence of oligomers can be clearly detected for low molecular weight P4 from run 10 and quantified by MALDI-MS (top).

Figure 11 shows a representative SEC elugram of a polymer from monomer **4** (run 13) synthesized in bulk, in comparison to the diluted synthesis performed in solution (run 10). The monomer **4** was injected also to the GPC and it can be observed, that the oligomers from solution polymerization still contain a monomer fraction (eluting at 30.4 mL). Interestingly, in the oligomer, there is a shoulder to higher elution times (ca. 31-32 mL), indicating the presence of cyclic monomer which should elute later than the linear counterpart. The main peaks in the MALDI section of the figure correspond to the oligomers, ranging from dimers to pentamers (for example: the peak at 995 g mol⁻¹ corresponds to the molecular ion of [2M+K]⁺) observed in the elugram of the oligomer (run 10), while the neighboring peaks exhibit an interval of 14 g mol⁻¹ (methylene units) which is most likely attributed to ruthenium-hydride formation, resulting in double bond isomerizations, during ADMET in the particular conditions (in solution) using catalyst **C2**.^{49,50} This isomerization was not observed in the MALDI spectrum of a relatively low molecular weight sample of polymer **P2** ($M_n = 3,000$ g mol⁻¹, Figure 12). This is reasonable as isomerization would produce a

phosphoric acid allyl ester that cannot undergo further metathesis (see above) resulting in a precise polymer.

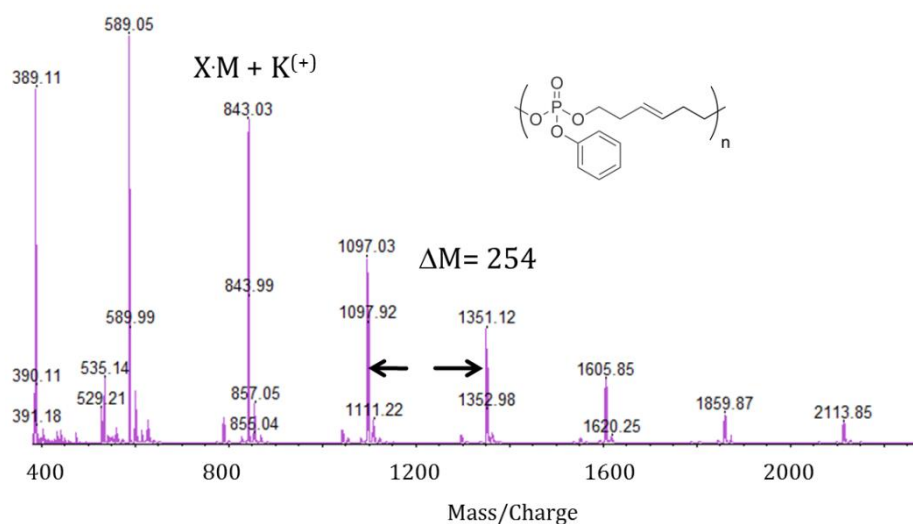


Figure 12: MALDI spectrum of a relatively low molecular weight polymer **P2** obtained by quenching the reaction using (dithranol as a matrix and potassium trifluoroacetic acid (KTFA) as cationization agent were used).

This systematic process allows the study of ideal models of functionalized PPEs with precisely placed substituents and simply by choosing the proper catalyst and monomer, in the absence of solvent and under reduced pressure, leads to quantitative yield of the desired polymer. In this regard, a monomer bearing longer side chains was synthesized (**4**). The reactions of **4** proceed in the same manner as for the other monomers, in this case observing a quick viscosity increase. After a screening on different parameters as reported in Table 1, the optimum conditions for the polymerization of **4** was found to be at 60 °C, 0.3 mol% of Grubbs' first generation catalyst, and for 10-12 h polymerization time ($M_w = 57,300$ $M_n = 38,000$ PDI 1.5). **4** was also investigated in a one-pot copolymerization with **3** in a ratio 1:1 following the standard procedure, leading to a sticky gum ($M_w = 13,000$) soluble in CH_2Cl_2 or THF (run 17, Table 1). UPPEs with different molecular weights have been prepared following the ADMET approach. The resulting polymers are rich in trans olefins due to the ADMET mechanism, since the stereochemistry is controlled thermodynamically due to the equilibrium nature of the polymerization.⁵¹ Because the results for ADMET are highly de-

pendent on the catalytic system, only ruthenium-based catalysts were selected, free of Lewis acids, that favor metathesis chemistry over vinyl addition,⁵² and are only reactive towards olefins.⁵³ Figure 13 shows the ¹H NMR spectra of monomer **4** (bottom) and the respective polymer (**P4**) (middle) proving the complete disappearance of the terminal double bonds (5.8 ppm and 4.9 ppm) and the formation of internal double bonds (5.4 ppm). A zoom into the region of the terminal double bonds also allows the determination of the molecular weight of the polymers (see below). In a following step, a saturated PPE (**P5**) has been synthesized from **P4** via catalytic hydrogenation. In an ideal case the phosphates are separated by 20 carbon centers. This broadens the range of accessible materials by this synthetic strategy from UPPEs in order to prepare saturated PPEs. Metathesis chemistry, in fact, is giving promising results in the preparation of degradable materials from renewable resources.⁵⁴

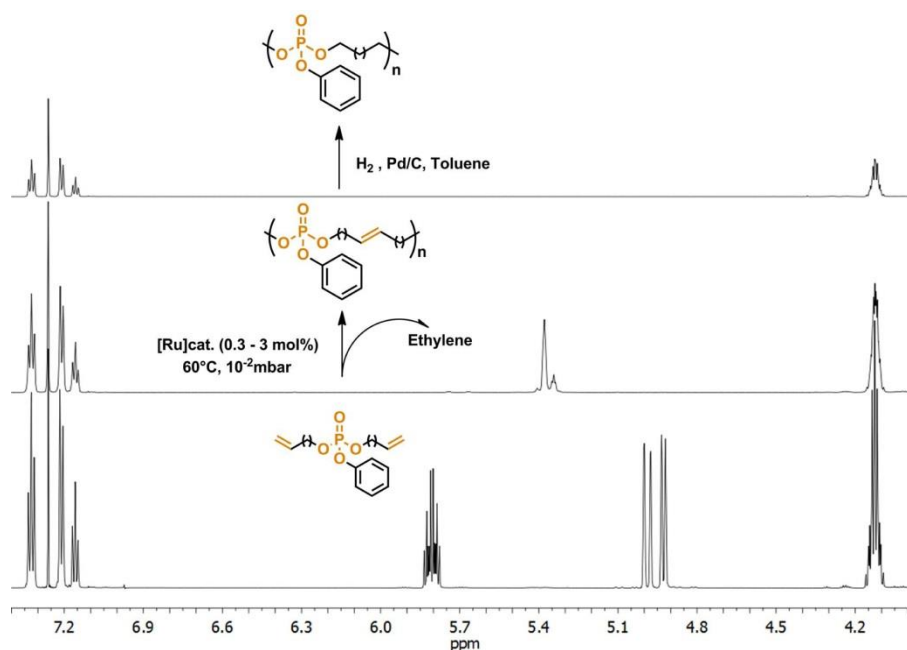


Figure 13: ¹H NMR investigation (700 MHz in CDCl₃ at 298.3 K) showing the aromatic and olefinic region of the spectra of monomer **4**, polymer **P4** and hydrogenated polymer **P5**.

P5 can be regarded as a degradable polyethylene with predetermined breaking points inside the backbone. ¹H NMR and ¹³C NMR spectroscopy proves complete reduction of all double bonds. In addition, GPC results prove that the phosphate linkages are stable under the hydrogenation condi-

tions (Pd/C, H₂, 8 bar) and fully saturated PPEs can be generated with different thermal properties (see below). The molecular weight of the saturated polymer **P5** (M_w 54,000 g mol⁻¹, PDI 1.90) estimated by GPC was in agreement with the starting material (M_w 53,000 g mol⁻¹, PDI 1.90). Like the other unsaturated polymers ³¹P NMR measurements revealed for **P5** only a single peak around -7 ppm, excluding the presence of di-substituted or mono-substituted phosphate in the material isolated. For all polymers, molecular weights were obtained from GPC in THF against polystyrene standards. In addition, ADMET produces only linear polymers that possess terminal double bonds as the respective end groups which are accessible for further reactions. With high resolution ¹H NMR spectroscopy these can be used to calculate an absolute molecular weight. For a low molecular weight PPE this spectrum is shown in Figure 14. By integration of the terminal olefinic signals, M_n's of 40,000, 60,000 and 140,000 g mol⁻¹ have been calculated respectively for the polymers **P2**, **P3**, **P4**. For M_n's higher than 50,000 g mol⁻¹ the method is limited of course, due to increase in the noise ratio and possible isomerization of the terminal end-group resulting in large errors.

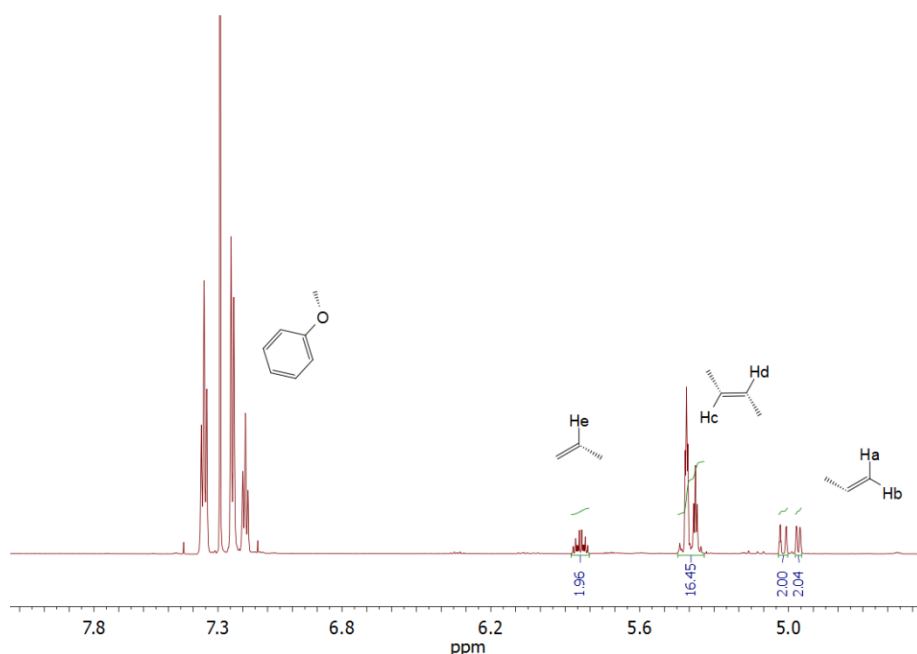


Figure 14: ¹H NMR spectrum (700 MHz) in CDCl₃ at 298.3 K showing the aromatic and olefinic signals of a polymer **P4** 4,000 g mol⁻¹ sample calculated by NMR.

The resonances labeled belong respectively to the phenyl pendant group (7.2 ppm), the terminal groups (a : 5.0 ppm, b : 4.9 ppm, e : 5.8 ppm) and internal (c : 5.38 ppm, d : 5.34 ppm) olefinic protons. ^1H - ^1H COSY of polymer **P4** (M_n 9,000 g mol $^{-1}$) further proves the presence of terminal double bond signals, which disappear after hydrogenation.

3.1.3 Thermal Characterization

The UPPEs synthesized in this study range from sticky gums to rubbers, which are readily soluble in common organic solvents such as CHCl_3 , CH_2Cl_2 and toluene. The flexible P-O-C groups in the backbone commonly result in PPEs with low glass transitions (-40 °C).⁵⁵ Interestingly it has been observed that the glass transition of a poly(lactide-*co*-ethylphosphate) copolymer depends inversely on the weight percentage of phosphoester segment in the copolymer.⁵ The Fox equation for these polymeric systems estimated the T_g at -30 °C for a PPE homopolymer, which is consistent with the role of an internal plasticizer of the phosphoester monomer itself. The thermal stability of the polymers **P2**, **P3**, **P4**, **P5** was examined by thermal gravimetric analysis (TGA) while the glass transition temperatures (T_g) and the melting points (T_m) were determined by differential scanning calorimetry (DSC) under nitrogen (Figure 4). The materials synthesized showed the typical low temperature glass transitions of PPEs, with a relevant contribution of the olefinic double bonds to the polymer microstructure for the polymers **P2**, **P3**, **P4** shifting the T_g to -30 to -70 °C. In addition, the melting temperatures of the polymers **P4** and **P5** (50,000 g mol $^{-1}$) change as the unsaturated backbone is hydrogenated. Even polymer **P4** exhibits a melting temperature at -7 °C upon heating and cooling, while the equivalent hydrogenated polymer **P5** shows melting at 44 - 45 °C due to the disappearance of the double bonds which act as a defect during the crystallization of the polymer (Figure 15). All the other unsaturated polymers exhibit different glass transitions at -32 °C for **P2** (14,000 g mol $^{-1}$) and -53 °C for **P3** (20,000 g mol $^{-1}$), without observing a melting peak.

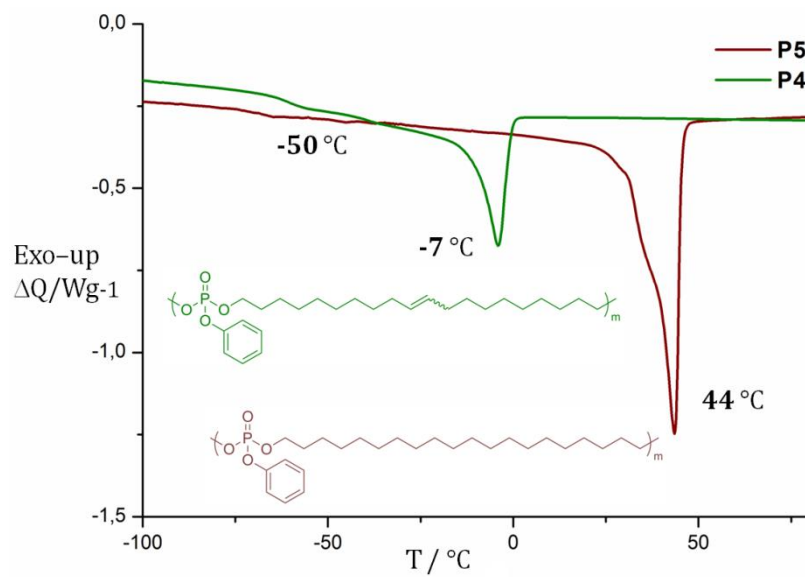
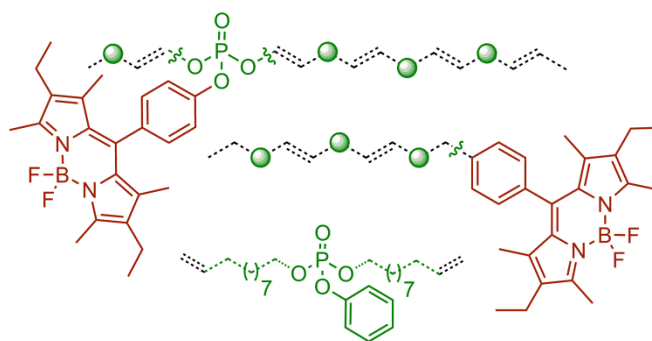


Figure 15. DSC thermograms of P4 and P5.

3.2 A metathesis Route for BODIPY Labeled Polyolefins

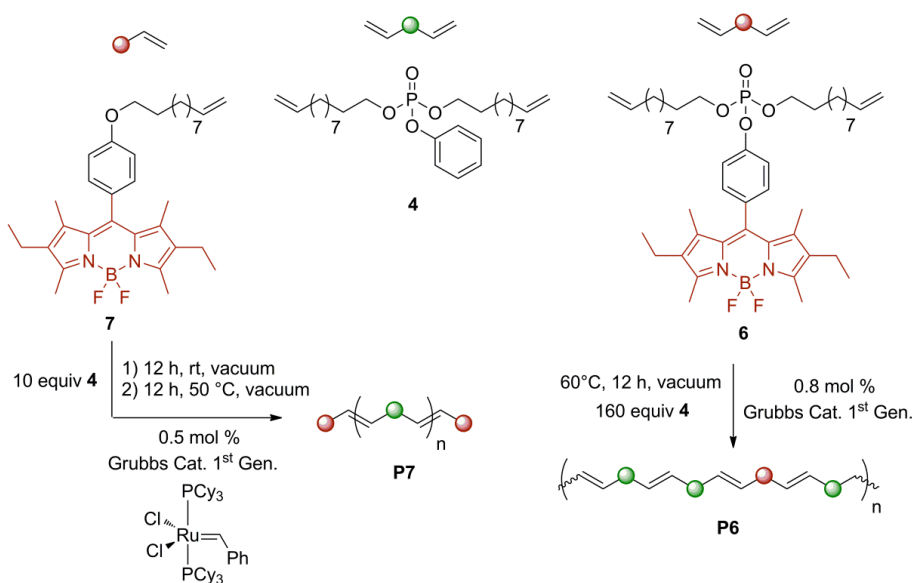
ADMET provides an efficient strategy for the labeling of polyolefins. The versatility of phosphorus chemistry allows designing substituted BODIPY monomers or chain stoppers for the synthesis of precise labeled (degradable) polyphosphoesters.



Scheme 8a. Metathesis approach toward BODIPY labelled Poly(Phosphoester)s

Chemical labeling is a great possibility to obtain traceable steadily-stained materials for versatile applications such as optical bioimaging and signal amplification in biological diagnostics.⁵⁶ In the family of organic dyes, the set based on **BODIPY** (boron-dipyrromethene or 4,4-difluoro-4-bora-3a,4a-diaza-s-indacene) has attracted increasing attention over the past decade.⁵⁷ BODIPY-based functional materials continuously expand their range of applications because of unique photo-physical properties, such as excellent thermal and photochemical stability, good solubility and intense absorption profile. BODIPY's chemical robustness allows the design of functional systems for paint, ink compositions, and electroluminescent devices.⁵⁸ One of the main features that makes this organic dye extremely attractive is the possibility to modify its molecular backbone in a straightforward manner. Great potential was recognized for biochemical purposes, making this stable dye become known and used among biologists, for example for the labeling of biomacromolecules such as DNA.⁵⁹ Because of their functionality and similarity to DNA, in recent years synthetic polyphosphoesters have attracted attention in biomaterial science.^{5,7} Typically, polyesters dominate the field, and are widely applied in pharmaceuticals and medical applications, because of their excellent

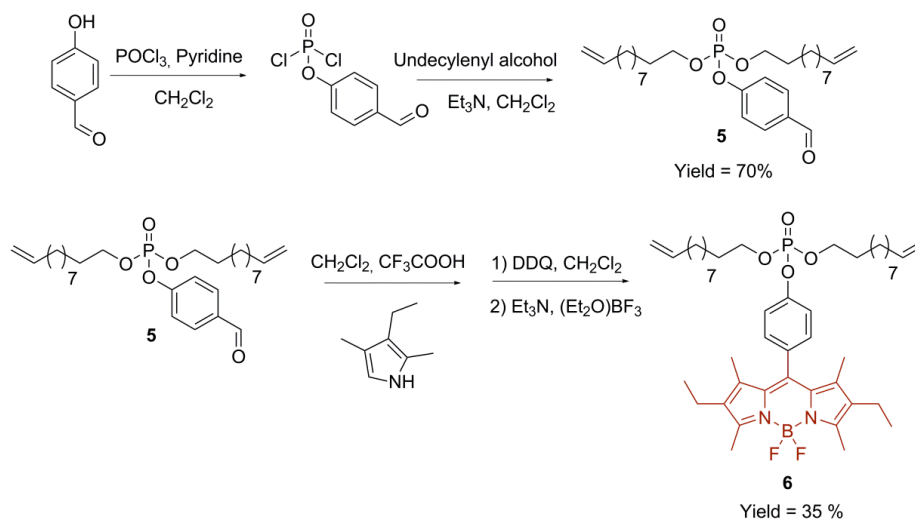
biocompatibility and degradability.⁶¹ The structural versatility of phosphorus, combined with a straightforward synthetic approach, allows generating novel functional polymerizable organophosphates. We have demonstrated how these compounds can undergo acyclic diene metathesis and thus be converted into linear synthetic polyphosphoesters.⁴⁵



Scheme 8b. Metathesis polycondensation of phenyl-di-(10-undecenyloxy)-phosphate **4** in presence of BODIPY dyes (**6** and **7**).

Different strategies for the synthesis of complex BODIPY–polymer conjugates mostly by anionic or radical polymerization has been reported.⁶⁰ In contrast, little attention was given to the precise incorporation of these dyes into degradable polymers, which has become of particular scientific and application relevance. Different synthetic strategies allow the synthesis of functional BODIPY derivatives via cross-coupling of organometallic compounds,⁶¹ click chemistry,⁶² radical or photochemical polymerizations.⁶³ This is the first report on a strategy (Scheme 8) based on ADMET for the facile preparation of precise labeled polymers that further expand the toolbox of biodegradable polyesters based on phosphorus. A ROMP metathesis strategy for the synthesis of fluorogenic polymers was developed by using norbornene derivatives and suitable fluorophores.⁶⁴ However this strategy is limited to only a few monomers that can be polymerized by this technique. Our model system offers many possibilities to design and label various types of polyolefins, because a wide

range of functional acyclic diene monomers is available for ADMET in combination with a robust synthetic protocol based on phosphorus oxychloride. Ruthenium-based complexes such as the catalysts of Grubbs provide, furthermore, an efficient and functional-group tolerant tool for olefin metathesis, under mild conditions with quantitative conversion.



Scheme 9. Synthesis of polymerizable BODIPY **6**.

3.2.1 BODIPY Dyes: Synthesis

Phosphorus oxychloride is a key compound for the synthesis of structural versatile organophosphates. This intermediate can be reacted with a variety of alcohols to obtain functional and polymerizable phosphoaldehyde **5** (Scheme 9) what is the perfect handle to build the BODIPY moiety onto the olefinic monomer. As phenyl-di-(10-undecenyloxy)-phosphate **4** is a liquid, it facilitates the bulk-metathesis co-polymerization of the olefinic BODIPYs allowing the generation of high molecular weight polymers.

In order to ensure covalent labeling of the polymer, **6** or **7** were used as co-monomer or chain stopper, respectively, during the polymerization. The relative amount of **6** allows tailoring the percentage of dye in the polymer, while BODIPY **7** acts as a terminating agent capping the polymer chains to allow adjusting the molecular weight and also the labeling position (at the chain ends in

this case). As proven by GPC equipped with a fluorescence detector (Figure 16) homogeneous labeling of the polymers is achieved.

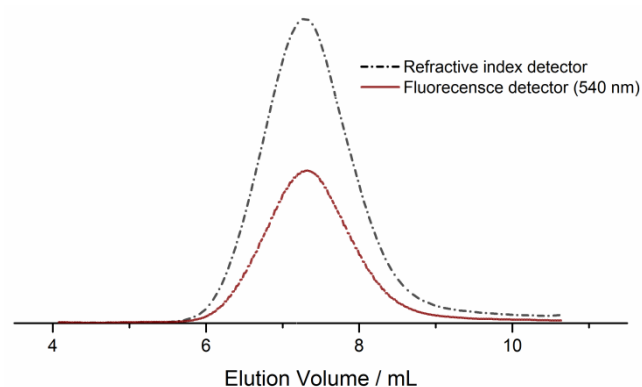


Figure 16. GPC elugram (in THF) for polymer **P6** showing the fluorescence (λ_{exc} = 540 nm) and the refractive index detection.

3.2.2 Photophysical Properties

One important point that should be emphasized here is the possible influence of the polymer chain on the spectroscopic properties of the dye and, conversely, the influence of the dye on the polymer chain conformation (Figure 17).

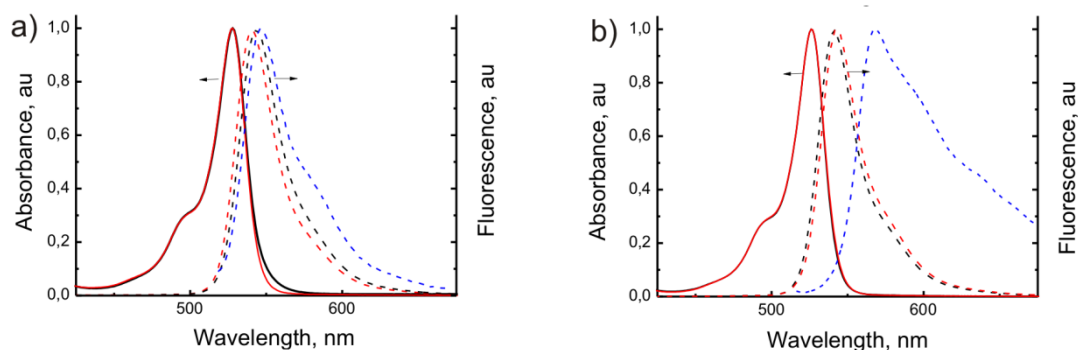


Figure 17. UV-visible (solid lines) and fluorescent spectra (dashed lines) for monomeric dyes and the respective polymers. (a) BODIPY **6** in toluene (black), polymer **P6** in toluene (red) and thin solid film (blue); (b) BODIPY **7** in toluene (black), polymer **P7** in toluene (red), and thin solid film (blue).

It is possible to tune the percent of labeling by tailoring the monomer ratios as both carry electron rich olefins, leading to a random incorporation into the polymer backbone and high molecular weights via ADMET, the photophysical properties of the dye stay undisturbed after polymerization when the polymer is dissolved in organic solvent (Figure 17 and Table 2).

Table 2. Summary of fluorescences of BODIPY polymer-conjugates in solution and film.

	entry	λ_{\max} nm	lifetime (τ) ns	Quantum yield (η)
SOLUTION	P6	542	4.8	0.70
	P6a	542	4.7	0.70
	P7	542	4.6	0.72
FILM	P6	547	2.4	0.51
	P6a	546	0.95	0.09
	P7	569	0.97	0.10

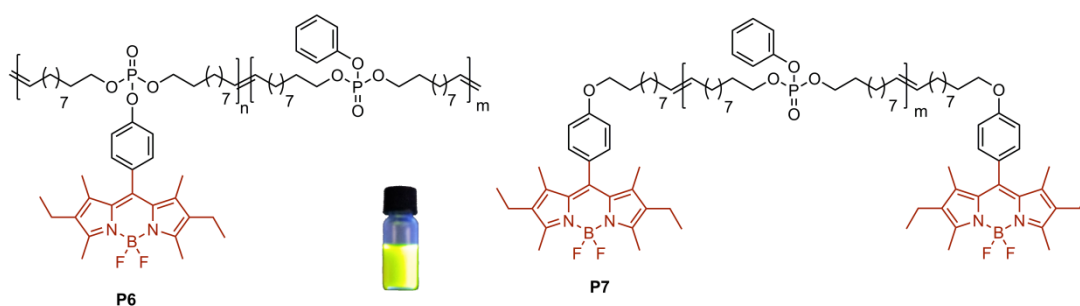
Further, an incorporation efficiency of 100% of **6** and **7** in the polymers was obtained (Table 3). The precise percentage of labeling is crucial to keep unchanged the conformation of the polymer chain, minimizing self-quenching between dyes in close proximity. In a second approach, we used metathesis to selectively label the end groups with **7** that acts as a chain stopper in the polycondensation reaction.

Table 3. Summary of photophysical properties of BODIPY polymer-conjugates.

	(M_w) ¹ , g mol ⁻¹	(M_n) ² , g mol ⁻¹	Polydispersity, (M_w) ¹ / (M_n) ²	Absorption (λ_{\max}), nm	Extinction, (ϵ_p) ³	Labeling efficiency, φ ⁴ , %
P6	170,000	80,000	2.1	528	1,13	~100
P6A	150,000	75,000	2.0	528	7,49	~100
P7	30,000	20,000	1.5	526	4,78	~100

(1) Weight-average and (2) number-average molecular weight determined by gel permeation chromatography (GPC) in THF vs. polystyrene standards from RI-detector. (3) extinction coefficient of the (ϵ_m [L mol⁻¹ cm⁻¹]) polymer ; (ϵ_p [L g⁻¹ cm⁻¹]) dissolved in toluene; (4) labeling efficiency (φ) was calculated as $\varphi = \frac{\omega_p}{\omega_s}$, where ω_p is weight fraction of the fluorescent monomer in the polymer and ω_s is weight fraction of the fluorescent monomer in the monomer mixture. ω_p was calculated as $\omega_p = \frac{A_p M_m}{\epsilon_m m_p}$, where $A_p = \epsilon_p$ is absorbance of the polymer solution with concentration 1 g L⁻¹, M_n is the molecular weight of the fluorescent monomer, ϵ_m – we assume that the molar extinction of the BODIPY unit is the same in the monomer and polymer, $m_p = 1$ g is mass of the polymer in solution.

In a one-step reaction, this chain stopper, allowed to introduce precisely and homogeneously the fluorescent moieties at the ends of the polymer backbone in a quantitative manner; it can also be used for labeling of other compounds by cross metathesis, making it a valuable compound for future works. More importantly, this strategy allows tailoring the desired molecular weight as **7** is quantitatively incorporated. Telechelic polymer **P7** (M_w 30,000 g mol⁻¹, polystyrene standards in THF, PDI= 1.5) with high optical absorptivity per weight of polymer was obtained. These polymers (Scheme 10) are promising candidates for example, to generate fluorescent nanoparticles that could find applications as degradable drug delivery vehicles and to monitor their cell uptake *in vitro*.



Scheme 10. Structures of labeled polyphosphoesters synthesized via ADMET. The vial shows the fluorescence of polymer **P6** in toluene.

An important property of the labeled polymer **P7** is that the fluorescence quantum yield is very similar to the monomer (**7**) in solution but differs in the polymeric film. The decrease of the quantum yield is likely to originate from self-quenching because of the rather high dye content. The direct copolymerization of **6** allows to generate the high molecular weight labeled polyphosphoester **P6** (M_w 170,000 g mol⁻¹, GPC polystyrene standards in THF PDI = 2.1). By this approach, we were able to increase seven times the amount of fluorescent co-monomer into the polymer chain **P6A** compared to **P6**. This tunable labeling keeps the properties of the mother polymer less affected, demonstrating with **P6A** the possibility to obtain a bright material with a high extinction coefficient and strong fluorescence without self-quenching (Table 3, Table 4).

Table 4. Summary of photophysical properties of BODIPYs synthesized.

	Absorption (λ_{max}), nm	Extinction, (ϵ_{m})¹	Fluorescence (λ_{max}), nm	Fluorescence lifetime (τ), ns	Fluorescence quantum yield (η)
BODIPY (6)	528	67000	545	4,6	0,71
BODIPY (7)	526	64000	545	4,9	0,69

(1) extinction coefficient of the (ϵ_{m} [L mol⁻¹ cm⁻¹]) BODIPYs ; (ϵ_{p} [L g⁻¹ cm⁻¹]) dissolved in toluene.

3.2.3 BODIPY Labeled Polyolefins: Considerations

Two new BODIPY **6** and **7** derivatives have been synthesized which can be used to label polymers and other olefinic compounds via olefin metathesis. The metathesis approach offers the possibility to adjust the quantity and labeling position at tunable positions, i.e. along the chain or at the chain end – or also via cross metathesis to other compounds. As a model we prepared unsaturated polyphosphoesters which were labeled along the chain or at the chain ends by controlling the molecular weights.⁶⁵ This one-step olefin metathesis with mono- or difunctional BODIPY-based dyes is a general protocol to label polymers that can be prepared by ADMET for example to follow their cell uptake behavior.

3.3 Telechelic Polyphosphoesters^{1a}

By definition, a telechelic polymer is a di-end-functional polymer where both ends possess the same functionality. Polymers which have different end groups are termed di-end-functional polymers or heterotelechelic polymers.⁶⁵ A telechelic polymer or oligomer is a prepolymer capable of entering into further polymerizations or other reactions through its reactive end-groups. It can be used for example to synthesize block copolymers.⁶⁵ Reactive end-groups in telechelic polymers can stem from the initiator or termination or chain-transfer agents in chain polymerizations, but not from monomers as in polycondensations and polyadditions.⁶⁶ Since their

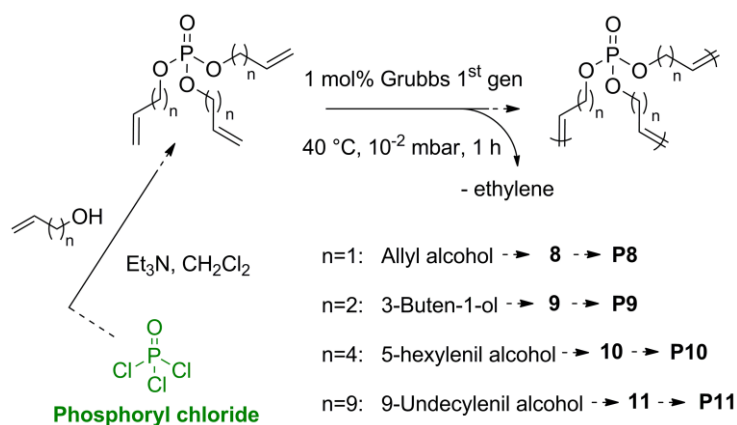
^{1a} In collaboration with Mark Steinmann, Diplomarbeit 2013, manuscript in preparation.

monomer of the repeat unit were directly mixed together with Grubbs catalyst 1st generation, which is a typical catalyst for metathesis reactions. The backbone is based on UPPEs, made by the ADMET polymerization. Furthermore a Chain termination reactant (CTR) was added to the reaction mixture, which carries nine methylene groups, between their olefin and precursor, like alcohol groups, were used to cap the polymer chain ends to yield difunctional telechelic material. The CTRs with nine methylene groups have two advantages : the lengths is the same as the lengths of the methylene groups between the phosphates; the size of the CTR is big enough to have less volatile or a higher boiling point respectively, which is useful because the synthesis applies vacuum. The molecular structures of the telechelic polymers differ by the group at the chain end, which is a direct result of the identity of the CTR used to end-cap the polymer chains during the ADMET reaction. The CTR serves to limit the molecular weight of the polymer and to cap the chain-ends with a desired functional group. The use of the CTR directly in polymerization reaction allows synthesizing telechelic UPPEs with good molecular weight control. Telechelic diols presented in this work would serve as a macro monomer lead to Polyurethanes (PU) with novel interesting features. Furthermore any chosen telechelic macro monomer could be polymerized to yield innovative polymers with new properties depending on the architecture and degree of polymerization of the introduced polymer chains, such as polyesters by telechelic dicarboxylates.

3.4 Hyperbranched Polyphosphoesters

Hyperbranched (hb), i.e. statistically branched, polymers were always considered as materials suitable for large-scale applications in coatings or resins, as their synthesis is usually achieved in one polymerization step only yielding highly functional materials with peculiar properties.⁷⁰ Coatings companies, for example, have found breeding grounds and since the first reports on hyperbranched polymers many formulations from high solid coatings to barriers for flexible packaging have been developed.⁷¹ A branch-on-branch structure with a large number of terminal groups, gives excellent flow and processing properties to these polymers superior to most linear polymers.⁷⁰ From the early beginning, different methodologies have been developed for the synthesis of hb polymers: step-growth polymerization techniques are probably the most frequently ap-

plied strategies.⁷² Generally, these approaches are based on AB_n monomer in which the single A-group reacts in an ideal case only with the B groups of the monomer via polycondensation or polyaddition.⁷³ The polymerization of a mixture of monomers of the type A₂/B₃, is also regarded to lead to highly branched structures often based on commercially available materials.⁷⁴ These structural peculiarities lead to amorphous materials, since branching prevents crystallization, resulting in low viscosities in bulk and in solution.^{70, 75} In spite of the abovementioned benefits, often harsh reaction conditions need to be applied for the synthesis of hb polymers. Recently Grubbs et al. employed olefin metathesis to prepare hb polymers under mild conditions.⁷⁶ We present structurally novel hbUPPEs that are generated by metathesis polymerization. For the first time, hbUPPEs (Scheme 12) were prepared within a two-step protocol via olefin metathesis using the phosphate moieties as trifunctional branching points.



Scheme 12. A straightforward strategy: Schematic representation of monomer synthesis and AT-MET polymerization conditions for the synthesis of hbUPPEs.

3.4.1 Monomer Design

The polymerization with quantitative conversion of A₃-type monomers produces soluble processable materials with variable structure (Scheme 12), with an intrinsic low viscosity and high level of internal and end group functionalization. Only the structural versatility of phosphorus (starting from POCl₃) allows the straightforward preparation of several A₃-type functional monomers. Herein we synthesized tri-(but-3-en-1-yl)-phosphate(**9**), tri-(5-hexen-1-yl)-phosphate (**10**), tri-(undec-

10-en-1-yl)-phosphate (**11**) having a variable chain length between the double bond and the phosphate unit by the choice of the alcohol in order to vary the branching point density within the hb polymers. These A₃ monomers were polymerized with Grubbs catalyst 1st generation in bulk to generate hbUPPEs. Control over molecular weights avoiding gelation has been obtained by fine tuning of the reaction conditions, with temperature and catalyst amount being the key during the preparation of soluble branched materials. The high level of terminal double bond functionalization (Figure 18), combined with the low glass transition temperatures (ca. -90 °C) of the hbUPPEs make these systems as mobile and closed matrixes for the dispersion of highly hydrophobic moieties. The metathesis of **9** was used as a model monomer to study the growth of the olefin rich hbUPPEs without a complementary B₂-type monomer, in presence of the appropriate ruthenium catalyst.

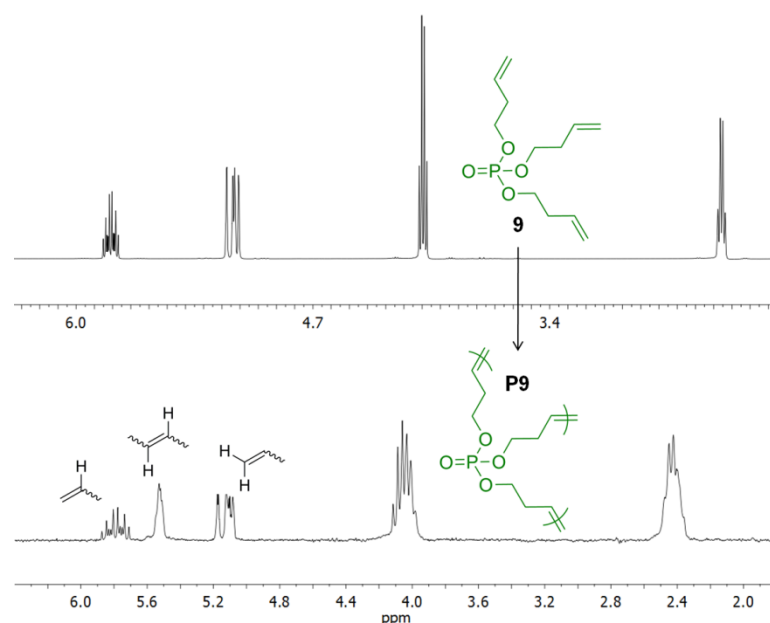


Figure 18. ¹H NMR (500 MHz in CDCl₃ at 298.3 K) showing high level of terminal end group functionality after the controlled metathesis polymerization of **9**.

The polymerization via Grubbs-type catalysts of **9** can be followed by ¹H NMR as the terminal olefinic resonances of the starting monomer at 5.8 and 5.1 ppm, respectively, change into much broader peaks after polymerization and also internal polymeric double bonds (at ca. 5.5 ppm) can be detected (Figure 18). These results prove, combined with SEC equipped with a viscosity detector, the highly branched and polyfunctional structure of the hbUPPEs (Figure 19). Olefin metathesis is

able to polymerize an A_3 monomer without the need of a complementary B_2 monomer. This was first shown by the group of Meier with the polymerization of a Glyceryl triundec-10-enoate to yield highly branched materials.⁷⁷ Control over the molecular weight during the hyperbranching polymerization of suitable A_3 monomers is controlled by the addition of chain stoppers in order to perform the one-step and one-pot reaction and to prevent highly cross-linked insoluble structures.⁷⁸ The ring-opening polymerization (ROP) approach was also applied to prepare a water-soluble hyperbranched polyphosphate drug carrier which was recently synthesized by self-condensation ROP of 2-(2-hydroxyethoxy)-ethoxy-2-oxo-1,3,2-dioxaphospholane.²⁴ The structural versatility of phosphorus, combined with our straightforward synthetic approach, allows generating novel functional polymerizable organophosphates. These compounds can undergo acyclic triene metathesis (ATMET) and thus be converted into hbPPEs. Since the monomers are liquid at room temperature, the polymerizations were carried out in bulk, by the addition of the appropriate amount of catalyst (usually ca. 0.1-0.5 mol%) under argon.

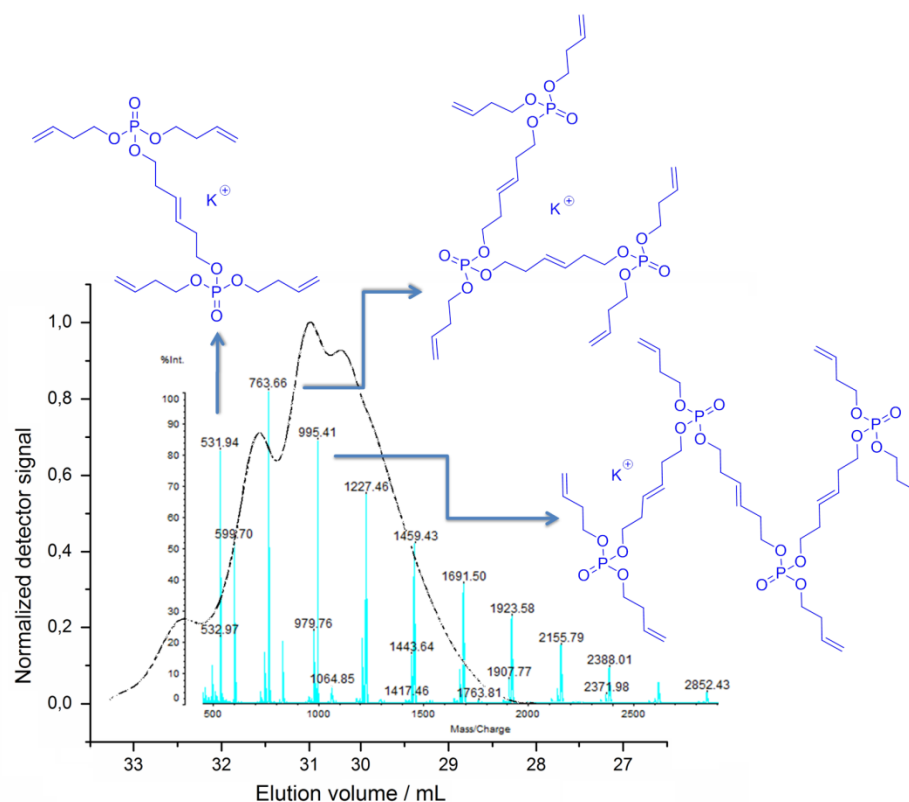


Figure 19. Overlay of a MALDI-ToF mass spectrum and a SEC elugram indicating oligomeric metathesis compounds of **P9**. (0.6 mol% G1 catalyst, r.t. for 8 h).

Because the results for ADMET are highly dependent on the catalytic system, only ruthenium-based catalysts were selected.⁵² Considering molecular weight dispersity, for a linear ADMET system a value of $M_w/M_n=2$ is the most probable distribution for a linear polycondensation, as conversion reaches 100%.⁴⁶ Nonlinear polycondensations, such as the metathesis of acyclic trienes, lead to systems with higher dispersity values. In our case, highly branched PPEs can be prepared with tailorable molecular weights having dispersities which did not limit the applications of these materials, as discussed later.

Tri-allyl phosphate **1** was synthesized to be used as an A_3 monomer for the acyclic triene metathesis (ATMET) to generate *hb* unsaturated PPEs with high phosphorous content (**P1**). To the best of our knowledge, for the first time, an olefin metathesis polymerization on a tri-allyl ester was reported, since allyl esters, -amides or -ethers are known to have very low metathesis activity.⁴⁷ In this case, the A_3 monomer proved efficient polymerization as it can be calculated from ^1H NMR (Figure 20) and ESI-MS analysis of early reaction steps (Figure 21) with final molecular weight up to $2,500\text{ g mol}^{-1}$.

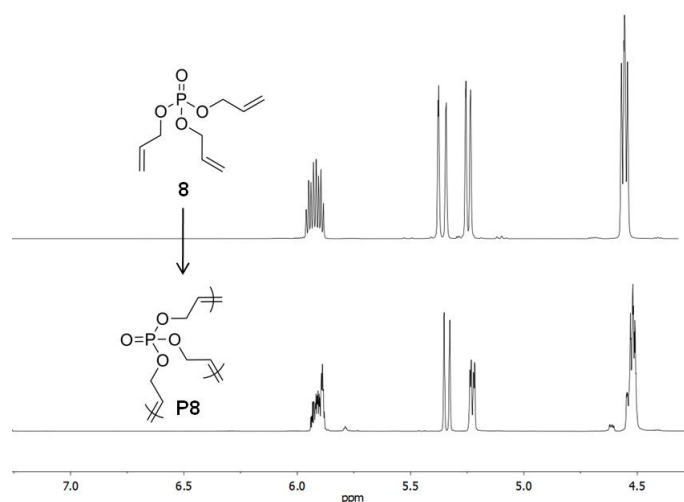


Figure 20. ^1H NMR (500 MHz in CDCl_3 at 298.3 K) showing high level of terminal end group functionality after the controlled metathesis polymerization of **8**.

All ATMET polymerizations exhibited quantitative conversion of **8** and lead to soluble, processable materials with variable structure with an intrinsic low viscosity (M_w 's typically ca. $2,500\text{ g/mol}$, GPC

in THF vs PS). The high level of end group functionality makes **P8** a suitable candidate as additive in flame retardant coatings since the presence of double bonds provides a reactive group for a classical bi-component system.

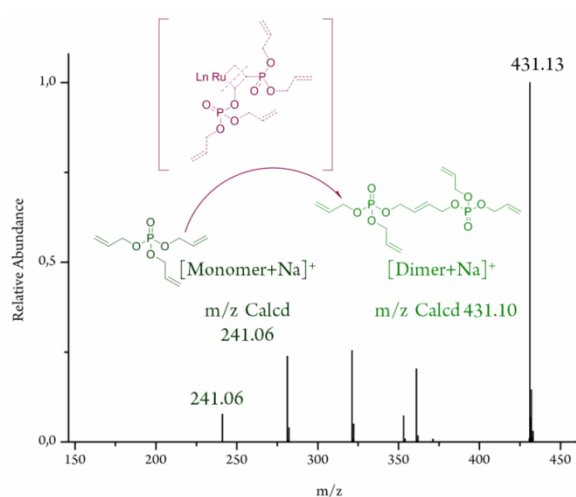


Figure 21. Evidence of dimeric structure from ESI-MS: early metathesis step.

This system allowed preparing a UPPE with a very high P-content (17%) and degree of branching with the smallest possible backbone that is accessible via metathesis chemistry. From the ^{31}P NMR of **P8** a branched structure is shown, as the different structural units in a *hb* polymer (linear, dendritic, terminal as well as cis/trans double bonds) resonance at different chemical shift (Figure 22).

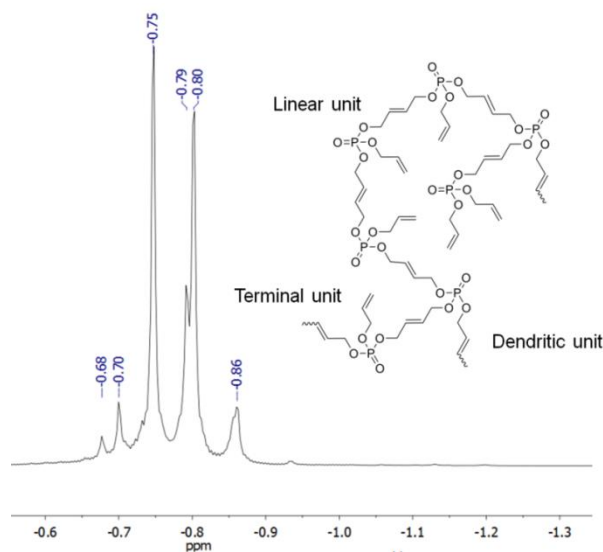


Figure 22. ^{31}P NMR of **P8** (202 MHz, CDCl_3).

3.4.2 Kinetics of Polymerization and Structural Considerations

In order to control the polymerization of A₃-type monomers and to prevent cross-linking of the materials, temperature showed to have a key role as a control parameter. As shown in Figure 18 and 20, this strategy without using a chain stopper ensured high level of terminal double bonds functionalization while keeping the material soluble and preventing crosslinking.

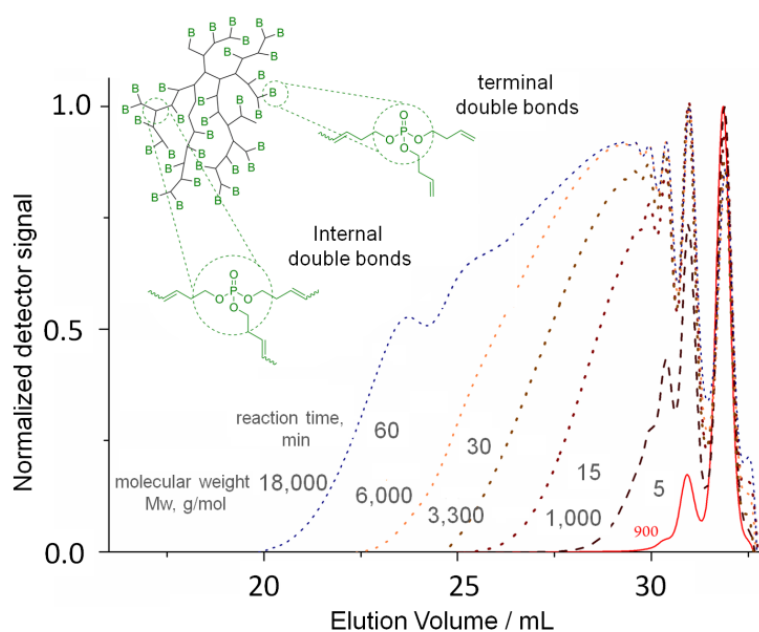


Figure 23. SEC elugrams showing the kinetics of the polycondensation of 1 over a period of 140 min (0.8 mol% G1 catalyst, 30 °C).

The polymerization of **9** was conducted in presence of 0.8 mol% Grubbs 1st generation catalyst at 40-45 °C, under vacuum in absence of solvent and polymers **P9** were obtained after 90 min reaction time with M_w 's of ca. 16,000 - 18,000 g/mol (from GPC). Because of the low viscosity of **P9**, stirring was still possible after consumption of the monomer ensuring homogeneous mixing with a quantitative monomer conversion. In order to determine the onset of gelation, the kinetics (at 40 °C) of the polycondensation of **9** was monitored via GPC (Figure 23). In a fashionable way, the polymerization of tri-(5-hexen-1-yl)-phosphate (**10**), tri-(undec-10-en-1-yl)-phosphate (**11**) reached an optimum molecular weight at 16,000 g/mol resulting into a glassy transparent material (**P10**, **P11**) after purification (Table 5). The materials prepared showed good solubility in the common organic

solvents with a low viscosity in solution. SEC equipped with a viscosity detector further proves the highly branched structures as all Kuhn Mark Houwink parameters of the hbUPPEs are lower than 0.5 as common for hb polymers.⁷⁰

Table 5. Metathesis polymerizations: Molecular weights, polydispersities, glass transitions, melting points and Staudinger indices.

Entry	$M_w^{(a)}$	$M_n^{(a)}$	$\mathcal{D}^{(b)}$	$T_g^{(c)}$	$\alpha^{(d)}$
P8	2,500	1,000	2.6	-100	/
P9	18,000	7,000	2.6	-85	0.44
P10	15,500	3,500	4.4	-88	0.26
P11	20,500	5,600	3.7	+5 (melting)	0.17

[a] in g mol^{-1} , determined by gel permeation chromatography (GPC) in THF vs. polystyrene standards; [b] M_w/M_n , molecular weight dispersity from GPC, [c] glass transition in $^{\circ}\text{C}$ (from DSC), [d] Kuhn Mark Houwink parameter (determined from GPC/viscosity experiments in THF).

Chapter 4

Applications

Outline

This chapter will describe targets and the applications of the novel poly(phosphoester)s described in this thesis. The synthetic route allows customizing linear, hyperbranched, labeled and telechelic phosphorous based architectures with unique properties. A main focus will be given to poly(phosphoester)s as oxygen scavengers for optical upconversion applications. The synthetic route also allows one to design functional materials for tissue engineering as well as for flame retardancy, demonstrating the versatility of the systems for covering different research areas with common and cheap starting materials.

4.1 Optical Upconversion

The possibility to tune chemical and physical properties in polymeric materials has a strong impact on a variety of technologies, including photovoltaics. One of the prominent research areas of modern material science for photovoltaics involves spectral conversion. Optical upconversion (UC) refers to a collection of processes that permit the conversion of optical radiation into light of a shorter wavelength. Anti-Stokes emission (Figure 24) was observed long ago for processes that involved thermal excitation, but the shifts attainable through thermal excitation are very small, generally of the order of a few kT .⁷⁹

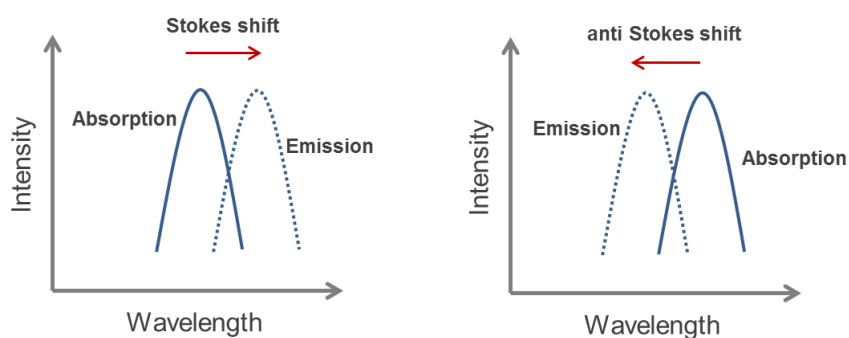
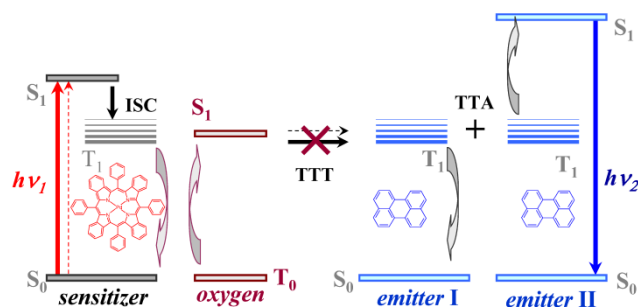


Figure 24. Schematic illustration of the Stokes (downconversion) and anti-Stokes (upconversion) shifts. Solid and dotted lines represent absorption and emission spectra, respectively.

Thus, optical upconversion remained a curiosity until the advent of lasers, which promoted the discovery of a diverse range of UC processes in which the emission and excitation energies are different by many multiples of kT , i.e., clearly in violation of Stokes' law. Evidently, no energy is created in such UC processes; rather, the various UC schemes rely on different approaches to harness and combine the energy of multiple photons. Examples include nonlinear-optical processes such as second and third harmonic generation, and simultaneous absorption of multiple photons.⁸⁰ Nonlinear-optical materials have come to play an important role in a variety of technological applications, but since they require coherent, high-intensity excitation by (pulsed) highpower lasers, they cannot be exploited in applications where the upconversion of low-power, non-coherent, continuous-wave excitation is either desirable or a must. Several alternative processes that allow for

low-power upconversion have been known since the 1960s. Upconversion based on energy-transfer processes, excited state absorption, cooperative upconversion involving multiple ions, or photon avalanches can be observed in certain materials doped with transition-metal (d) or rare-earth (f) ions, which exhibit long excited-state lifetimes and offer accessibility of multiple energy levels with similar spacings.⁸¹ UC at low power densities (<100 mW cm²) and of noncoherent light can also be achieved by way of triplet-triplet annihilation (TTA-UC) in multi-chromophore systems that comprise a triplet sensitizer and an emitter.⁸² The effect was first demonstrated fifty years ago by Parker and Hatchard,⁸³ who employed solutions of anthracene and phenanthrene to upconvert ultraviolet (UV) light.



Scheme 13. Energy scheme of the processes involved in TTA-UC. The process involves population of the first singlet excited state of a sensitizer (S_1) upon absorption of incident light, intersystem crossing (ISC) to the triplet excited state (T_1), triplet-triplet energy transfer from the sensitizer to an emitter (T_1), and triplet-triplet annihilation (TTA) of two emitter triplets to populate the emitter singlet excited state (S_1), which decays radiatively (fluorescence).

The generally accepted mechanism for this process is that light is absorbed by the sensitizer, whose first singlet excited state is converted into a triplet upon intersystem crossing (ISC). Triplet-triplet energy transfer (TTET) to an emitter and triplet-triplet annihilation (TTA) of two emitter triplets eventually populate an emitter first singlet excited state, which decays radiatively and leads to delayed fluorescence by the emitter (Scheme 13). Interestingly, for almost half a century, TTA-UC, also referred to as sensitized photon upconversion, had been limited to liquid solutions of sensitizer-emitter pairs. The recent discovery that TTA-UC can also be realized in solid polymer matrices,⁸⁴ which on account of their processability and mechanical characteristics are more suitable

ble for many potential applications than liquid solutions, has further fueled the interest in this process. Both sensitizer and emitter ensembles can transfer their triplet energy to molecular oxygen and are thus depopulated and no upconversion is detected.⁸⁵ Further, the hereby generated singlet oxygen is highly reactive, leading to oxidation of the sensitizer and emitter molecules. Passive protection strategies – i.e. decreasing oxygen permeability by means of encapsulation of the UC-active substances in polymer films⁸⁶ or nano- and micro-carriers⁸⁷ - although effective for some minutes or hours, are insufficient for technological application due to their short lifetime. It is inevitable to guarantee an efficient TTA-UC process in materials that can be easily processed on a large scale to get upconversion ready for diverse applications that range from the optimization of photovoltaic devices to bioimaging.⁸⁸

4.1.1 Strategies for Designing TTA-UC in Polymeric Systems

The simplest, and so far most widely used approach to create upconverting polymeric materials involves simply blending the sensitizer and the emitter into a “photophysically inert” polymer matrix, which merely serves as a mechanical support for the chromophores. While this route is particularly attractive as it requires minimal synthetic efforts, the main obstacle is to molecularly dissolve the chromophores at concentrations that are sufficiently high to support the required electronic interactions, i.e., exciton migration and annihilation. Unless special measures are taken, the solubility of small molecules in polymers is often limited to a few percent. Thus, under equilibrium conditions phase separation and dye aggregation are bound to occur, if their concentrations are chosen above the solubility limit.

As the first example of TTA-UC in solid polymer systems, the groups of Castellano and Weder demonstrated that exciton diffusion can be achieved in solid polymer films, by blending comparably low concentrations (0.17 and 0.01 wt%, respectively) of the previously employed sensitizer PdOEP (Pd-octaethylporphyrin) and emitter DPA (diphenylanthracene) into a rubbery host polymer – an ethylene oxide/epichlorohydrin copolymer.⁸⁹ This matrix was selected on the account of its adequate transparency, high dye solubility, and suitable mechanical properties, but most im-

portantly because of its low crystallinity and low glass transition temperature ($-37\text{ }^{\circ}\text{C}$), which impart rubbery behavior as well as rotational and possibly translational mobility to the dissolved dye molecules. The fact that the effect is observed at low chromophore content supports the conclusion that the rubbery matrix indeed permits the required bimolecular processes, presumably, as designed, on account of adequate chromophore mobility.

Considering that triplet excited states are readily quenched by oxygen, the observation of upconversion seems to suggest that blending the upconverting chromophores into a polymer protects them at least partially from this effect. Building upon this initial study, the groups of Weder and Castellano conducted a systematic study that explored how the nature of the elastomeric matrix and the temperature influence the upconverting properties.⁸⁹ Using the above-described blend and similar materials based on a series of thermoplastic polyurethane elastomers as matrices, it was shown that cooling the PdOEP/DPA-containing elastomer films to below the glass transition temperature of the respective polymer completely suppresses the upconverted emission. Conversely, the upconverted emission intensity dramatically increased with increasing temperature. This behavior was completely reversible through several heating and cooling cycles.

A comparison of samples containing the same concentrations of chromophores in different polymer hosts showed that the intensity of the upconverted DPA emission was greatest in the softest (lowest modulus) of the polymers studied. Together with the above-discussed thermal activation effect, this illustrates the importance of translational mobility for the observation of efficient TTA-UC, which in these low-dye content materials is clearly mediated by diffusion-controlled steps. Interestingly, TTA-UC has in the meantime also been realized in blends of upconverting dye pairs in glassy host polymers. For example, Merkel and Dinnocenzo have reported upconversion with an efficiency of 0.02% in glassy poly(methyl methacrylate)(PMMA) comprising 0.005 wt% of PtOEP as sensitizer and 0.09% of DPA as emitter.⁹⁰ Thus, in this case TTA-UC was observed under conditions where the dye molecules are immobilized. Weder proposed a melt-process to create homogeneous high-dye-content blends of PMMA and up to 0.16 and 25 wt% of PdOEP and DPA, respectively.⁹¹ These materials were made by melt-mixing the components at $210\text{ }^{\circ}\text{C}$ (where the mixture is thermodynamically miscible), and quenching the materials to below T_g , thereby kinetically trapping

homogeneously blended materials. Unlike solution-cast reference blends of a similar dye content, which had a phase-separated morphology and showed no appreciable upconversion, TTA-UC occurred readily in these molecularly mixed blends.

The study strikingly illustrates the importance of processing, and the opportunities and possible pitfalls that can arise in the context of the influence that processing has on the final morphology, which in turn exerts a dominating influence on the TTA-UC mechanism. Balushev et al. have studied the mechanistic basis for TTA-UC in solid polymer matrices, as the mechanisms for exciton transport and annihilation are not imminently clear.⁹² More generally, these findings suggest that a precise architectural control can help to maximize the efficiency and to minimize parasitic energy recycling effects.

4.1.1.1 Mechanistic Considerations for Upconversion in Solid Materials

While TTA-UC has only recently been realized in solid materials, all the steps required in the process have been extensively studied individually in different types of solids.⁹³ From absorption to energy transfers to the various limiting processes, every key step has been theorized.⁹⁴ As should be evident from the above description, solid materials must comprise a sensitizer and an emitter in a manner (concentration, morphology) that enables the underlying photophysical processes. Obviously, auxiliary matrix materials should not interfere with the electronic processes by absorbing incident or emitted radiation or quenching any of the excited states.

In addition, it is desirable to exclude O₂, in order to prevent quenching of the excited triplet states. The essential step for TTA-UC is the formation of an encounter complex between two emitter molecules in their triplet excited states and this requires either a high level of translational mobility of these species (as in solution) or, alternatively, efficient exciton migration/diffusion. Both approaches have been utilized to achieve upconversion in solid materials. Indeed, weak blue upconverted emission could be observed in these materials, but the quantum yield was very low. A

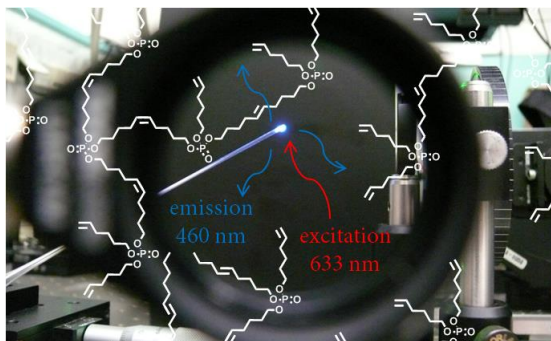
detailed characterization of these materials revealed that this was due to the formation of a phase-separated morphology, i.e. the PtOEP and the DPA crystallized separately, which severely limited the energy transfer between the sensitizer and the emitter. It would seem that this problem could be solved by optimizing the morphology of such solid mixtures, but in reality, the co-crystallization of organic molecules is very difficult to control.⁹⁵

4.1.1.2 Oxygen Quenching

Oxygen solubility and permeability of a polymer matrix have a significant influence on the overall efficiency of the UC process, if operated under ambient conditions. The knowledge acquired in other domains (packaging, gas-exchange membranes, etc..) ⁹⁶ will be of paramount importance for the implementation of polymeric TTA-UC materials. Permeant transport across a polymer involves (i) the sorption of a gas molecule upon collision with the surface, (ii) the solution of the penetrant, (iii) a diffusive random walk along the voids or free-volume of the material, and (iv) the desorption on the other side of the material.⁹⁷

The solubility and diffusivity of a penetrant molecule are governed by the shape and size of the molecule in question, the affinity of the gas for a given polymer, and the morphology of the polymeric material. In semicrystalline materials, dense crystalline regions can generally not be penetrated by diffusing species such as oxygen and slow down diffusion by increasing the tortuosity within the material. In the amorphous regions, molecular mobility dictates local fluctuations and consequently the diffusivity of the penetrants. Consequently, the latter is greatly diminished upon glass formation.⁹⁸ In summary, the nature and morphology of the polymer will impact oxygen solubility and diffusivity, and significantly influence the upconversion efficiency through impacting quenching of triplet excited states by ambient oxygen.

4.1.2 Hyperbranched Poly(phosphoester)s for Active Oxygen Scavenging



An efficient exploitation of renewable energy has become crucial to sustain the increasing energetic demand. Small improvements in terms of efficiency have strong positive repercussions on economy and life. Efficient harvesting of solar energy is one of the most promising solutions to the energetic problem. One of the main challenges is to maximize efficiency using low cost materials. While the overall efficiency of conventional silicon solar cells has continued to improve in recent years, the technology faces a theoretical Shockley–Queisser limit at around 33%.⁹⁹ Silicon solar cells cannot make use of about 20% of the solar spectrum, as these photons with energy below the band-gap are lost as they are not absorbed. Upconversion (UC) of these photons is a promising approach to fill this gap.¹⁰⁰ We developed a structurally diverse library of hyperbranched unsaturated poly(phosphoester)s for highly efficient upconversion in open air (Figure 25) working as active protective materials.

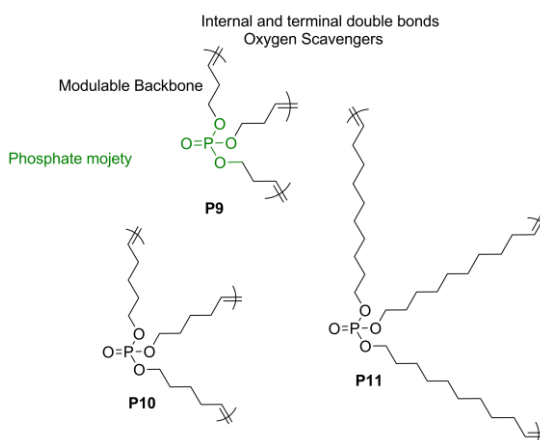


Figure 25. Hyperbranched unsaturated poly(phosphoester)s (hbUPPEs) with variable distance between the branching points were applied as oxygen scavengers.

These polymers can be synthesized conveniently on a large scale. Clear structure-property relationship between the polymer structure and the UC efficiency was developed. TTA-UC was demonstrated to occur in open air in a polymeric matrix with efficiencies much higher than the corresponding standard value assembled in a glove box. The possibility to tune chemical and physical properties in rubbery materials can have a strong impact on a variety of technologies, including photovoltaics, on a market scale due to their long life time (Figure 26).

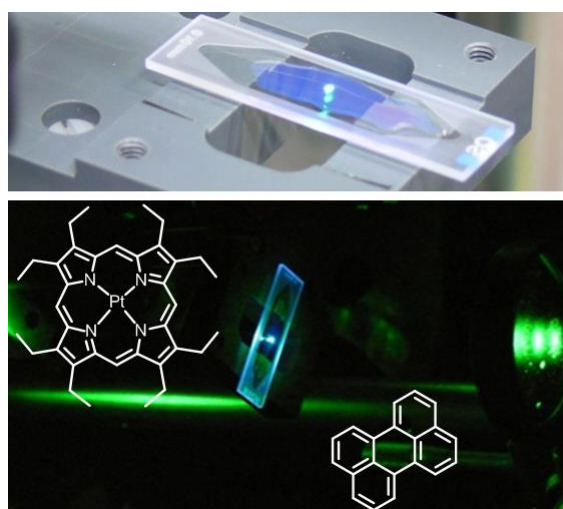


Figure 26: Photographs showing the mixture of perylene - PtOEP in **P11** and photon UC from green to blue light. Due to the viscosity of a polymeric sample the film can also be tilted.

The physical properties of the hbUPPEs, allowed us to evaluate for the first time the possibility to obtain TTA-UC on a large scale. In hyperbranched unsaturated polyphosphates, TTA-UC can be performed with high efficiencies under ambient atmosphere (Figure 26). However, conventional systems have to be protected against oxygen in order to reach a similar (usually less efficient) effect. The hbUPPEs were selected on the account of their transparency and suitable mechanical properties. The low crystallinity and low glass transition temperature impart rubbery behavior as well as the possibility to obtain polymer matrices with high dye content as they mix well with each other. This synthetic strategy is particularly attractive as it requires minimal synthetic efforts. A crucial point during the matrix-synthesis was to obtain an optimal length of the alkenyl chain, specified for the desired photophysical process. All polymers provided a long-term protection

against oxygen quenching of the process of TTA-UC. Increasing the chain length, the protective action of the newly synthesised polymers (**P10** and **P11**) is strong and does not depend on the macromolecular organization of polydisperse material. The efficient oxygen quenching is mostly due to two effects: i) an active chemical protection by scavenging singlet oxygen by the terminal and internal double bonds of the polymer, and ii) by the intrinsic passive protection of the viscous polymer matrix hindering oxygen diffusion – many hb polyesters are known to be impermeable for oxygen.¹⁰¹ Our synthetic strategy, compared to others for the preparation of hb materials, allowed us to obtain relative abundance of terminal double bonds active systems for oxygen protection.

4.1.3 Towards Solar Upconversion: Broadband Excitation

For the first time we demonstrate the possibility of broadband excitation of TTA-UC in a polymer film under ambient conditions (Figure 27). This has a great practical importance in the light of the earlier mentioned applications.

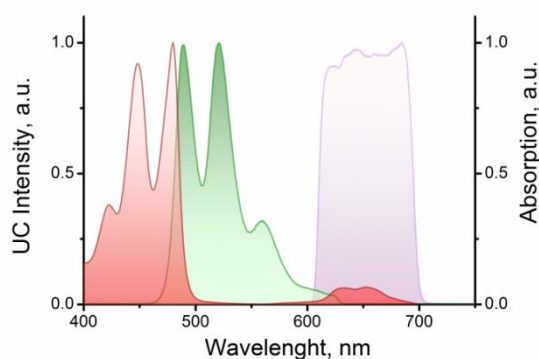


Figure 27: Luminescence spectra of the TTA-UC of a polymer film **P11** with broadband excitation: blue - λ (wavelength)-profile of the excitation source; red - absorption spectra of UC mixture; green - UC fluorescence. 21% O₂, thickness of the sample is $d = 100 \mu\text{m}$.

To obtain absorption spectra with maximal width synthesized library of structurally different porphyrins have been synthesized by Dr. Yuri Avlasevich at the MPIP (EP 13 185 751.8 / 2013) that possess variable absorption wavelength. Thus, in this experiment we report successful

effort of concentration of “red” and “near infrared” photons and their simultaneous conversion in photons with higher energy (“green” photons). This is a very significant step in pushing TTA-UC towards realization in a wide variety of applications, like TTA-UC devices for solar cells applications, food packaging and storing, sensing biocompatible nanoparticles, with the main advantage of measuring the phosphorescent emission (over long period) of any dyes without using glove-box conditions.

4.1.4 Oxygen-Scavenging Activity

It is well-known that singlet oxygen reacts with double bonds.¹⁰² The natural carotenoid lycopene is reported as the most efficient biological singlet oxygen scavenger.¹⁰³ The exact reaction depends on the nature of these double bonds via three main types of additional reactions as well as potential electron transfer. The purpose of an oxygen scavenger is to limit the amount of oxygen available for deteriorative reactions that can lead to reduced functionality of the product. For foods and pharmaceutical products, deteriorative reactions include lipid oxidation, nutritional loss, changes in flavour and aroma, alteration of texture, and microbial spoilage. Oxygen scavengers are the most patented of all active packaging technologies.¹⁰¹ Designing an oxygen scavenging system for a specific type of application is quite complex and is still not well understood. A protection strategy particularly designed for performing photo-chemical processes and especially for the process of TTA – UC is not described till now. The hbUPPEs enable not only the polymeric passive but also an active protection of any bio- and photo-active organic materials against singlet oxygen which is created during the chemical or photochemical reactions by means of deactivating, or chemical bonding of the singlet oxygen. Building up an effective protection mechanism against quenching by molecular oxygen and the subsequent generation of highly-reactive singlet oxygen is imperative for long-lifetime and efficient TTA-UC processes in ambient environments. As the polymer synthesized provide an efficient protective system, we also reported that suitable organophosphates can be used as specially designed organic solvents to enable long-lifetime TTA-UC in ambient atmosphere. The newly-synthesized family of organic phosphates bearing unsaturated hydro-

carbon tails serve as an UC-solvent with low viscosity, thus the efficiency of the TTA-UC process is identical with the efficiency in the standard solvent toluene. However, it simultaneously delivers long-term protection (over 1000 h) against the molecular oxygen quenching, allowing this efficiency to be reached and maintained under ambient conditions (Figure 28).

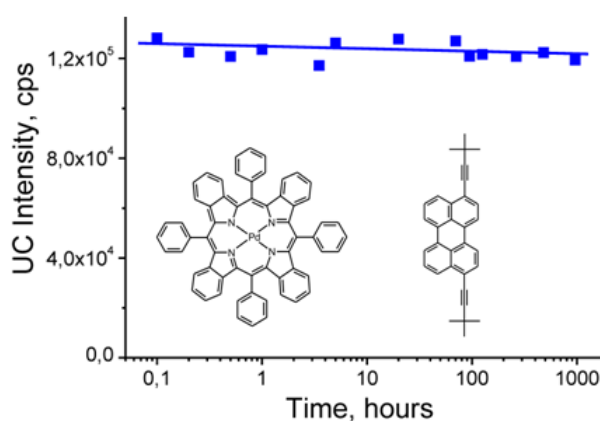
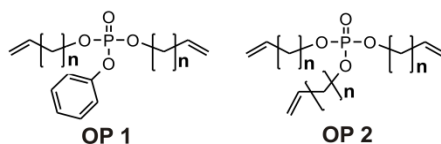


Figure 28: Long-term stability of the UC-fluorescence, for inset UC-couple dissolved in tri-(5-hexenyloxy)-phosphate in ambient conditions. Excitation intensity - 5 mW cm^{-2} ; laser spot diameter - $3000 \text{ }\mu\text{m}$. The solid line is guide to the eye. Daylight conditions, no additional spectral filters are used.

The synthetic procedure provides control of the phosphate functionality, e.g. viscosity, ability to dissolve UC-dyes and oxygen scavenging properties through variation of the hydrocarbon chains length, ratio between aliphatic and aromatic parts and number of terminal double bonds. The generalized chemical structures of the studied organophosphates are presented in Scheme 15.



Scheme 14: General chemical structures of the organophosphates investigated as protecting solvents for the process of TTA-UC. The chain length n was varied between 1 and 9 ($n = 1, 2, 3 \dots 9$).

In oxygen saturated solvents containing metallated macrocycles, during the optical excitation the generation of singlet oxygen is a dominant process when molecular oxygen is available. In this case the sensitizer triplet state is effectively quenched, and the process of TTA-UC is not observable. This explains the experimental data that at oxygen-saturated starting conditions, initially no upconversion is observable. However, as the molecular oxygen concentration is reduced with time (in a process we will discuss) the UC-fluorescence builds up and steady-state UC-emission is reached after a significantly longer rise time in comparison with oxygen-free starting conditions (more than 1000 times longer).

In the presence of high amount of organophosphates (entire solvent for the UC-dyes) fast oxidation, predominantly of the terminal double bonds occurs. Thus, the whole amount of the molecular oxygen is quickly consumed after the start of illumination through generation of singlet oxygen and its subsequent reaction with the terminal double bond. Thereafter, the process of TTA-UC becomes the prevalent relaxation path of the excited sensitizer triplet state. The organophosphates synthesized are colorless, odorless, nonvolatile, and low-viscosity liquids. All investigated phosphates perfectly dissolve various UC-dyes without evidences of dye aggregation.

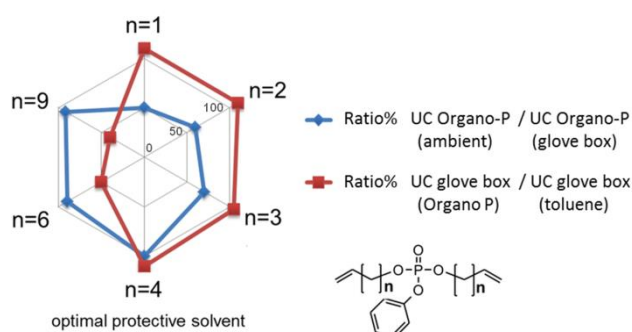


Figure 29: (*red filled squares*) – Ratio between the UC-Q.Y. for standard UC-couple (PtOEP / perylene) dissolved in organophosphates OP1, measured in ambient atmosphere or at glove-box conditions; (*blue filled diamonds*) – Ratio between the UC-Q.Y. for standard UC-couple (PtOEP / perylene) dissolved in organophosphates or toluene, measured at glove-box conditions.

As shown in Figure 29 (blue circles) the UC-Q.Y. in oxygen-free atmosphere for all the organophosphates bearing shorter alkyl ($n \leq 4$) chains is even higher than the UC-Q.Y., when the active dyes are dissolved in the standard solvent – toluene. In contrary, the organophosphates bearing longer chains, i.e. $n \geq 4$ demonstrate pronounced protective properties in oxygen-saturated environment. However, the optimal chain length is $n = 4$ and all following investigations will be conducted with it. To understand the effect of the central atom on the reactivity and oxygen-scavenging ability, we performed investigated the effect of substituting boron, carbon and nitrogen to phosphorous in the monomer precursors to the **P9** unsaturated polymers, by means of first-principles electronic structure calculations. The distribution patterns of the highest occupied molecular orbitals (HOMOs) and lowest unoccupied molecular orbitals (LUMOs) of tri-(but-3-en-1-yl)-phosphate are displayed in Figure 30.

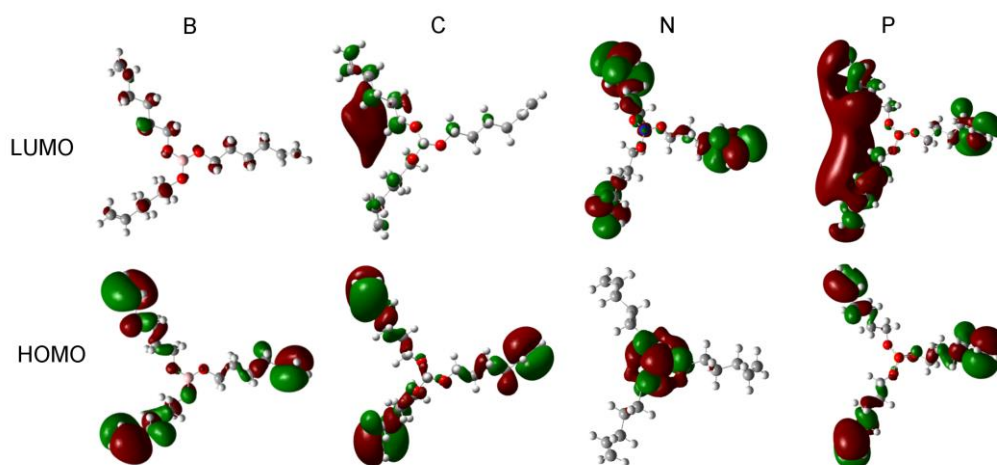


Figure 30. The distributions of HOMO and LUMO for tri-(but-3-en-1-yl)-phosphate. The central atom of the molecule is replaced with B, C, N and P. The positive and negative values are shown in green and red, respectively, with an isosurface value of ± 0.02 a.u.

In the case of B, C, and P, the HOMOs are mostly localized on the terminal C-C double bonds, while the N-substituted case is an exception and HOMO is localized on the lone pair of the central N atom. On the other hand, LUMOs are completely different, depending on the substituents.

The LUMO of the B-substituted molecule is completely delocalized with no specific preference, whereas C-substitution yields a more localized LUMO distribution between two branches. For the N-substituted molecule the LUMO is mainly localized on the terminal double bonds and decreasing towards the center. The most significant LUMO distribution is found for the P-substituted molecule: the LUMO is delocalized between two terminal C-C double bonds of two different side-chains of the molecule. Being the HOMO and the LUMO localized in the same region, tri-(but-3-en-1-yl)-phosphate is significantly more reactive than the counterparts with different substituents, thus resulting a more efficient oxygen scavenger. The energetics of the oxygen scavenging reaction and its atomistic mechanism have been also studied by first-principles calculations (Figure 31).

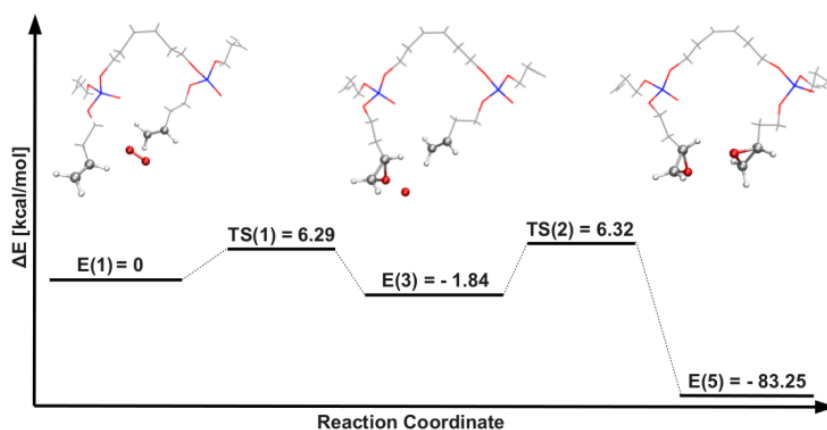


Figure 31. Computed reaction profile. Energies are in kcal/mol. Nonparticipating parts of the molecules into the reaction are omitted for clarity.

A tri-(but-3-en-1-yl)-phosphate dimer in *cis*- configuration is considered, interacting with an O_2 molecule excited in singlet state. Since the most reactive part of these molecules are the terminal double bonds, we considered the reaction of O_2 with the C=C bonds. The reaction occurs in two steps. The first step involves the reaction of O_2 with one of the terminal C=C double bonds so that a metastable intermediate configuration ((3) as shown in Figure 31). This step involves an activation barrier of 6.30 kcal/mol, and the intermediate has a relative energy of -1.84 kcal/mol with respect to the initial configuration. In the final product, the remaining oxygen atom is bonded

to the second C=C bond available. The second step is eased by the flexibility of the unsaturated side-chains. The formation of the final configuration is not only thermodynamically favored with an energy -83.3 kcal/mol with respect to the configuration but also kinetically accessible with an activation barrier of 6.3 kcal/mol. In order to support the theoretical calculations, “inversion recovery experiments” were used to measure the relaxation times of the protons, carbons and phosphorus (Figure 32).

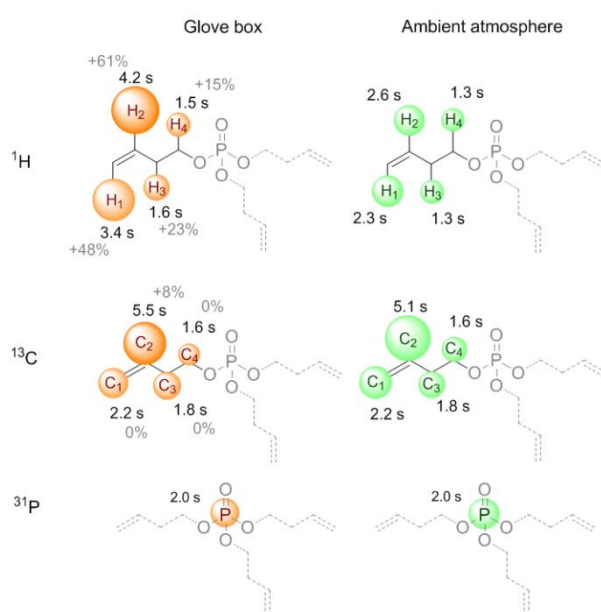


Figure 32: T_1 relaxation times of tri-(but-3-en-1-yl)-phosphate at different oxygen levels quantified by ^1H , ^{13}C and ^{31}P NMR (ambient atmosphere: 21% O_2 ; Glove-box: 2ppm O_2).

For the measurements, relaxation delays of 20 s for protons, 20 s for phosphorus and 40 s for the carbons were needed. The dipole interaction of the protons, carbons and phosphorus atoms with the unpaired spins of oxygen leads to a change in respective relaxation times depending on the distances of both. The measured relaxation times values of the double bond protons show a strong dependency on the oxygen concentration. The increased relaxation times of the butene-fragment by approximately 48% (H1), 61% (H2), 23% (H3) and 15% (H4) under glove box conditions (i.e. oxygen free) suggest a strong interaction with the partially paramagnetic oxygen for normal ambient atmosphere oxygen concentrations. The biggest effects are concentrated on the carbon-carbon

double bond, which suggests an interaction of the free electron pair of O₂ molecules with the π -orbitals of the double bond (Figure 32).

4.1.5 Upconversion in Organophosphates : Considerations

This work was developed through a collaboration between several departments at the Max Planck Institute for Polymer Research. Synthetically we designed, prepared and evaluated the mechanism of these new materials ; the group of Stanislav Baloushev characterized the systems described in upconversion applications, while Davide Donadio and Manfred Wagner supported us to explain the working mechanism of the materials. We demonstrate the application of a family of organic solvents, specially designed to enable the general long-term operation TTA-UC in ambient atmosphere.

This is a very significant step in pushing TTA-UC towards realization in a wide variety of applications. The identified organophosphates and polymers achieve UC efficiencies in ambient conditions just as high as the benchmark solvents in inert atmospheres. Simultaneously, the system introduces a huge excess of ‘sacrificial’ terminal double bonds to scavenge singlet oxygen. This leads to our clear experimental evidence for the long-lived TTA – UC in ambient atmosphere (over 1000 h). The identified family of organophosphates combines in a single material the obligatory parameters for sustainable TTA-UC operation in ambient atmosphere: low viscosity and sacrificial oxygen protection with pronounced long-term effect.

4.2 Flame Retardants

Flame retardants are a key component in reducing the devastating impact of fires on people, property and the environment. They are added to or treat potentially flammable materials, including textiles and plastics. The term “flame retardant” refers to a function, not a family of chemicals. A variety of different chemicals, with different properties and structures, act as flame retardants and these chemicals are often combined for effectiveness. These compounds can either be physically mixed with the base material (additive flame retardants) or chemically bonded to it (reactive flame retardants). Mineral flame retardants are typically additive while organohalogen and organophosphorus compounds can be either reactive or additive.¹⁰⁴

The annual consumption of flame retardants is currently over 1.5 million tonnes per year, which is the equivalent of a sales volume of approx. 1.9 billion Euro (2.4 billion US-\$). As of 2008 the United States, Europe and Asia have an annual consumption rate for flame retardants at 1.8 million metric tons and valued at \$4.20-4.25 billion dollars. According to the Ceresana Research, the market for flame retardants is increasing due to rising safety standards worldwide and the increase use of flame retardants. It is forecasted that the global flame retardant market will generate \$5.8 billion (US). As of 2010, the Asia-Pacific region was the largest market for flame retardants which was approximately 41% of global demand followed by North America, and Western Europe.

Brominated and chlorinated flame retarding materials have found to have very good flame retarding properties for a broad range of polymers. They work especially in the gas phase, where halogen radicals recombine with highly reactive hydrogen and hydroxyl radicals formed during combustion and pyrolysis.¹⁰⁵ Due to toxicological concerns and environmental issues, polychlorinated biphenyls were the first halogenated flame retardants to be banned in 1977. The attention has then gone towards polybrominated flame retardants. However, similar concerns have been raised for these kind of halogenated flame retardants.¹⁰⁶ Therefore, the trend moved towards environmentally friendlier and less toxic phosphorous flame retardants. Phosphorous based flame retardants equally work in the gas phase by scavenging of reactive radicals. In addition, phosphorous based flame retardants can act in the condensed phase where they induce charring and hence form

protective heat and gas barriers.¹⁰⁷ The leaching out of the flame retardants of the polymeric matrixes has been considered as problematic, since the flame retardants are often hazardous.¹⁰⁸ Blooming out can be prevented by the application of oligomeric and polymeric flame retardants, or by covalently attaching the flame retardants to the polymeric backbones.¹⁰⁹

4.2.1 Flame Retarding Mechanisms

Flame retardants are added to different materials or applied as a treatment to materials (e.g., textiles, plastics) to prevent fires from starting, limit the spread of fire and minimize fire damage. Some flame retardants work effectively on their own; others act as “synergists” to increase the fire protective benefits of other flame retardants. A variety of flame retardants is necessary because materials that need to be made fire-resistant are very different in their physical nature and chemical composition, so they behave differently during combustion. The elements in flame retardants also react differently with fire. As a result, flame retardants have to be matched appropriately to each type of material. Flame retardants work to stop or delay fire, but, depending on their chemical makeup, they interact at different stages of the fire cycle (Figure 33).¹¹⁰

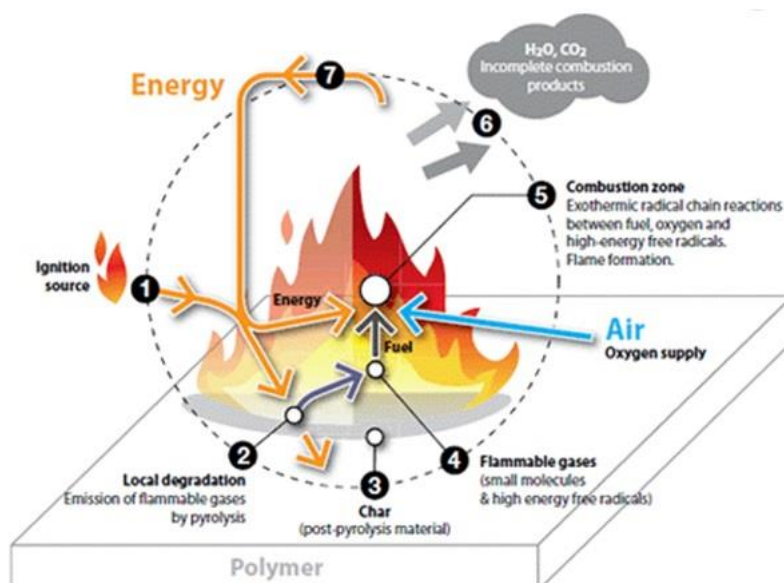


Figure 33 : The fire cycle.

Any energy source (heat, small flame or incandescent material) can be the initial ignition source(1). Energy transmitted by the ignition source to the polymer creates a degradation where pyrolysis takes place (2). Pyrolysis is a process that degrades the polymers long chain structure into smaller hydrocarbon molecules, the flammable gases (4), which are emitted to the gas phase. In the condensed phase, the result is an inert carbonized material, called “char”. In the gas phase, flammable gases are mixed with oxygen from the air. The proper mix of oxygen and fuel is reached in the combustion zone (5), where hundreds of exothermic chemical reactions take place involving high-energy free radicals, fuel and oxygen. A perfect combustion would theoretically produce H₂O and CO₂. In a real system, incomplete combustion products are also emitted during a fire (Polycyclic Aromatic Hydrocarbons, carbon monoxide, etc) (6). Energy (7) emitted during exothermic reactions is transmitted to the polymer and reinforces pyrolysis. This allows the reaction to sustain itself.

When flame retardants are present in the material, they can act in three key ways to stop the burning process. They may work to:

- ✚ Disrupt the combustion stage of a fire cycle, including avoiding or delaying “flashover” or the burst of flames that engulfs a room and makes it much more difficult to escape.
- ✚ Limit the process of decomposition by physically insulating the available fuel sources from the material source with a fire-resisting “char” layer.
- ✚ Dilute the flammable gases and oxygen concentrations in the flame formation zone by emitting water, nitrogen or other inert gases.

4.2.2 Phosphorous-based Flame Retardants

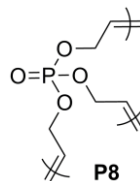
Phosphorous based flame retardants have become very popular as alternative to halogen containing flame retardants, due to environmental and health concerns rising for the corrosive and toxic decomposition products of for example brominated and chlorinated products.¹⁰⁵ There is a broad range of organic and inorganic phosphorous (like red phosphorous) based flame retardant

materials, since all oxidation states of phosphorus can be used for flame retarding purposes. Furthermore, polymeric organophosphorous systems have started to become increasingly important. Phosphorous containing flame retardants can act both in the gas phase and in the condensed phase. In the gas phase, they mainly act through flame inhibition by the formation of PO radicals that recombine with the very reactive hydrogen and hydroxy radicals, and thus interrupt the highly exothermic radical processes in the combustion zone.

The gas phase activity of phosphorous results in the reduction of the heat release.¹¹¹ However, flame inhibition results in incomplete combustion, yielding higher CO and smoke production. Furthermore, phosphorous based flame retardants can act in the condensed phase through the formation of protective char or a vitreous surface layer by the enhancement of charring and the formation of inorganic glasses, such as polyphosphates.¹¹² Phosphorous can promote charring in the condensed phase by dehydration of the polymer, which results in cyclisation reactions, by inducing cross-linking, and through aromatization.¹¹³

4.2.2.1 Hyperbranched Phosphorous Based Flame Retarding Materials

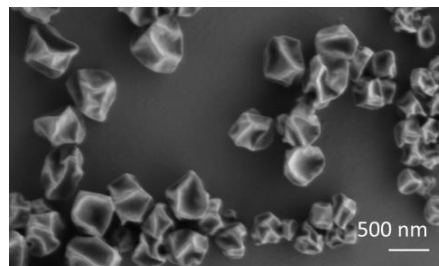
A new trend in the flame retarding community goes towards the use of polymeric flame retardants. One subgroup of these polymeric flame retardants is the domain of hyperbranched polymers. The hyperbranched polymers which have been reported as flame retardants are polysiloxanes,¹¹⁴ polyamines as charring agents,¹¹⁵ and polyphosphates.¹¹⁶ Especially the latter based on bisphenol-A and phosphoryl trichloride have been increasingly reported as reactive flame retardants in epoxy resins. Furthermore, hyperbranched polyphosphates also show gas phase activity, as the released PO radicals can scavenge reactive radicals from the gas phase. Central point of this work (In collaboration with Prof. Bernhard Schartel at the BAM of Berlin) has been the examination of the flame retarding properties of a novel hyperbranched allylic polyphosphate (Scheme 14), synthesized via Acyclic diene metathesis (ADMET) as described above in chapter 3.4.



Scheme 15. Polymer tested as flame retardant.

The molecular weight (Mw) of **P8** is 2500 g/mol, containing 12 wt% of phosphorous. **P8** with its aliphatic backbone and its phosphate groups is a promising flame retardant with good performances in PC, PET and epoxy resins. Its phosphate groups can on the one hand decompose to yield PO radicals, scavenging H and OH radicals in the gas phase. The temperature of the flame is therefore reduced. On the other hand, the phosphate groups can decompose into acid derivatives, which catalyze the formation of char from either its own polymeric backbone or the polymeric backbone of the matrix. In addition, the phosphate groups can have cross-linking abilities with the matrix, further increasing the amount of residue. The phosphate functionalities may also withdraw water from the pyrolysis zone and hence reduce polymer decomposition by hydrolysis. **P8** is thus a highly effective multifunctional novel flame retardant (Masterarbeit Hyperbranched Polyphosphates as novel Flame Retarding Materials, KAROLINE TÄUBER, Freie Universität Berlin).

4.3 Olefin Metathesis for the Preparation of Hollow Nanocapsules



The following work (Selective Interfacial Olefin Cross Metathesis for the Preparation of Degradable Nanocapsules. *ACS Macro Lett.* **2014**, 3, 40) was carried on in in collaboration with Kerstin Malzahn and Clemens K. Weiss (both MPIP). Synthetically we developed the first synthesis of hollow nanocapsules with an aqueous core via olefin cross metathesis. The reaction was tailored that it proceeds selectively at the oil-water interface of aqueous nanodroplets in an inverse miniemulsion (Figure 34). The cross metathesis takes place between an acrylated polysaccharide and unsaturated organophosphates under mild conditions.

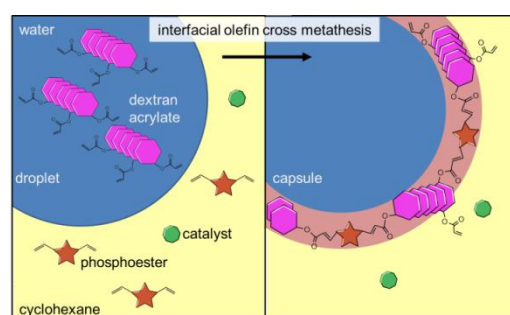
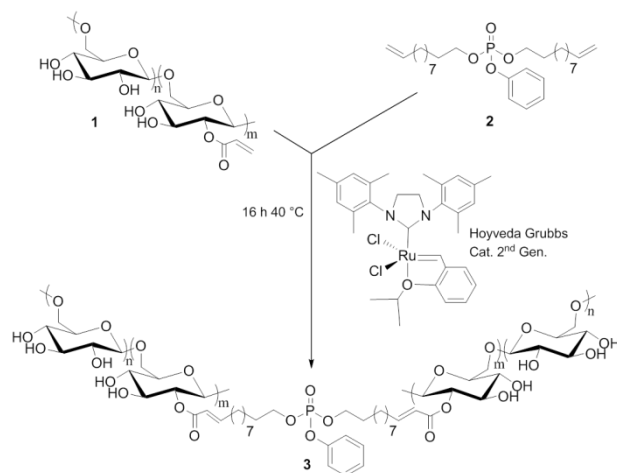


Figure 34. Schematic representation of the interfacial olefin cross metathesis at the water-oil interface of a nanodroplet in an inverse miniemulsion process for the formation of stable nanocapsules.

This general protocol allows the synthesis of biocompatible and polyfunctional nanocapsules via the bioorthogonal olefin metathesis, thus generating a highly versatile methodology for the design of future materials for biomedical applications, but also for materials science. Functionalization of the nanocapsules was demonstrated with fluorescent labels which can be either attached to the pendant phosphoester within the crosslinker, exploiting the versatility of the phosphorus chemistry, or via coupling to the capsules' surface.



Scheme 16. Schematic representation of the interfacial reaction between acrylated dextran (1) and phenyl-di(dec-10-en-1-yl)-phosphate (2) leading to a cross-linked polymer network (3).

The polymer obtained (Scheme 16) after the capsule formation was insoluble in all common solvents, which indicated that DexA was cross-linked during the reaction, as expected. Accordingly, direct proof that metathesis reaction occurred can only be demonstrated via ^{13}C and ^{31}P solid state NMR. Prior to NMR analysis a soxhlet extraction with methanol and dichloro-methane (good solvents for monomer and homopolymer respectively) was performed to purify the capsules from unbound material and residual monomer. No polymeric material was recovered in the organic solvent. The ^{31}P NMR spectrum unambiguously confirms the incorporation of the phosphate into the cross-linked polymer (Figure 35) showing a resonance for the phosphoester at -7.7 ppm.

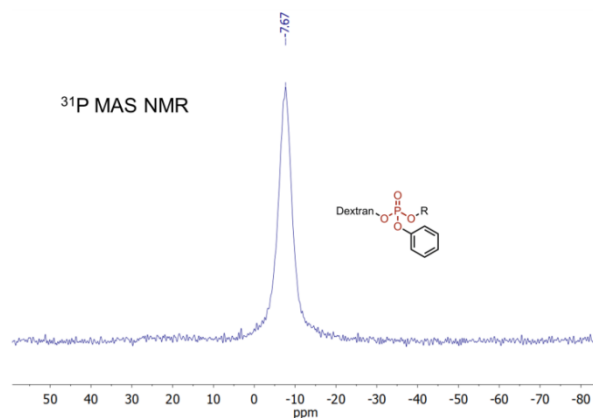


Figure 35. ^{31}P solid state NMR spectra of the nanocapsules.

In conclusion, the first nanocapsules with an aqueous core prepared by olefin metathesis are presented. This convenient protocol allows a mild bio-orthogonal crosslinking of degradable and biocompatible polymers at the oil-water interface. It combines two materials with high potential for future applications: Polyphosphoesters and polysaccharides, here dextran, which are known for their biocompatibility and degradability.

4.4 Tissue Engineering

Taking advantages of the synthetic approach developed, we developed with basic commercial available starting compounds new suitable Polyphosphoesters for different kind of applications (Paclitaxel-loaded polyphosphate nanoparticles: a potential strategy for bone cancer treatment. *J. Mater. Chem. B*, **2014**). The viability of our methods can find breeding grounds also in a classical application for synthetic polyphosphates, since they were used from the beginning (see introduction) as polymers to build drug delivery systems because of their similarity to DNA.

In collaboration with Evando Alexandrino and Sandra Ritz, we tested at the MPIP some of the polymers synthesized and described in this thesis work, for the preparation of polyphosphate nanoparticles loaded with Paclitaxel by the simple miniemulsion/solvent-evaporation technique as a model for chemotherapeutic delivery (Figure 36). This first report demonstrates how polyphosphate **P5** can be a promising material for the development of systemic or local bone cancer treatment, even by direct application or by formation of composites with calcium phosphate cements.

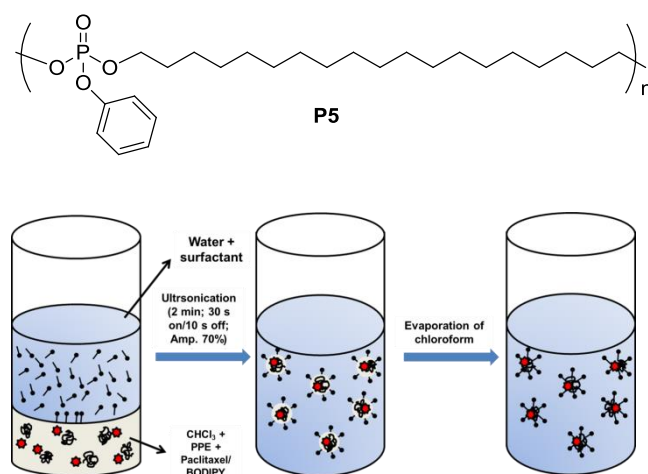


Figure 36. Top) Structure of polyphosphoester **P5** used. Down) miniemulsion/solvent-evaporation protocol used for the production of BODIPY loaded PPE nanoparticles.

This versatility allows the development of new degradable polymeric carriers with inherent bone targeting adhesion ability by the interaction of the nanoparticles with a calcium phosphate material used for bone regeneration (Figure 37). The novel polyphosphate nanoparticles were investigated in detail further proven to be efficiently loaded with different hydrophobic drugs (up to 15 wt%).

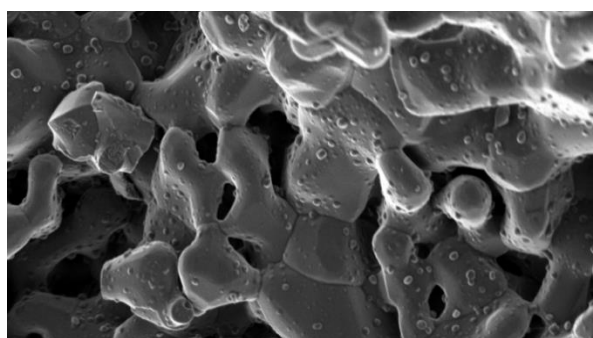


Figure 37. Scanning electron images (scale bar 2 μm) of the calcium phosphate cement after exposition to a dispersion of nanoparticles of **P5**.

Bone as a site of cancer growth can be either by: bone sarcomas, which include osteosarcoma and Ewing's sarcoma,¹¹⁷ or - more common - it can be a consequence of other tumors that spread by metastasis to the bone tissue.¹¹⁸ Among the types of cancer that spread by metastases to the bone tissue, breast and prostate cancer stand out, presenting metastases in approximately 70% - 80% in advanced stages of the disease.¹¹⁸ The most common treatment for primary bone tumors or bone metastases is a combination of different techniques, such as surgical removal, fixation and chemotherapy, treatment with radioisotopes or by radiation strategies.¹¹⁹ We introduced a new class of potentially biodegradable and biocompatible syntetic polyphosphates that can be used to develop nanoparticles with inherent bone targeting adhesion abilities. In vitro studies also proved that the polyphosphate nanoparticles are non-toxic against HeLa cells for concentrations up to 600 $\mu\text{g ml}^{-1}$ or 300 $\mu\text{g ml}^{-1}$, respectively, and that the polyphosphate nanoparticles loaded with Paclitaxel exhibit a similar cytotoxicity as the commercial available Taxomedac® against osteosarcoma cells. Further studies are in progress to understand the drug transfer mechanism, material degradation as well as in vivo validation are required to assess the potential for a clinical application.

Chapter 5

Thiol-ene Addition, Alternative Routes



5.1 An Alternative Route for Synthetic Poly(phosphoester)s

With this thesis we focused on the preparation of novel synthetic poly(phosphoester)s by using olefin metathesis as unique and highly versatile polymerization technique. This approach allowed us to build different architectures for different kind of applications, considering that all the materials have the phosphate as unit in the main chain. After modifying the polymer backbone but also the functionalities, in order to tailor the degradability of our system, it was interesting also the modification of the phosphate group in the polymer chains. Synthetically this idea was reflected into a poly(phosphoester) system by changing the phosphate structure, with poly(phosphoramidate) ones, in this case in the main chain (Figure 39).

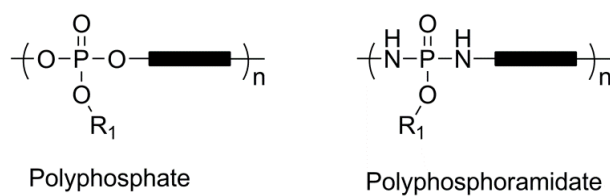


Figure 38. Poly(phosphate)s, poly(phosphoramidate)s.

Recently, Wooley et al. demonstrated how poly(phosphoramidate)s having side groups connecting to a phosphoester backbone through a phosphoramidate bond, can be easily cleaved by acids.^{25b} These acid-label materials, motivated us to synthesize poly(phosphoramidate)s with phosphoramidate bonds in the main-chain, in order to increase the degradability of these polymers. Ideally, following our synthetic approach developed, we based our polymerizations on olefin metathesis by preparing monomer **12** as model system for polyphosphoramidates with a short and degradable main chain (Figure 40).

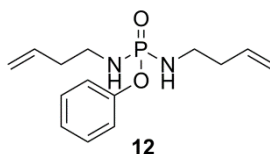


Figure 39. Model monomer **12** based on 3-buten-1-amine.

Surprisingly, the metathesis polymerizations of **12** did not give any polymeric material by using the analogues conditions for the synthesis of all the other poly(phosphate)s, probably due to catalyst coordination. For this reason, keeping robustness and efficiency, as alternative polymerization route based on double-bonds reactivity we thought about a thiol-ene addition reaction as strategy to make **12** a valuable monomer.

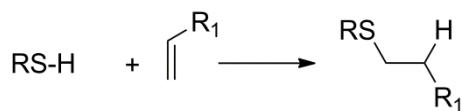
5.1.1 Thiol-ene Addition

Thiol-ene addition reactions are known for more than a century.¹²⁰ The reaction is well known to proceed via a radical mechanism.¹²¹ Generally, radical reactions are known to be quite fast reactions, and thiol-ene additions offer some additional features such as orthogonality, which have made this reaction to be considered as one of the click reactions and very popular during the last years.¹²² Although the efficiency of this reaction requires the unsaturation in the terminal position and strongly depends on the thiol compound used,¹²³ it has been successfully used for a large number of end- and side-group functionalizations.¹²⁴ Noteworthy, this reaction is not limited to alkenes, but alkyne compounds can also be used.

A “click” reaction, as defined by Kolb et al.,¹²⁵ is one that is modular, wide in scope, gives (nearly) quantitative yields, generates inoffensive (if any) byproducts that are easily removed by non-chromatographic methods and is stereospecific. From a practical standpoint, such reactions should be simple to perform and preferably be insensitive to water and oxygen, be accomplished with readily available starting materials and reagents, be performed under solventless conditions or in environmentally benign media such as water and facilitate simple product isolation. The attention has recently been paid to a series of thiol-based reactions including the thiol-ene,¹²⁶ thiol-alkyne,¹²⁷ thiol-isocyanate,¹²⁸ thiol-para-fluorostyrene¹²⁹ and thiol-bromoprocesses.¹³⁰

The term “thiol-ene” is used to denote the addition of a thiol to an olefin (“ene”) regardless of reaction mechanism. The thiol-ene reaction is, simply, the hydrothiolation of a C-C double bond, Scheme 18. Historically, in the materials science field the reaction has been most widely em-

ployed as a means of preparing near-perfect networks and films as exemplified by the work of Hoyle and co-workers,¹³¹ and Bowman et al.¹³²

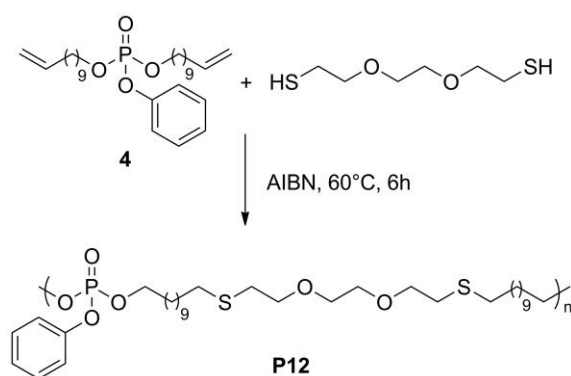


Scheme 17. The hydrothiolation of C-C double bond with anti-Markonikov orientation.

There are several features associated with the thiol-ene reaction that make it a particularly attractive, facile and versatile process.

- ✚ Hydrothiolation reactions can proceed under a variety of conditions including by a radical pathway,¹³³ via catalytic processes mediated by nucleophiles, acids, bases,¹³⁴ in the apparent absence of an added catalyst in highly polar solvents such as water or DMF.¹³⁵
- ✚ A wide range of enes serve as suitable substrates, including activated and non-activated species as well as multiply-substituted olefinic bonds. However, reactivity can vary considerably depending on the reaction mechanism and substitution pattern at the C-C double bond.
- ✚ Virtually any thiol can be employed, including highly functional species, although reactivity can cover several orders of magnitude depending on the S-H bond strength and the cleavage mechanism, i.e. homolytic vs. heterolytic lysis.
- ✚ These reactions are generally extremely rapid and can be complete in a matter of seconds (even at ambient temperature and pressure), are tolerant to the presence of air/oxygen and moisture (provided the concentration of oxygen does not approach that of the thiol), and proceed with (almost) quantitative formation of the corresponding thioether in a regioselective fashion.

Generally, the thiol-ene reaction has been conducted via a radical mechanism, often photochemically induced. Under such conditions it proceeds via a typical chain process with initiation, propagation and termination steps. Initiation involves the treatment of a thiol with an initiator, resulting in the formation of a thiyl radical, plus other byproducts. Simple thermalysis of the S-H bond can also be employed as a means of generating thiyl radicals.¹³⁶ Propagation is a two step process involving first the direct addition of the thiyl radical across the C-C double bond yielding an intermediate carboncentred radical followed by chain transfer to a second molecule of thiol to give the thiol-ene addition product, with anti-Markovnikov orientation, with the concomitant generation of a new thiyl radical. Possible termination reactions involve typical radical-radical coupling processes. To test the performance of the thiol-ene reaction for the synthesis of PPEs, phenyl-dodecyl-undecylenyl-phosphate **4** was polymerized via thiol-ene addition by using the inexpensive commercially available triglycoldimercaptan as described in Scheme 19. The reaction under the given conditions gave quantitatively polymer **P12** (M_n 20,000, PDI=2. GPC in THF vs polystyrene). The colourless polymer obtained ($T_g = -12$ °C) showed good solubility in common organic solvents such as CH_2Cl_2 or THF, while can be purified after reprecipitating in hexane or methanol.



Scheme 18. Synthesis of polymer **P12** via thiol-ene addition.

While we only recently recognized and exploited as a “click” process, the polymerization of **4**, in both its metathesis and thiol-ene forms, has already been demonstrated to be a powerful and versatile method for site specific functionalization as a convenient conjugation tool.

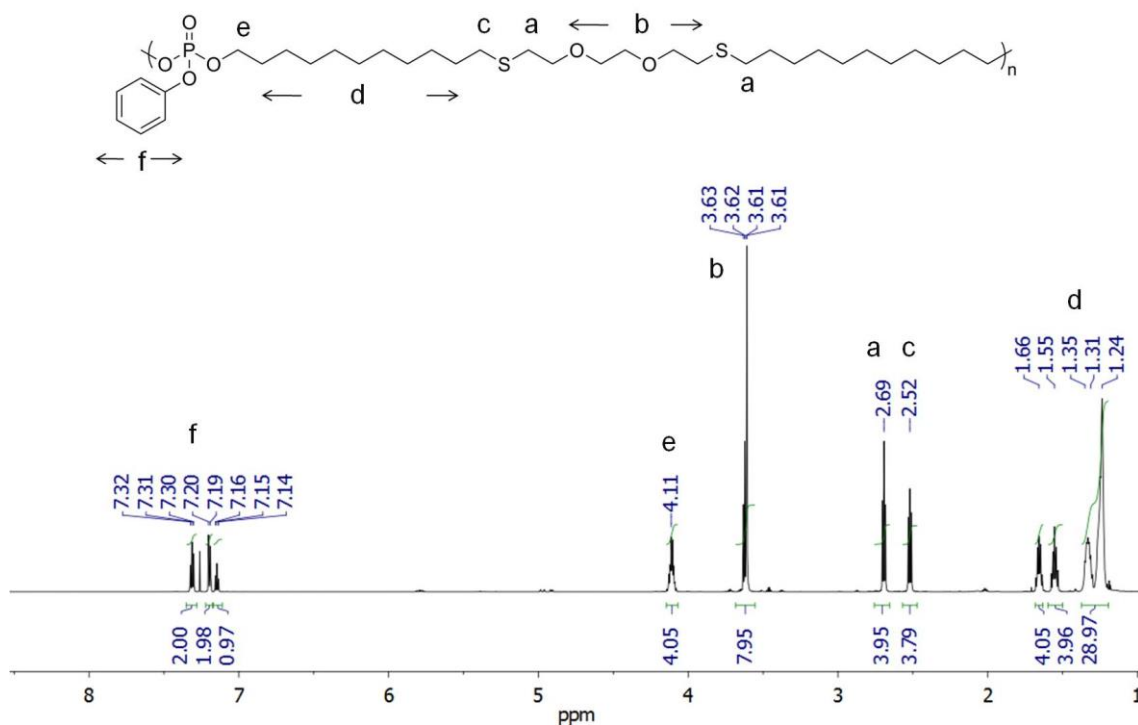
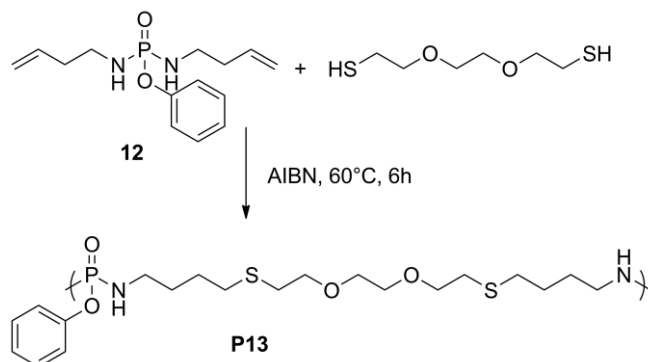


Figure 40. ^1H NMR spectrum, 700 MHz of. polymer **P12**.

The combination of phosphorus chemistry and thiol-ene additions open a breeding field for the preparation of novel degradable polymers where the backbone can be tailored easily by varying the di-thiol, while the side chain on the phosphorous atom can be designed before on the monomer (Figure 40). In a similar way proceed the polymerization via the thiol-ene addition of monomer **12** for the preparation of polyphosphoramides in the main chain (Scheme 19).



Scheme 19. Synthesis of polymer **P13**.

Colorless polymer **P13**, was obtained with a maximum molecular weight M_n of 8,000 and a polydispersity of 2. The structure can be resolved easily by $^1\text{H-NMR}$ (Figure 41). Given that research efforts are still in their infancy with respect to exploiting this reaction in materials synthesis, it is likely that its true potential has yet to be realized. Actually, our research group is focusing in some preliminary test to understand the behavior and applicability of these polymers as biomaterials, evaluating their degradability and biocompatibility.

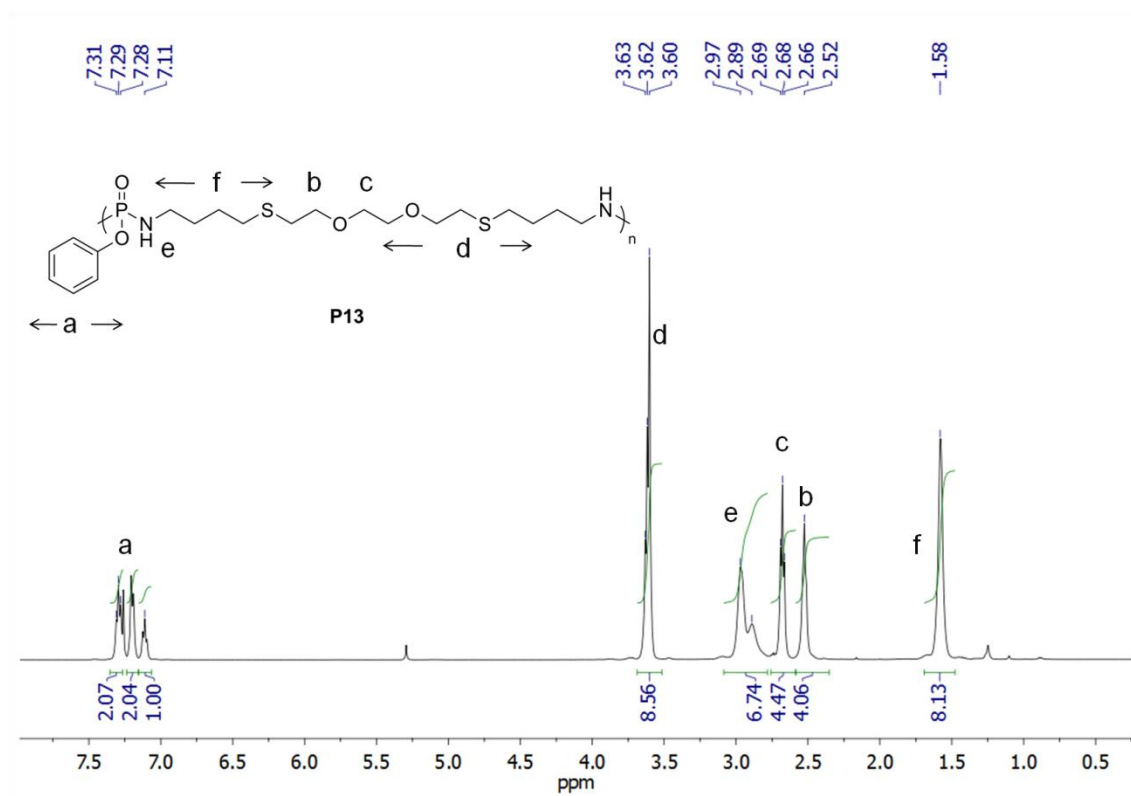


Figure 41. $^1\text{H-NMR}$ spectrum, 500 MHz of polymer **P13**.

Chapter 6

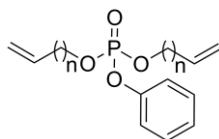
Experimental Section

Outline

The following chapter describes the synthesis and novel compounds and materials presented in this thesis work. Intermediates, monomers and polymers will be described through general procedures with their corresponding characterizations and spectroscopic data.

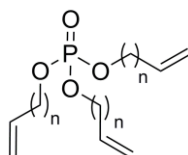
- General procedure a for the synthesis of phenyl-di-(alkenyl)-phosphate
- General procedure b for the synthesis of tri-(alkenyl)-phosphate
- Representative procedures for metathesis polymerizations
- Data for intermediates, polymerizable organophosphates and BODIPY dyes
- Data for polymers

General Procedure (a) for the Synthesis of Phenyl-di-(alkenyl)-phosphate.



To a dried three-necked, 250 mL round bottom flask fitted with a dropping funnel, 0.1 mol of the appropriate alcohol and 0.1 mol of triethylamine were added under argon atmosphere in 80 mL of dry CH_2Cl_2 . Then 0.05 mol of phenyl dichlorophosphate dissolved in 20 mL of dry CH_2Cl_2 were added dropwise to the above flask at 0 °C. Then, the reaction was allowed to warm up to room temperature and stirred for an additional 12 h. The mixture was concentrated under reduced pressure, dissolved in diethyl ether and filtered. The crude was washed twice with brine and the organic layer was dried over anhydrous sodium sulfate, filtered, and concentrated in vacuo. The compounds were purified by chromatography over neutral alumina (or silica) using dichloromethane as eluent or by distillation under reduced pressure to give clear oils. The structures were determined by ^1H NMR, ^{13}C NMR, ^{31}P NMR spectroscopy as well as electrospray ionization mass spectrometry (ESI-MS).

General Procedure **(b)** for the Synthesis of Tri-(alkenyl)-phosphate.



To a dried three-necked, 250 mL round bottom flask fitted with a dropping funnel, 0.1 mol of the appropriate alcohol and 0.1 mol of triethylamine were added under argon atmosphere in 80 mL of dry CH₂Cl₂. Then 0.03 mol of phosphoryl chloride dissolved in 20 mL of dry CH₂Cl₂ were added dropwise to the above flask at 0 °C. Then, the reaction was allowed to warm up to room temperature and stirred for additional 12 h. The mixture was concentrated under reduced pressure, dissolved in diethyl ether and filtered. The crude was washed twice with brine and the organic layer was dried over anhydrous sodium sulfate, filtered, and concentrated *in vacuo*. The compounds were purified by chromatography over neutral alumina (or silica) using dichloromethane as eluent or by distillation under reduced pressure to give clear, colorless oils. The purity and chemical structure was determined by ¹H NMR, ¹³C NMR, ³¹P NMR spectroscopy as well as electrospray ionization mass spectrometry (ESI-MS).

Representative Procedures for Metathesis Polymerizations.

ADMET in bulk. In a dry Schlenk tube fitted with a magnetic stirring bar, the monomer (2 mL) was placed under an argon atmosphere. Temperature was raised up to 60 °C, and the appropriate catalyst (0.5 mol%) was suddenly added. After ethylene started to evolve, a controlled vacuum of $5 \cdot 10^{-2}$ mbar was applied to remove the condensate. After 8-12 h, the reaction was cooled to room temperature, diluted with a solution containing tris(hydroxymethyl)phosphine (5 mol%), triethylamine (5 mol%) in 10 mL of dry CH_2Cl_2 , and stirred for 1 h. Then water was added and stirring was continued for an additional 1 h to decolorize the brownish solution. The mixture was extracted with CH_2Cl_2 and washed twice with brine. The organic layer was dried over anhydrous sodium sulfate, filtered, and concentrated in vacuo. The polymer, obtained with a quantitative yield, is then dissolved in the minimum volume of chloroform and precipitated into hexane or methanol (which is a non-solvent for the polymer, but a good solvent for both monomers) when requested, and dried.

ADMET Reaction in solution. The monomer (100 mg) and the Grubbs' catalyst (0.2 mol%) were dissolved in CH_2Cl_2 (2 mL) or toluene under argon atmosphere and stirred at 40 °C for 12 h. The same procedure as described for the reaction in bulk was used to isolate the polymer.

Telechelic UPPEs. In an argon atmosphere the monomer (200 mg), appropriate CTR (amount depend on the ratio between monomer and CTR) and Grubbs catalyst 1st generation (0.4 mol%) were placed in a glass Schlenk tube equipped with a magnetic stir bar. The reaction was carried out under intermittent vacuum ($\sim 10^{-1}$ mbar) at room temperature for the 24 h or until gas evolution decreased. From then on high vacuum ($< 10^{-3}$ mbar) was applied. The temperature was increased to 45 °C on the 2nd day and 50 °C for further 2 days. The mixture gradually became more viscous. The reaction was removed from the Schlenk line on the fourth day. The work up procedure described for ADMET bulk polymerization was used (yield: 90-95%).

Synthesis of phenyl-diallyl-phosphate (1). Following the general procedure(A) described above and using allyl alcohol, phenyl-diallyl-phosphate was obtained as a clear oil with a yield of 75% after column chromatography over silica using as eluent dichloromethane (R_f : 0.3). ^1H NMR (700 MHz, CDCl_3) δ : 7.31(t, $J = 7.7$ Hz = 2H), 7.21(d, $J = 7.7$ Hz, 2H), 7.16(t, $J = 7.7$ Hz, 1H), 5.94-5.89 (ddt, $J = 18$ Hz, $J = 10.5$ Hz, $J = 5.6$ Hz, 2H), 5.35 (ddt, $J = 18$ Hz, $J = 1.4$ Hz, 2H), 5.23 (d, $J = 10.5$ Hz, 2H), 4.65-4.59 (m, 4H). ^{13}C NMR (176 MHz, CDCl_3): 150.70, 150.66, 132.18, 132.14, 129.77, 125.17, 120.10, 120.08, 118.64, 68.86, 68.83. ^{31}P NMR (283 MHz, CDCl_3) δ : -6.20. ESI-MS (m/z): 277.05 $[\text{M}+\text{Na}]^+$, 531.14 $[2\text{M}+\text{Na}]^+$ (Calcd for $\text{C}_{12}\text{H}_{15}\text{O}_4\text{P}$: 254.07).

Synthesis of phenyl-di-(3-buten-1-yl)-phosphate (2). Following the general procedure(A) described above and using 3-buten-1-ol, phenyl-di-(3-buten-1-yl)-phosphate was obtained as a clear oil with a yield of 70% after column chromatography over silica using as eluent dichloromethane (R_f : 0.3). ^1H NMR (500 MHz, CDCl_3) δ : 7.33-7.31 (m, = 2H), 7.20 (d, $J = 7.7$ Hz, 2H), 7.16(t, $J = 7.7$ Hz, 1H), 5.79-5.73 (ddt, $J = 16.8$ Hz, $J = 10$ Hz, $J = 3.5$ Hz, 2H), 5.11 (ddt, $J = 16.8$ Hz, $J = 1.4$ Hz, 2H), 5.08 (d, $J = 10$ Hz, 2H), 4.20-4.13 (m, 4H), 2.44-2.42 (m, 4H). ^{13}C NMR (176 MHz, CDCl_3): 150.69, 150.65, 133.12, 129.70, 125.05, 120.04, 120.01, 117.91, 67.54, 67.50, 34.60, 34.56. ^{31}P NMR (283 MHz, CDCl_3) δ : -6.40. ESI-MS (m/z): 305.07 $[\text{M}+\text{Na}]^+$, 587.18 $[2\text{M}+\text{Na}]^+$ (Calcd for $\text{C}_{14}\text{H}_{19}\text{O}_4\text{P}$: 282.10).

Synthesis of phenyl-di-(4-penten-1-yl)-phosphate. Following the general procedure(A) described above and using 4-penten-1-ol, phenyl-di-(4-penten-1-yl)-phosphate was obtained as a clear oil with a yield of 75% after column chromatography over neutral alumina using as eluent dichloromethane (R_f : 0.8). ^1H NMR (500 MHz, CDCl_3) δ : 7.33 (t, $J = 7.7$ Hz = 2H), 7.21(d, $J = 7.7$ Hz, 2H), 7.16(t, $J = 7$ Hz, 1H), 5.77(m, 2H), 5.04-4.98 (m, 4H), 4.15 (m, 4H), 2.16-2.11 (m, 4H), 1.81-1.76 (m, 4H). ^{13}C NMR (126 MHz, CDCl_3): 150.92, 150.87, 137.21, 129.83, 125.12, 120.12, 120.09, 115.72, 67.95, 67.90, 29.60, 29.54, 29.48. ^{31}P NMR (202 MHz, CDCl_3) δ : -6.17. ESI-MS (m/z): 333.31 $[\text{M}+\text{Na}]^+$, 643.64 $[2\text{M}+\text{Na}]^+$ (Calcd for $\text{C}_{16}\text{H}_{23}\text{O}_4\text{P}$: 310.33).

Synthesis of phenyl-di-(5-hexenyloxy)-phosphate(3). Following the general procedure (A) described above and using 5-hexen-1-ol, phenyl-di-(5-hexenyloxy)-phosphate was obtained as a clear oil with a yield of 75% after column chromatography over silica using as eluent dichloromethane (R_f : 0.4). ^1H NMR (500 MHz, CDCl_3) δ : 7.32 (t, $J = 7.7$ Hz = 2H), 7.21(d, $J = 7.7$ Hz, 2H), 7.16(t, $J = 7$ Hz, 1H), 5.79-5.73 (ddt, $J = 16.8$ Hz, $J = 10.5$ Hz, $J = 3.5$ Hz, 2H), 5.00-4.94 (ddt, $J = 16.8$ Hz, $J = 1.4$ Hz, 2H), 4.96-4.95 (m, 2H), 4.14 (m, 4H), 2.07-2.04 (m, 4H), 1.71-1.63 (m, 4H), 1.46 (q, $J = 7.7$ Hz, 4H). ^{13}C NMR (126 MHz, CDCl_3): 150.89, 150.86, 138.29, 129.80, 125.08, 120.08, 115.05, 68.47, 68.43, 33.21, 29.74, 29.70, 24.74. ^{31}P NMR (202 MHz, CDCl_3) δ : -6.11. ESI-MS (m/z): 361.16 $[\text{M}+\text{Na}]^+$, 699.30 $[2\text{M}+\text{Na}]^+$, 1277.48 $[3\text{M}+\text{Na}]^+$ (Calcd for $\text{C}_{18}\text{H}_{27}\text{O}_4\text{P}$: 338.16).

Synthesis of phenyl-di-(7-octen-1-yl)-phosphate. Following the general procedure(A) described above and using 7-octen-1-ol, phenyl-di-(7-octen-1-yl)-phosphate was obtained as a clear oil with a yield of 65% after column chromatography over silica using as eluent dichloromethane (R_f : 0.6). ^1H NMR (500 MHz, CDCl_3) δ : 7.33 (m, 2H), 7.22-7.15(m, 3H), 5.79 (m, 2H), 5.00-4.92 (m, 4H), 4.12 (m, 4H), 2.03 (m, 4H), 1.68(m, 4H), 1.38-1.30 (br, 12H). ^{13}C NMR (126 MHz, CDCl_3): 150.99, 150.93, 139.03, 129.80, 125.06, 120.13, 120.09, 114.49, 68.66, 68.62, 33.77, 30.34, 30.28, 28.86, 28.69, 25.38. ^{31}P NMR (202 MHz, CDCl_3) δ : -6.11. ESI-MS (m/z): 417.22 $[\text{M}+\text{Na}]^+$, 811.44 $[2\text{M}+\text{Na}]^+$ (Calcd for $\text{C}_{22}\text{H}_{35}\text{O}_4\text{P}$: 394.23).

Synthesis of phenyl-di-(undec-10-en-1-yl)-phosphate(4). Following the general procedure(A) described above and using 10-undecen-1-ol, phenyl-di(undec-10-en-1-yl)-phosphate was obtained as a clear oil with a yield of 80% after column chromatography over neutral alumina using as eluent dichloromethane (R_f : 0.7). ^1H NMR (700 MHz, CDCl_3) δ : 7.32 (t, $J = 7.7$ Hz = 2H), 7.21(d, $J = 7.7$ Hz, 2H), 7.16(t, $J = 7.7$ Hz, 1H), 5.83-5.77 (ddt, $J = 16.8$ Hz, $J = 10$ Hz, $J = 3.5$ Hz, 2H), 5.00-4.97 (ddt, $J = 10$ Hz, $J = 3.5$ Hz, $J = 1.4$ Hz, 2H), 4.93-4.91 (ddt, $J = 10$ Hz, $J = 1.4$ Hz, 2H), 4.16-4.09 (m, 4H), 2.04-2.01 (m, 2H), 1.69-1.65 (m, 4H), 1.39-1.32 (m, 8H), 1.26 (m, 18H). ^{13}C NMR (176 MHz, CDCl_3) δ : 150.98, 150.94, 139.29, 129.77, 125.02, 120.10, 114.27, 68.69, 68.66, 33.93, 30.37, 30.33, 29.55, 29.04. ^{31}P NMR (283 MHz, CDCl_3) δ : -6.11. ESI-MS (m/z): 501.33 $[\text{M}+\text{Na}]^+$, 979.67 $[2\text{M}+\text{Na}]^+$, 1458.00 $[3\text{M}+\text{Na}]^+$ (calcd for $\text{C}_{28}\text{H}_{47}\text{NaO}_4\text{P}$: 501.31).

Synthesis of 4-Formylphenyl Phosphorodichloridate. A solution of triethylamine (5.7 mL, 0.041 mmol, 1.0 eq) in methylene chloride (10 mL) was added dropwise to a mixture at 0 °C of 4-hydroxybenzaldehyde (5 g, 0.041 mol, 1.0 eq) and POCl₃ (38 mL, 0.41 mol, 10 eq) in methylene chloride (100 mL) under an argon atmosphere. The mixture was stirred then additionally at r.t. for 1 h. Subsequently the crude was concentrated under reduced pressure, 50 mL of diethyl ether were added, and the mixture was filtered to remove precipitates. The solvents and the excess of POCl₃ were removed in vacuo (<10⁻² mbar). A yellowish viscous oil was obtained with a yield of 7.8 g (60%). The compound was used without further purification. ¹H NMR (500 MHz, CDCl₃) δ: 10.03 (s, 1H), 7.98 (d, *J* = 9 Hz, 2H), 7.49 (d, *J* = 9 Hz, 2H). ¹³C NMR (126 MHz, CDCl₃) δ: 190.31, 153.60, 134.86, 131.92, 127.35, 121.32. ³¹P NMR (202 MHz, CDCl₃) δ: 3.10.

Synthesis of 4-(10-undecenyloxy)benzaldehyde. To a solution of 4-hydroxybenzaldehyde (3 g, 0.024 mol, 1.0 eq), undecylenyl alcohol (5.4 mL, 0.027 mol, 1.1 eq) and triphenylphosphine (7 g, 0.027 mol, 1.1 eq) in anhydrous THF (100 mL) was added dropwise a THF solution of diethyl azodicarboxylate (DEAD) (4.2 mL, 0.027 mol, 1.1 eq in 50 mL). After stirring for 20-24 h at room temperature, the reaction mixture was concentrated and the crude directly purified by column chromatography on silica gel (elution with dichloromethane, *R_f*: 0.7). The pure product was isolated as a colorless oil (yield 5.9 g, 90%). ¹H NMR (500 MHz, CDCl₃) δ: 9.9 (s, 1H), 7.85 (d, *J* = 8.5 Hz, 2H), 7.01 (d, *J* = 8.5 Hz, 2H), 5.84 (m, 1H), 4.97 (m, 2H), 4.06 (t, *J* = 6.5 Hz, 2H), 2.06 (q, *J* = 6.5 Hz, 2H), 1.83 (quin, *J* = 6.5 Hz, 2H), 1.5-1.3 (br, 12H). ¹³C NMR (126 MHz, CDCl₃) δ: 190.93, 164.40, 139.31, 132.12, 129.88, 114.88, 114.28, 68.56, 33.93, 29.61, 29.54, 29.45, 29.24, 29.19, 29.05, 26.09.

Synthesis of 4-formylphenyl-di-(10-undecenyloxy)phosphate (5). To a dried three-necked 250 mL round bottom flask, 5 g (0.021 mmol, 1.0 eq) of 4-Formylphenyl Phosphorodichloridate dissolved in dry methylene chloride (100 mL) were added under an argon atmosphere. To the solution above, which was cooled to 0 °C, 10-undecen-1-ol (8.8 mL, 0.044 mol, 2.1 eq) and triethylamine (6.1 mL, 0.044 mmol, 2.1 eq) were added slowly with a syringe through a septum. Then, the reaction was stirred for 1 h at 0 °C and additionally 24 h at room temperature, before the mixture was concentrated under reduced pressure, dissolved in diethyl ether and filtered. The

crude was washed twice with brine, dried over anhydrous sodium sulfate, filtered and concentrated in vacuo. The compound was purified by chromatography over silica using dichloromethane as eluent to give a clear viscous oil (R_f : 0.2). Yield: 7.4 g (70%). ^1H NMR (700 MHz, CDCl_3) δ : 9.97 (s, 1H), 7.88 (d, J = 8.5 Hz, 2H), 7.38 (d, J = 8.5 Hz, 2H), 5.82-5.77 (m, 2H), 5.00-4.97 (m, 2H), 4.93-4.91(m, 2H), 4.15(q, J = 6.5 Hz, 4H), 2.01 (q, J = 7 Hz, 4H), 1.69 (qui, J = 7 Hz, 4H), 1.38-1.32 (br, 8H), 1.26 (br, 16H). ^{13}C NMR (176 MHz, CDCl_3) δ : 190.84, 155.70, 155.66, 139.29, 139.27, 133.35, 131.78, 120.66, 120.63, 114.30, 69.11, 69.07, 33.92, 30.35, 30.31, 29.56, 29.51, 29.22, 29.19, 29.04, 25.50. ^{31}P NMR (283 MHz, CDCl_3) δ : -6.80. MS-ESI (m/z): 507.34 $[\text{M}+\text{H}]^+$ (calcd. for $\text{C}_{29}\text{H}_{48}\text{O}_5\text{P}$: 507.32).

Synthesis of acyclic diene polymerizable BODIPY (6). To a dried three-necked 500 mL round bottom flask, 4-formylphenyl-di-(10-undecenyloxy)phosphate **5** (90 mg, 0.177 mmol) and 3-ethyl-2,4-dimethyl pyrrole (44 mg, 0.355 mmol) were added in 100 mL of dry CH_2Cl_2 under argon atmosphere. One drop of trifluoroacetic acid (TFA) was added, and the solution was stirred at room temperature for 4 h. After that, a solution of 2,3-dichloro-5,6-dicyanobenzoquinone (DDQ) (41 mg, 0.180 mmol) in 50 mL dry CH_2Cl_2 was added dropwise, and stirring was continued for 1 h, followed by the addition of triethylamine (273 μL , 1.8 mmol) and boron trifluoride diethyl etherate (321 μL , 1.8 mmol). After stirring for 10 h, the reaction mixture was washed with brine and dried over sodium sulfate anhydrous. The solvent was evaporated, and the residue was purified by column chromatography on silica gel (elution with Hexane/ethyl acetate, 7 : 3, R_f : 0.7). The pure product was isolated as a waxy solid. Yield: 51 mg (35%). ^1H NMR (500 MHz, CD_2Cl_2) δ : 7.36 (d, J = 8.5 Hz, 2H), 7.28 (d, J = 8.5 Hz, 2H), 5.80(m, 2H), 4.95 (m, 4H), 4.13 (m, 4H), 2.48 (s, 6H), 2.32 (q, J = 7.5 Hz, 4H), 2.03 (m, 4H), 1.69 (m, 4H), 1.40-1.23(br, 30H), 0.98 (t, J = 7.5 Hz, 6H). ^{13}C NMR (126 MHz, CD_2Cl_2) δ : 154.40, 152.12, 139.89, 139.82, 139.02, 133.62, 132.75, 131.32, 130.89, 130.43, 130.20, 121.29, 121.25, 114.39, 69.32, 69.27, 34.35, 30.85, 30.79, 30.04, 29.98, 29.69, 29.53, 17.55, 14.95, 12.83, 12.24. ^{31}P NMR (202 MHz, CD_2Cl_2) δ : -6.80. MS-ESI (m/z): 781.58 $[\text{M}+\text{H}]^+$, 803.57 $[\text{M}+\text{Na}]^+$, 1584.14 $[\text{2M}+\text{Na}]^+$ (calcd. for $\text{C}_{45}\text{H}_{68}\text{BF}_2\text{N}_2\text{O}_4\text{P}$: 780.50).

Synthesis of chain stopper BODIPY (7). To a dried three-necked 500 mL round bottom flask, 4-(10-undecenyloxy)benzaldehyde (0.728 mmol, 200 mg) and 3-Ethyl-2,4-dimethyl pyrrole (1.464 mmol, 181 mg) were added in 100 mL of dry CH₂Cl₂ under argon atmosphere. One drop of trifluoroacetic acid (TFA) was added, and the solution was stirred at room temperature for 3 h. After that, a solution of 2,3-dichloro-5,6-dicyanobenzoquinone (DDQ) (0.7307 mmol, 166 mg) in 100 mL dry CH₂Cl₂ was added dropwise, and stirring was continued for 1 h, followed by the addition of triethylamine (7.3 mmol, 1 mL) and boron trifluoride diethyl etherate (7.3 mmol, 0.9 mL). After stirring for 10 h, the reaction mixture was washed three times with brine and dried over sodium sulfate anhydrous. The solvent was evaporated, and the residue was purified by column chromatography on silica gel (elution with dichloromethane, *R_f*: 0.5). The pure product was isolated as a red solid (yield 120 mg, 30%). ¹H NMR (700 MHz, CDCl₃) δ : 7.14(d, *J* = 8.5 Hz, 2H), 7.00(d, *J* = 8.5 Hz, 2H), 5.82(m, 1H), 4.96 (m, 2H), 4.01 (t, *J* = 7 Hz, 2H), 2.52 (s, 6H), 2.30 (q, *J* = 7.7 Hz, 4H), 2.04 (q, *J* = 7 Hz, 2H), 1.83(quin, *J* = 6.5 Hz, 2H), 1.49(m, 2H), 1.4-1.3 (br, 16H), 0.98 (t, *J* = 7 Hz, 6H). ¹³C NMR (176 MHz, CDCl₃) δ : 159.70, 153.58, 140.55, 138.61, 132.75, 131.36, 129.55, 127.81, 115.13, 114.30, 68.32, 33.96, 29.66, 29.58, 29.42, 29.28, 29.09, 26.22, 17.23, 14.79, 12.63, 12.01.

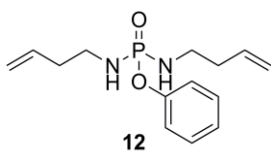
Synthesis of triallyl phosphate(8). Following the general procedure (b) described above and using allyl alcohol, triallyl phosphate was obtained as a clear oil with a yield of 80% after column chromatography over neutral alumina using as eluent dichloromethane (*R_f*: 0.7) or after distillation (b.p. 60 °C, 4 · 10⁻² mbar). ¹H NMR (500 MHz, CDCl₃) δ: 5.92-5.84(m, 3H), 5.33-5.18 (m, 6H), 4.50-4.47 (m, 6H). ¹³C NMR (126 MHz, CDCl₃): 132.46, 132.41, 118.22, 68.14, 68.09. ³¹P NMR (202 MHz, CDCl₃) δ: -0.80. ESI-MS (*m/z*): 241.06 [M+Na]⁺ (Calcd for C₉H₁₅O₄P: 218.07).

Synthesis of tri-(but-3-en-1-yl)-phosphate (9). Following the general procedure (b) described above and using 3-buten-1-ol, tri(but-3-en-1-yl) phosphate was obtained as a clear oil with a yield of 70% after column chromatography over neutral alumina using as eluent dichloromethane (*R_f*: 0.7). ¹H NMR (500 MHz, CDCl₃) δ: 5.83-5.75(m, 3H), 5.15-5.08 (m, 6H), 4.09-4.05 (m, 6H), 2.45-2.41 (m, 6H). ¹³C NMR (126 MHz, CDCl₃): 133.50, 117.84, 66.89, 66.84, 34.80, 34.74. ³¹P NMR (202 MHz, CDCl₃) δ: -1.11. ESI-MS (*m/z*): 283.11 [M+Na]⁺ (Calcd for C₁₂H₂₁O₄P: 260.12).

Synthesis of tri-(5-hexenyloxy)-phosphate(10). Following the general procedure(b) described above and using 5-hexen-1-ol, tri-(5-hexenyloxy)-phosphate was obtained as a clear oil with a yield of 80% after column chromatography over neutral alumina using dichloromethane as eluent to give a colorless oil (R_f : 0.6). ^1H NMR (700 MHz, CDCl_3) δ : 5.77 (m, 3H), 5.00-4.98 (m, 3H), 4.96-4.94 (m, 3H), 4.02 (q, $J = 7$ Hz, 6H), 2.07(q, $J = 7$ Hz, 6H), 1.68 (m, 6H), 1.47 (m, 6H). ^{13}C NMR (176 MHz, CDCl_3) δ : 138.35, 115.01, 67.61, 67.57, 33.27, 29.84, 29.80, 24.84. ^{31}P NMR (283 MHz, CDCl_3) δ : -0.67. ESI-MS m/z 345.23 $[\text{M}+\text{H}]^+$, 367.22 $[\text{M}+\text{Na}]^+$, 689.44 $[2\text{M}+\text{H}]^+$, 711.42 $[2\text{M}+\text{Na}]^+$ (Calcd for $\text{C}_{18}\text{H}_{43}\text{O}_4\text{P}$: 344.21).

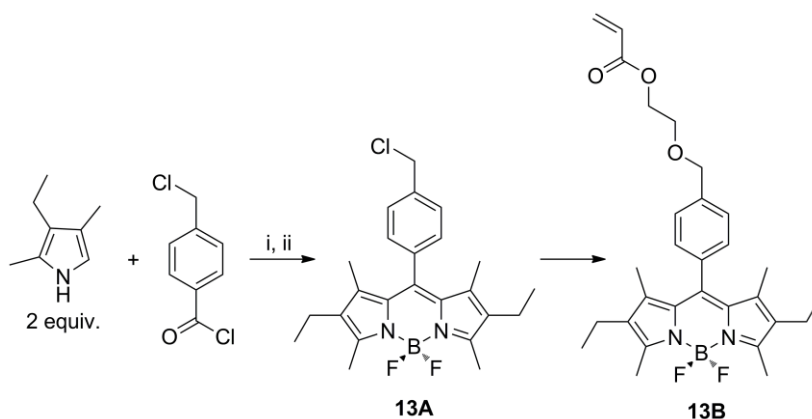
Synthesis of tri-(undec-10-en-1-yl)-phosphate(11). Following the general procedure described above and using 10-undecen-1-ol, tri-(undec-10-en-1-yl) phosphate was obtained as a clear oil with a yield of 60% after column chromatography over neutral alumina using dichloromethane as eluent to give a colorless oil (R_f : 0.5). ^1H NMR (700 MHz, CDCl_3) δ : 5.77 (m, 3H), 5.00-4.98 (m, 3H), 4.93-4.91 (m, 3H), 4.02 (q, $J = 7$ Hz, 6H), 2.02(q, $J = 7$ Hz, 6H), 1.66 (m, 6H), 1.36-1.27 (br, 36H). ^{13}C NMR (176 MHz, CDCl_3) δ : 139.27, 114.26, 67.80, 67.76, 33.92, 30.45, 30.42, 29.59, 29.53, 29.27, 29.23, 29.05, 25.59. ^{31}P NMR (283 MHz, CDCl_3) δ : -0.62. ESI-MS (m/z): 545.45 $[\text{M}+\text{H}]^+$, 577.44 $[\text{M}+\text{Na}]^+$ (Calcd for $\text{C}_{33}\text{H}_{63}\text{O}_4\text{P}$: 544.45).

Synthesis of 12. 3-Buten-1-amine (5 g, 0.07 mol) and triethyl-



amine (9.7 mL, 0.07 mol) were dissolved in 10 mL of dry methylene chloride. This solution was added dropwise to phenyldichlorophosphate (19.5 g, 0.1 mol) and 50 mL of dry diethylether were over a period of 30

min at 0 °C. The reaction mixture was stirred additionally for 2 h at 0 °C. The precipitate obtained was removed by filtration and the filtrate solution was washed thoroughly with a saturated aqueous solution of brine and water. Then the washed organic layer was dried over MgSO_4 and concentrated by solvent evaporation. The product was further washed with hexane. The final product was isolated as a highly viscous light yellowish oil (Yield = 85%). ^1H NMR (700 MHz, CDCl_3) δ : 7.31 (t, 2H), 7.20 (m, 2H), 7.13(m, 1H), 5.76-5.70 (m, 2H), 5.10-5.06 (m, 4H), 3.07(m, 4H), 2.24 (m, 4H). ^{13}C NMR (176 MHz, CDCl_3) δ : 151.27, 151.23, 135.27, 129.76, 124.54, 120.53, 120.50, 117.71, 40.43, 36.06, 36.02. ^{31}P NMR (283 MHz, CDCl_3) δ : 11.56.



Synthesis of intermediate 13A. For the synthesis of compound **13A**, we followed the procedure described by Lopez Arbeloa *et. Al.* (*J. Phys. Chem.A* **2004**, *108*, 3315) as following reported. *p*-(Chloromethyl)benzoyl chloride (1.5 g, 8 mmol) was added dropwise to a stirred solution of freshly distilled 2,4-dimethyl-3-ethylpyrrole (2.2 mL) in dichloromethane (90 mL) at room temperature and under Ar, and the mixture was heated to 50 °C with stirring for 2 h. After the vacuum evaporation of the solvent, toluene (190 mL), dichloromethane (10 mL), and triethylamine (3.88 g, 38 mmol) were added to the residual solid, the mixture was stirred at room temperature for 30 min under Ar, and boron trifluoride diethyl etherate (7.82 g, 55 mmol) was then added. After heating to 50° for 1.5 h, the subsequent workup yielded a residue that was purified by column chromatography (silica gel, hexane-EtOAc mixture 9:1 as eluent, $R_f = 0.4-0.5$) and crystallization from hexane. Red crystals, yield 25%. (Spectroscopic data in agreement with the literature)

Synthesis of Acrylate BODIPY 13B. A solution of potassium acrylate (1 mmol) and **13A** (0.25 mmol) in DMF (30 mL) was stirred at room temperature for 5 days under an Ar atmosphere and in the dark. The subsequent workup yielded a residue that was purified by column chromatography (silica gel, hexane-EtOAc 9:1, $R_f : 0.3-0.4$, yield 50%). $^1\text{H NMR}$ (700 MHz, CDCl_3) δ : 7.49-7.48(m, 2H), 7.30(m, 2H), 6.51-6.48(m, 1H), 6.24-6.20(m,1H), 5.30(s, 2H), 2.53(s, 6H), 2.30(q, 4H), 1.31-1.25(m,12H), 0.98(t, 6H). $^{13}\text{C NMR}$ (176 MHz, CDCl_3) δ : 166.08, 153.99, 139.77, 138.47, 136.88, 135.83, 132.99, 131.52, 130.88, 128.71, 128.53, 128.33, 65.88, 29.85, 17.23, 14.75, 12.66, 11.92.

Synthesis of polymer (P2). Phenyl-di-(3-buten-1-yl)-phosphate (**2**) was reacted following the general procedure described above for ADMET bulk polymerization. ¹H NMR (700 MHz, CDCl₃) δ: 7.32-7.30 (m, = 2H), 7.19-7.14 (m, 3H), 5.47-5.44 (m, 2H), 4.10-4.08 (m, 4H), 2.40-2.35 (m, 4H). ¹³C NMR (176 MHz, CDCl₃): 150.79, 150.75, 129.86, 128.18, 127.23, 125.23, 120.10, 120.08, 67.83, 67.80, 67.59, 33.64, 33.60. ³¹P NMR (283 MHz, CDCl₃) δ: -6.38.

Synthesis of polymer (P3). Phenyl-di-(5-hexenyloxy)-phosphate (**3**) was reacted following the general procedure described above for ADMET bulk polymerization of. ¹H NMR (700 MHz, CDCl₃) δ: 7.32-7.31 (m, 2H), 7.21-7.20(m, 2H), 7.16-7.14(m, 1H), 5.33 (m, 2H), 4.13-4.11 (m, 4H), 1.97 (m, 4H), 1.68-1.65 (m, 4H), 1.42-1.39 (m, 4H). ¹³C NMR (176 MHz, CDCl₃): 150.90, 150.87, 130.30, 129.82, 125.10, 120.10, 68.54, 68.50, 67.09, 53.58, 32.04, 29.81, 29.75, 28.41, 25.38. ³¹P NMR (283 MHz, CDCl₃) δ: -6.12.

Synthesis of polymer (P4). Phenyl-di-(undec-10-en-1-yl)-phosphate (**4**) was reacted following the general procedure described above for ADMET bulk polymerization. ¹H NMR (700 MHz, CDCl₃) δ: 7.34-7.31 (m, 2H), 7.22-7.20 (m, 2H), 7.17-7.15(m, 1H), 5.41-5.34 (m, 2H), 4.15-4.09 (m, 4H), 2.02-1.96 (m, 4H), 1.69-1.65 (m, 4H), 1.38-1.21 (m, 24H). ¹³C NMR (176 MHz, CDCl₃): 151.00, 150.96, 130.48, 129.80, 125.05, 120.14, 120.11, 68.73, 68.69, 32.77, 30.40, 30.36, 29.82, 29.62, 29.57, 29.33, 29.26, 25.53. ³¹P NMR (283 MHz, CDCl₃) δ: -6.11.

Synthesis of polymer (P5). 200 mg of the polymer **P4**, 5 mL of toluene and 10 mg of 10% Pd/C catalyst were charged into a reactor and flushed with nitrogen. Hydrogenation was then performed with vigorous stirring under a hydrogen pressure of 8 bar at room temperature for 6 h. The solution was filtered over celite and the solid polymer isolated after solvent evaporation in quantitative yield. ¹H NMR (700 MHz, CDCl₃) δ: 7.34-7.31 (m, 2H), 7.22-7.20 (m, 2H), 7.17-7.15(m, 1H), 4.15-4.09 (m, 4H), 1.69-1.65 (m, 4H), 1.36-1.20 (m, 36H). ¹³C NMR (176 MHz, CDCl₃): 151.01, 150.97, 129.79, 125.04, 120.14, 120.11, 68.73, 68.69, 66.00, 30.42, 30.36, 29.89, 29.87, 29.73, 29.67, 29.27, 25.54. ³¹P NMR (283 MHz, CDCl₃) δ: -6.10.

Synthesis of labeled unsaturated polyphosphoesters (P6-P6a). In a dry Schlenk tube fitted with a magnetic stirring bar, BODIPY **6** (2 mg, 0.0025 mmol) and **4** (160 mg, 0.334 mmol)

were placed under an argon atmosphere. Temperature was raised up to 60 °C, and Grubbs catalyst 1st Generation was added (3 mg, 0.0036 mmol, 0.8 mol%). After ethylene started to evolve, a controlled vacuum of 5·10⁻² mbar was applied to remove the condensate. After 12 h, the reaction was cooled to room temperature, diluted with a solution containing tris(hydroxymethyl)phosphine (3.7 mg, 0.03 mmol), triethylamine (3 mg, 0.03 mmol) in 10 mL of dry CH₂Cl₂, and stirred for 1h. Then water was added and stirring was continued for an additional 1 h to decolorize the brownish solution. The mixture was extracted with CH₂Cl₂ and washed twice with brine. The organic layer was dried over anhydrous sodium sulfate, filtered, and concentrated in vacuo. The polymer, obtained with a quantitative yield, is then dissolved in the minimum volume of chloroform and precipitated into hexane (which is a non-solvent for the polymer, but a good solvent for both monomers). In an analogous way, as a general representative procedure, polymer **P6a** was prepared by mixing BODIPY **6** (10 mg, 0.0125 mmol) and **4** (120 mg, 0.250 mmol) in different ratio. ¹H NMR (700 MHz, CDCl₃) δ: 7.32 (t, *J* = 7 Hz = 2H), 7.21(d, *J* = 7 Hz, 2H), 7.15(t, *J* = 7 Hz, 1H), 5.37-5.34 (br, 2H), 4.12 (br, 4H), 2.01-1.95 (br, 4H), 1.67(m, 4H), 1.33-1.25 (br, 24H). ¹³C NMR (176 MHz, CDCl₃) δ: 150.94, 130.44, 130.39, 129.98, 129.76, 125.01, 120.11, 120.08, 68.69, 68.66, 32.74, 29.90, 29.80, 29.59, 29.54, 29.43, 29.30, 29.23, 27.36, 25.51. ³¹P NMR (283 MHz, CDCl₃) δ: -6.11.

Synthesis of end-labeled unsaturated polyphosphoester (P7). In a dry Schlenk tube fitted with a magnetic stirring bar, phenyl-di-(10-undecenyloxy)-phosphate **4** (160 mg, 0.333 mmol) and BODIPY **7** (6 mg, 0.011 mmol) were placed under an argon atmosphere. Grubbs catalyst 1st Generation was added (2.2 mg, 0.0026 mmol, 0.8 mol %), and the reaction was stirred for 12 h at r.t. with a controlled vacuum of 5·10⁻² mbar to remove the evolving ethylene. Then, temperature was raised up to 60 °C for additional 4 h. The reaction was cooled to room temperature, diluted with a solution containing tris(hydroxymethyl)phosphine (3.3 mg, 0.03 mmol), triethylamine (3 mg, 0.03 mmol) in 10 mL of dry CH₂Cl₂, and stirred for 1h. Then water was added and stirring was continued for an additional 1 hour to decolorize the brownish solution. The crude mixture was diluted with CH₂Cl₂ and washed twice with brine. The organic layer was dried over anhydrous sodium sulfate, filtered, and concentrated in vacuum. The polymer, obtained with a quantitative yield, is then dissolved in the minimum volume of chloroform and precipitated into hexane (which is a

non-solvent for the polymer, but a good solvent for both monomers). ^1H NMR (700 MHz, CDCl_3) δ : 7.32 (t, $J = 7$ Hz = 2H), 7.21(d, $J = 7$ Hz, 2H), 7.15(t, $J = 7$ Hz, 1H), 5.37-5.34 (br, 2H), 4.12 (br, 4H), 2.03-1.95 (br, 4H), 1.69-1.65(br, 4H), 1.33-1.25 (br, 24H). ^{13}C NMR (176 MHz, CDCl_3) δ : 150.98, 130.44, 129.98, 129.77, 125.01, 120.11, 120.08, 115.11, 68.70, 68.66, 32.75, 30.38, 30.34, 29.90, 29.80, 29.60, 29.54, 29.43, 29.30, 29.23, 27.36, 25.51. ^{31}P NMR (283 MHz, CDCl_3) δ : -6.11.

ATMET bulk polymerization of triallyl phosphate (P8). In a dry Schlenk tube fitted with a magnetic stirring bar, the monomer **8** (100 mL) was placed under an argon atmosphere. Temperature was raised up to 60 °C, and the Grubbs catalyst 1st gen. (0.3-0.5 mol%) was added. After ethylene started to evolve, a controlled vacuum of $5 \cdot 10^{-2}$ mbar was applied to remove the condensate. After 0.5 h, the reaction was cooled to room temperature, diluted with a solution containing tris(hydroxymethyl)phosphine (5 mol%), triethylamine (5 mol%) in 10 mL of dry CH_2Cl_2 , and stirred for 1h. Then water was added and stirring was continued for an additional 1 h to decolorize the brownish solution. The mixture was extracted with CH_2Cl_2 and washed twice with brine. The organic layer was dried over anhydrous sodium sulfate, filtered, and concentrated *in vacuo*. The polymer, obtained with a quantitative yield, is then washed with hexane (which is a non-solvent for the polymer, but a good solvent for monomer) when requested, and dried. ^1H NMR (700 MHz, CDCl_3) δ : 5.94-5.88 (br, 3H), 5.36-5.32 (m, 2H), 5.24-5.22 (m, 2H), 4.55-4.51 (br, 5H). ^{13}C NMR (176 MHz, CDCl_3) δ : 132.53, 132.49, 132.45, 132.41, 128.33, 128.29, 128.20, 128.16, 128.07, 128.03, 118.63, 118.57, 118.52, 118.45, 118.32, 68.40, 68.31, 68.28, 68.23, 68.20, 66.86, 66.83, 66.77, 66.74, 66.71, 62.86. ^{31}P NMR (283 MHz, CDCl_3) δ : -0.68, -0.70, -0.75, -0.79, -0.80, -0.86.

Synthesis of polymer P9. Tri-(but-3-en-1-yl)-phosphate (**9**) was reacted following the general procedure described above for ATMET bulk polymerization. ^1H NMR (700 MHz, CDCl_3) δ : 5.81-5.76(m, 3H), 5.52-5.53 (br, 3H), 5.15-5.09 (m, 6H), 4.08-4.00 (m, 13H), 2.46-2.39 (m, 13H). ^{13}C NMR (176 MHz, CDCl_3): 133.48, 128.31, 128.24, 128.20, 127.34, 127.28, 127.23, 117.88, 67.10, 66.89, 34.79, 34.75, 33.76, 28.75, 28.72. ^{31}P NMR (283 MHz, CDCl_3) δ : -0.71, -1.05, -1.08, -1.11.

Synthesis of polymer P10. Tri-(5-hexen-1-yl)-phosphate (**10**) was reacted following the general procedure described above for ATMET bulk polymerization. ^1H NMR (700 MHz, CDCl_3) δ :

5.81-5.75 (m, 3H), 5.38-5.35 (m, 6H), 5.02-4.95 (m, 6H), 4.04-4.00 (m, 16H), 2.09-2.00(br, 16H), 1.70-1.64 (br, 16H), 1.50-1.43 (br, 16H). ¹³C NMR (176 MHz, CDCl₃) δ: 138.36, 130.34, 129.80, 115.14, 115.03, 67.66, 67.62, 67.58, 33.28, 32.13, 30.07, 30.03, 29.93, 29.89, 29.84, 29.81, 26.84, 25.67, 25.51, 24.85. ³¹P NMR (283 MHz, CDCl₃) δ: -0.66(br).

Synthesis of polymer P11. Tri-(undec-10-en-1-yl)-phosphate (**11**) was reacted following the general procedure described above for ATMET bulk polymerization. ¹H NMR (700 MHz, CDCl₃) δ: 5.83-5.73 (m, 3H), 5.37-5.34 (br, 7H), 5.00-4.92 (m, 6H), 4.04-4.00 (br, 19H), 2.04-1.95(br, 19H), 1.66 (br, 19H), 1.36-1.28 (br, 125H). ¹³C NMR (176 MHz, CDCl₃) δ: 139.29, 130.45, 129.99, 114.29, 67.82, 67.80, 33.95, 32.78, 30.47, 29.84, 29.67, 29.62, 29.55, 29.35, 29.30, 29.07, 27.39. ³¹P NMR (283 MHz, CDCl₃) δ: 0.40, -0.62, -0.71.

Synthesis of polymer P12. In a dry one neck flask fitted with a magnetic stirring bar, phenyl-di-(undec-10-en-1-yl)-phosphate **4** (1g, 2.08 mmol) and (ethylenedioxy)diethanethiol (380 mg, 2.08 mmol) were placed under an argon atmosphere. Temperature was raised up to 70 °C, and AIBN (azobisisobutyronitrile) was added (10 mg, 0.06 mmol) as radical initiator, observing a quick increase of viscosity. After 12 h, the reaction was cooled to room temperature; the crude mixture was dissolved into CHCl₃ and reprecipitated into methanol. The polymer was obtained with a quantitative yield as a colourless material. ¹H NMR (700 MHz, CDCl₃) δ: 7.32 (m, 2H), 7.21(m, 2H), 7.15(m, 1H), 4.11 (m, 4H), 3.61 (m, 8H), 2.69 (m, 4H), 2.52(m, 4H), 1.66 (br, 4H), 1.55, 1.35-1.24 (br, 28H). ¹³C NMR (176 MHz, CDCl₃) δ: 150.93, 150.89, 129.73, 124.99, 120.07, 120.05, 114.24, 71.14, 70.38, 68.65, 68.62, 32.70, 31.47, 30.34, 30.30, 29.90, 29.60, 29.58, 29.57, 29.35, 29.19, 28.98, 25.47. ³¹P NMR (283 MHz, CDCl₃) δ: -6.12.

Synthesis of polymer P13. In a dry one neck flask fitted with a magnetic stirring bar, monomer **12** (500 mg, 1.8 mmol) and (ethylenedioxy)diethanethiol (325 mg, 1.8 mmol) were placed under an argon atmosphere. Temperature was raised up to 70 °C, and AIBN (azobisisobutyronitrile) was added (10 mg, 0.06 mmol) as radical initiator, observing a quick increase of viscosity. After 12 h, the reaction was cooled to room temperature; the crude mixture was dissolved into CHCl₃ and reprecipitated into methanol or hexane. The polymer was obtained with a quantitative

yield as a colourless material. ^1H NMR (500 MHz, CDCl_3) δ : 7.29 (m, 2H), 7.21(m, 2H), 7.15(m, 1H), 3.62 (m, 4H), 3.61 (m, 8H), 2.97 (m, 6H), 2.68 (m, 4H), 2.52(m, 4H), 1.6 (br, 8H). ^{13}C NMR (126 MHz, CDCl_3) δ : 151.36, 151.31, 129.73, 124.43, 120.48, 120.44, 71.15, 70.44, 70.41, 70.36, 41.07, 32.29, 31.57, 31.07, 31.02, 26.96. ^{31}P NMR (202 MHz, CDCl_3) δ : 12.13, 11.96, 11.81.



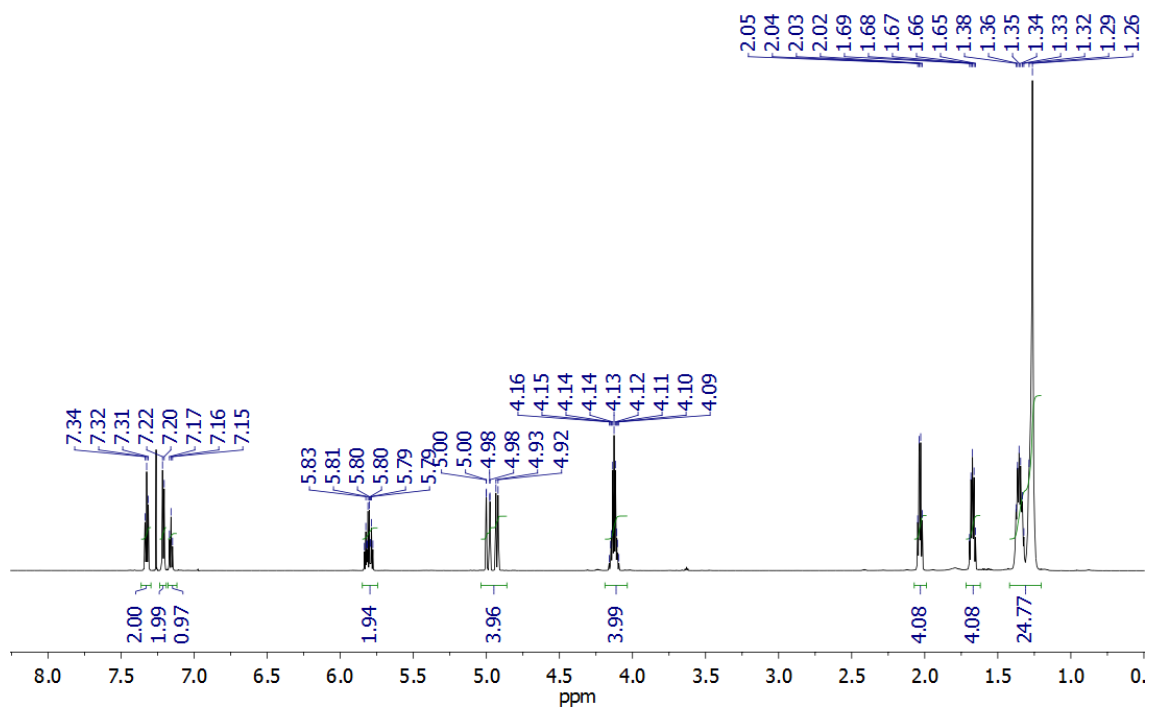
Chapter 7

Spectroscopic Selection

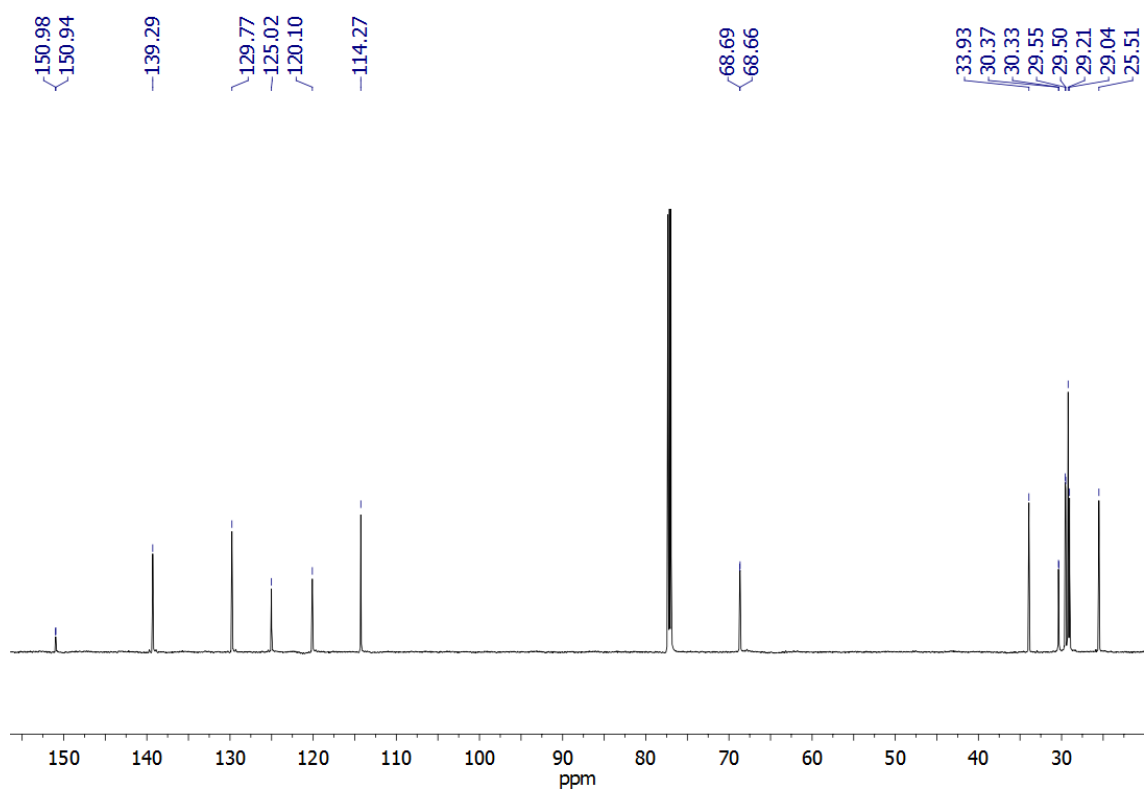
Outline

The following chapter reports a selection of NMR spectra, for the most representative compounds synthesized in this thesis work.

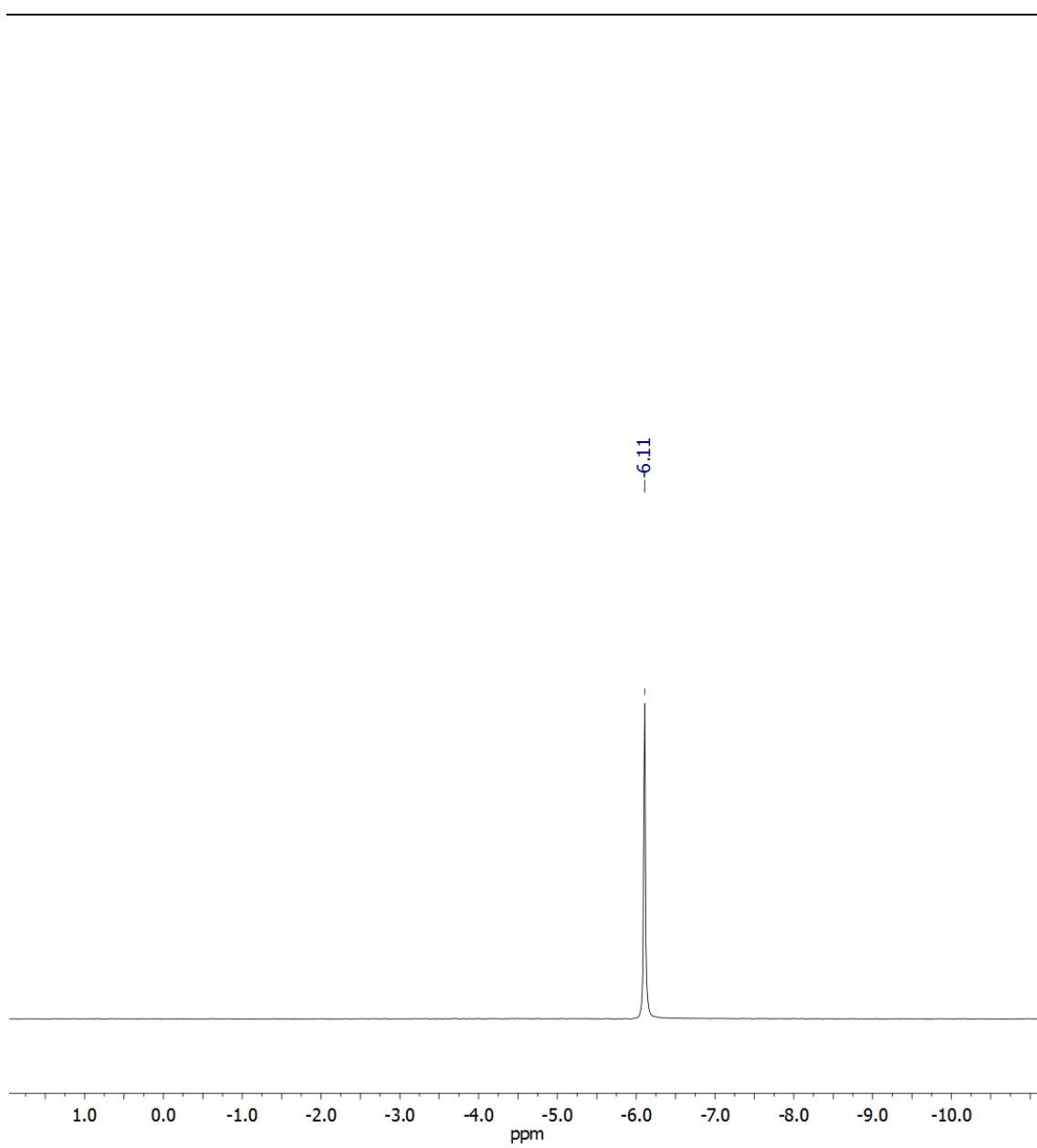
- Phenyl-di-(undec-10-en-1-yl)-phosphate **4**
- Triallyl-phosphate **8**
- 4-formylphenyl-di-(10-undecenyloxy)phosphate **5**
- Acyclic diene BODIPY **6**
- Labeled unsaturated polyphosphoester **P6**
- Chain-stopper BODIPY **7**
- End-labeled unsaturated polyphosphoester **P7**
- Unsaturated hyperbranched polyphosphoester **P11**



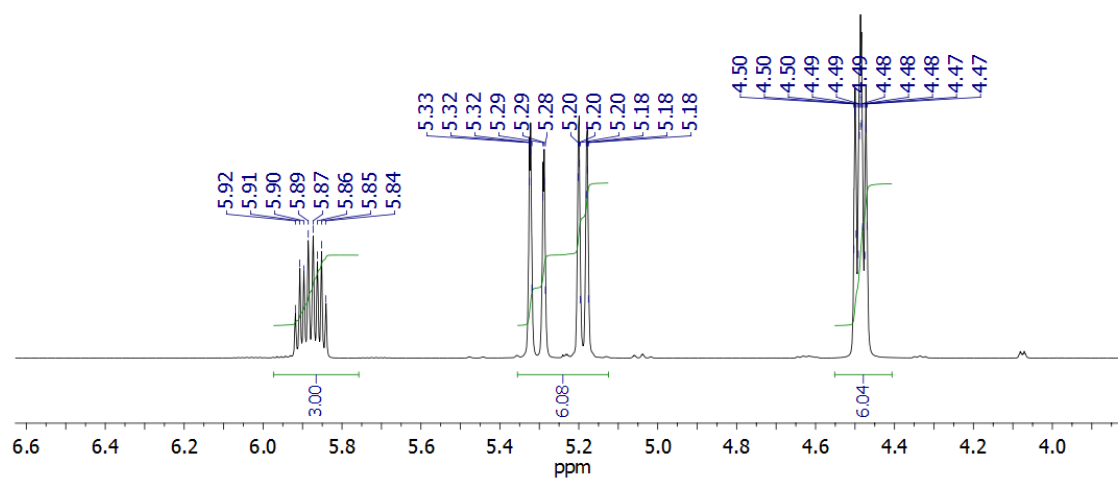
¹H NMR of phenyl-di-(undec-10-en-1-yl)-phosphate 4 (700 MHz, CDCl₃).



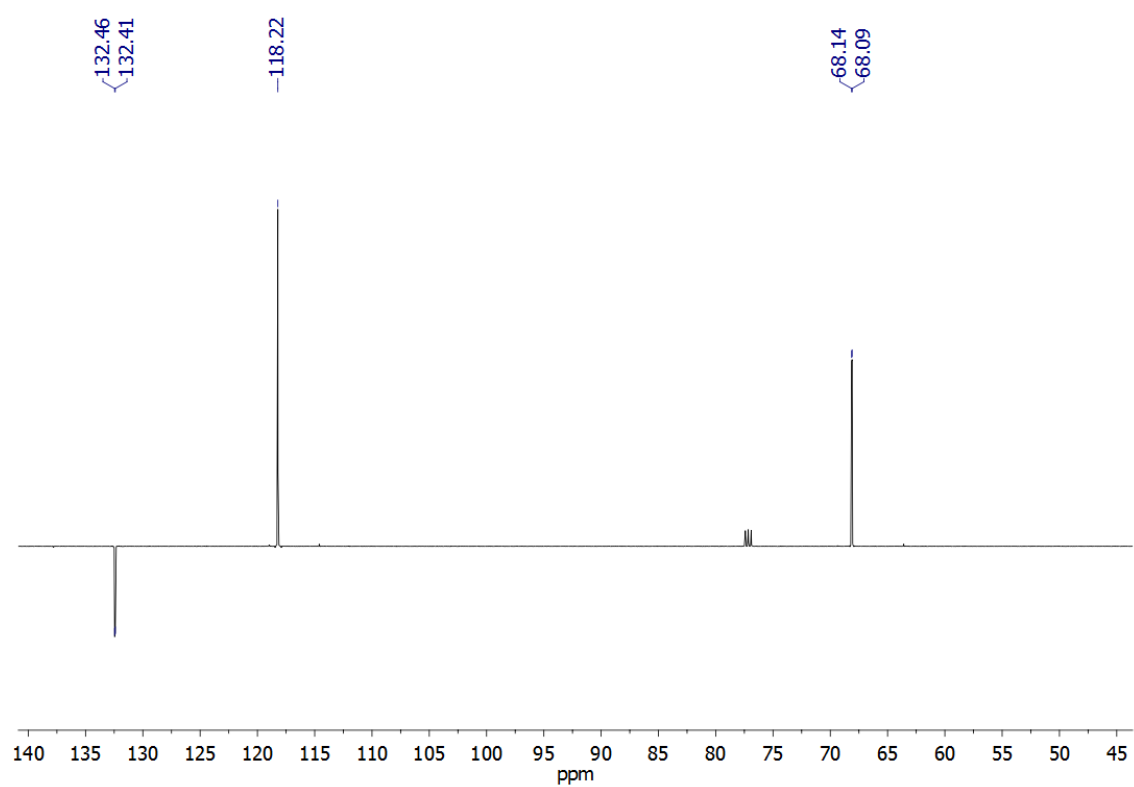
^{13}C NMR of phenyl-di-(undec-10-en-1-yl)-phosphate **4** (176 MHz, CDCl_3).



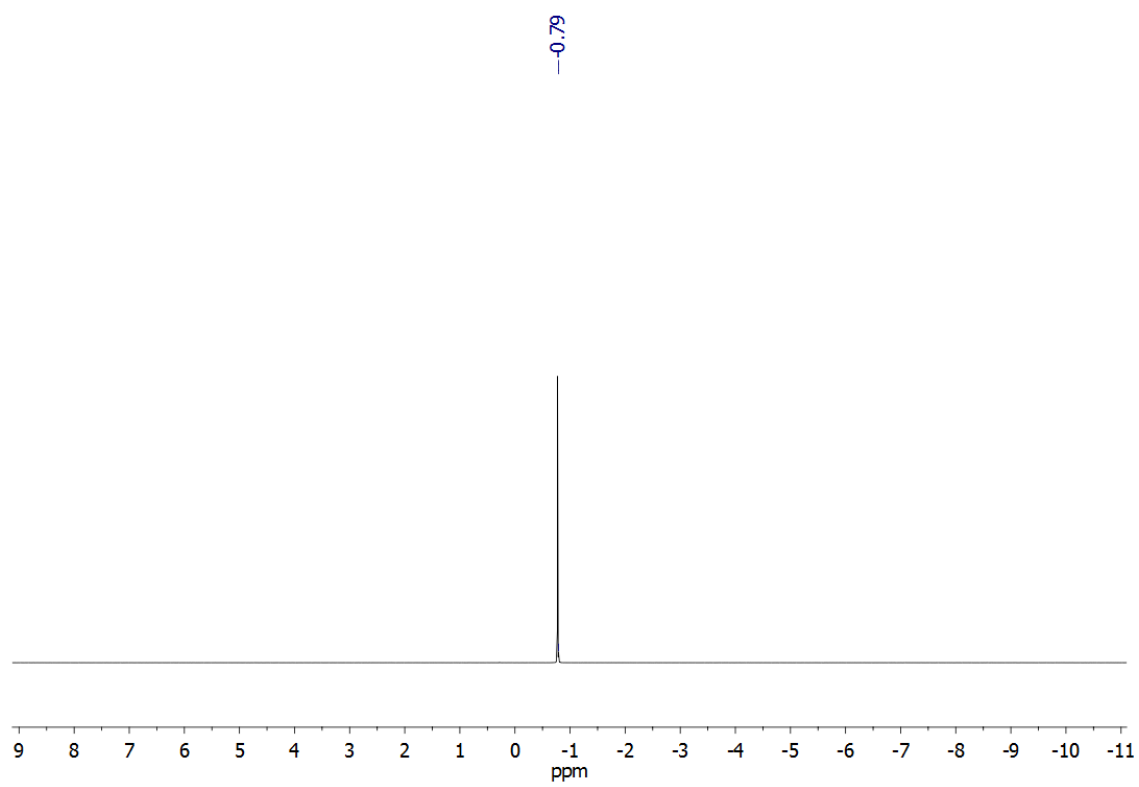
^{31}P NMR of phenyl-di-(undec-10-en-1-yl)-phosphate **4** (283 MHz, CDCl_3).



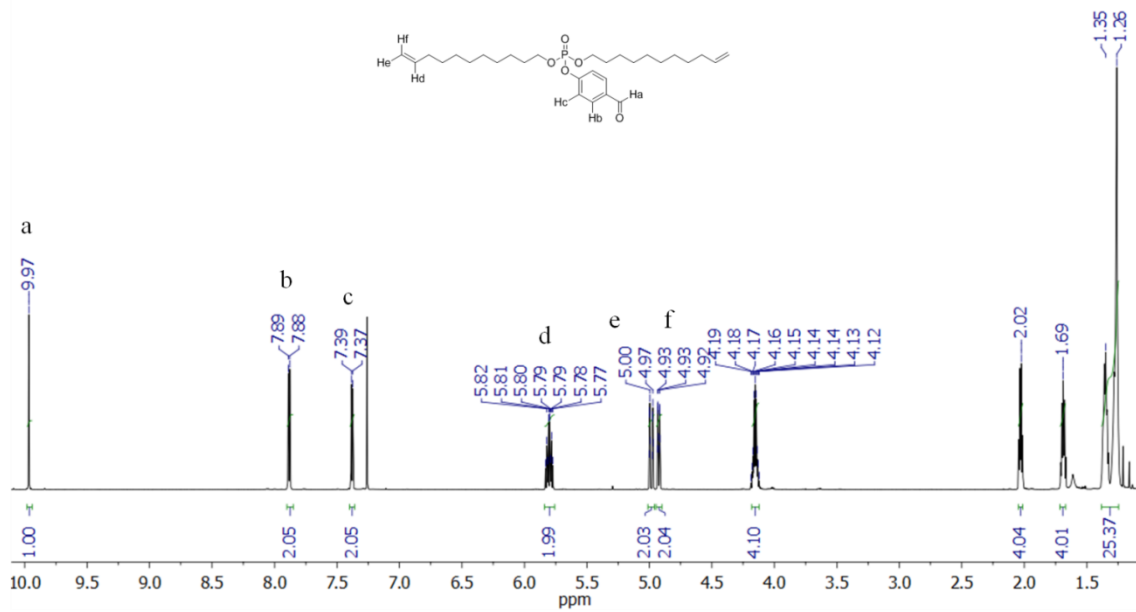
^1H NMR of triallyl-phosphate **8** (500 MHz, CDCl_3).



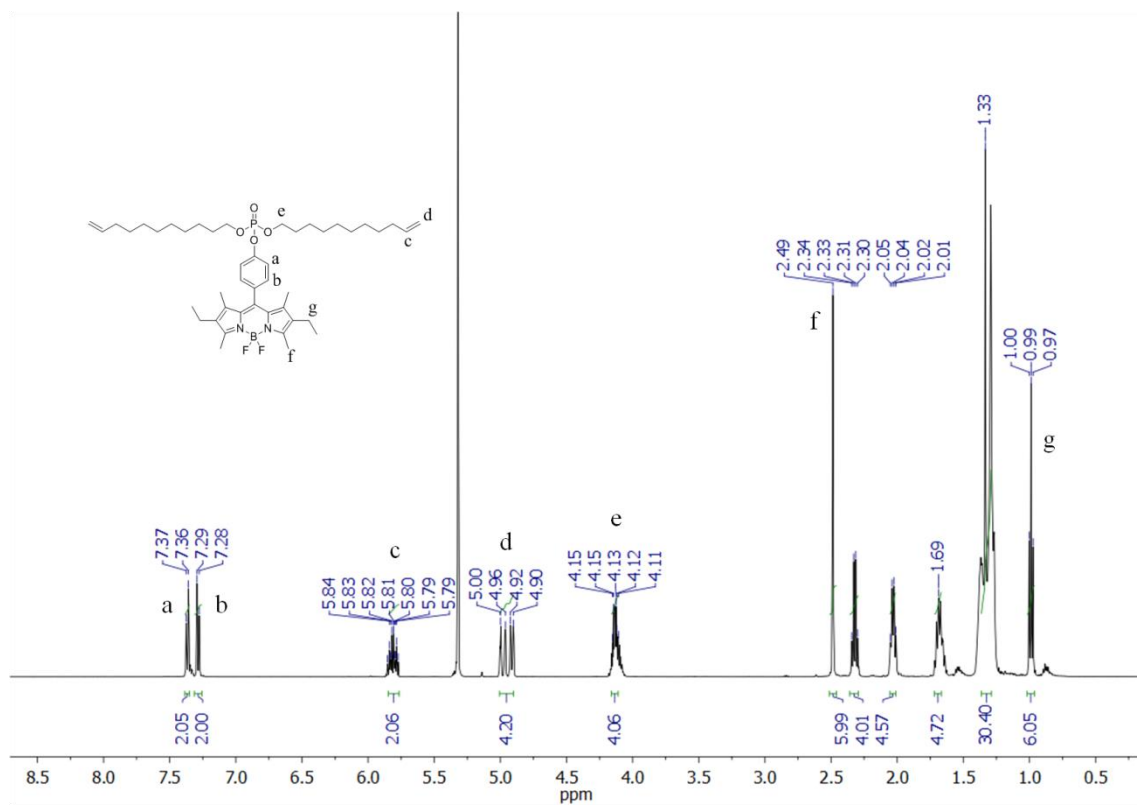
^{13}C NMR of triallyl-phosphate **8** (126 MHz, CDCl_3).



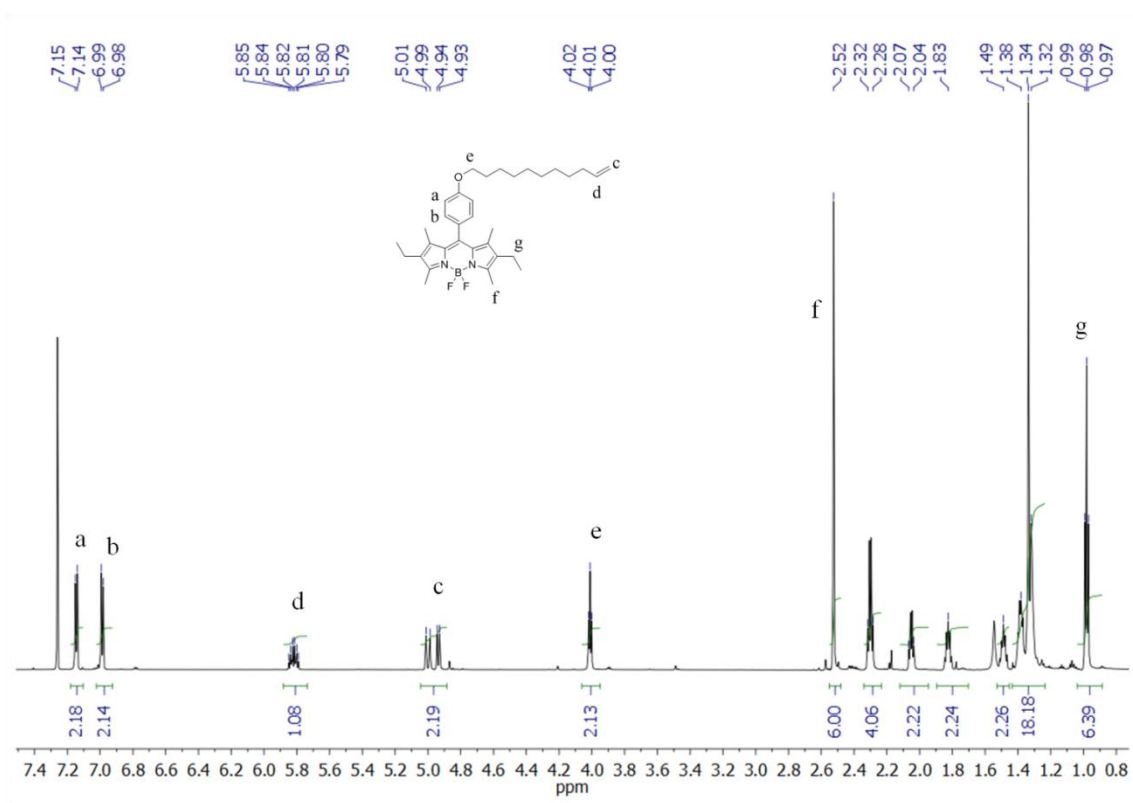
^{31}P NMR of triallyl-phosphate **8** (202 MHz, CDCl_3).



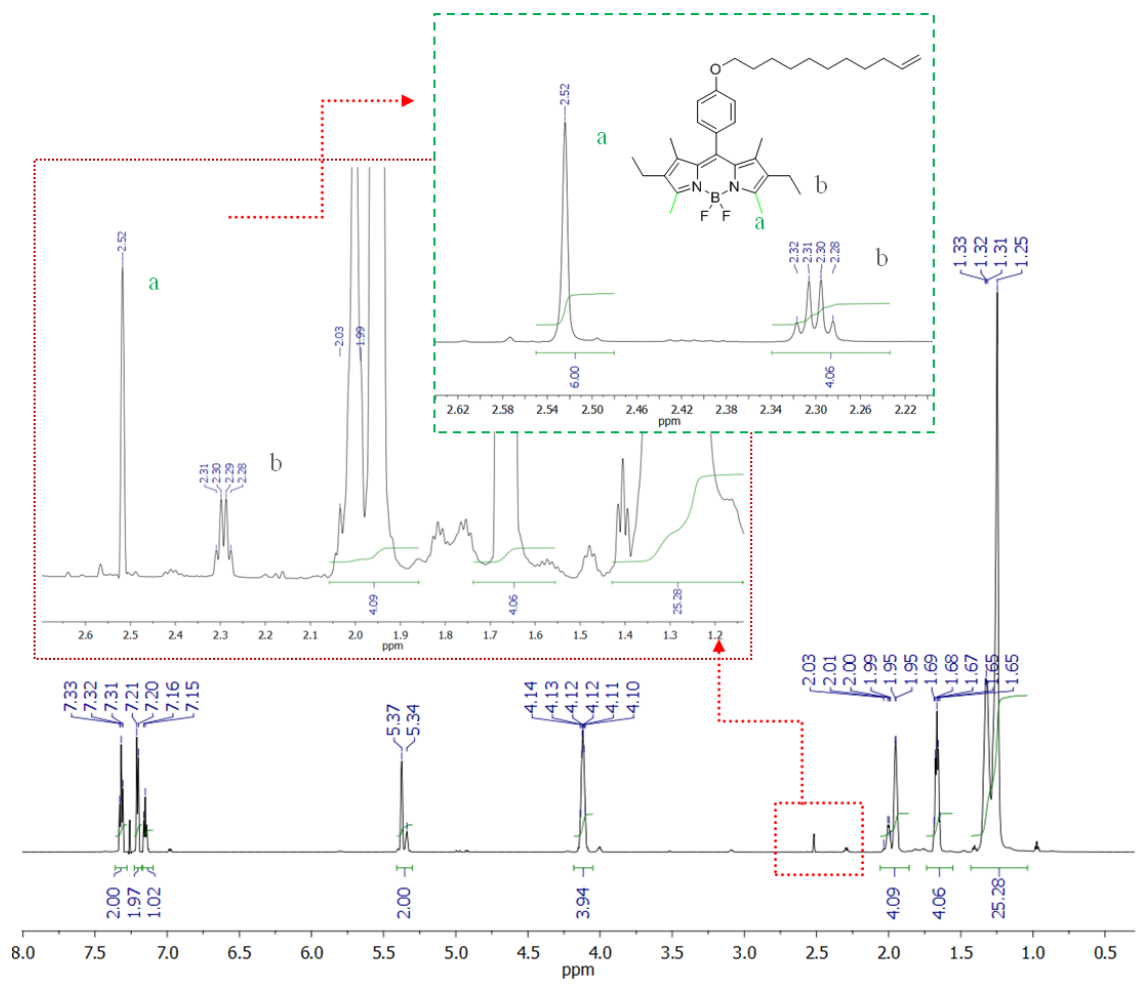
^1H NMR of 4-formylphenyl-di-(10-undecenyloxy)phosphate **4** (700 MHz, CDCl_3).



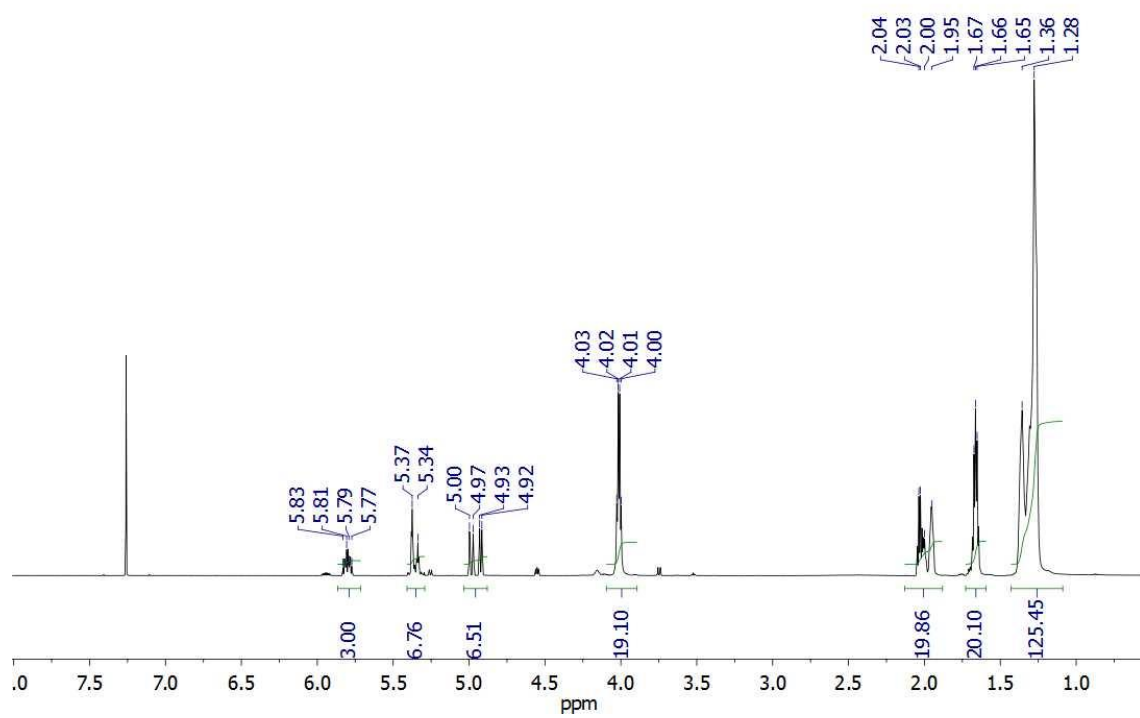
¹H NMR of acyclic diene BODIPY 6 (700 MHz, CD₂Cl₃).



¹H NMR of chain stopper BODIPY 7 (700 MHz, CDCl₃).



¹H NMR of end-labeled unsaturated polyphosphoester P7 (700 MHz, CDCl₃).



^1H NMR unsaturated hyperbranched polyphosphoester **P11** (700 MHz, CDCl_3).

Publications



(1) **Unsaturated Polyphosphoesters via Acyclic Diene Metathesis Polymerization.** Marsico, F.; Wagner, M.; Landfester, K.; Wurm, F. *Macromolecules* **2012**, *45*, 8511.

(2) **A Metathesis Route for BODIPY Labeled Polyolefins.** Marsico, F.; Turshatov, A.; Weber, K.; Wurm, F. *Org. Lett.* **2013**, *15*, 3844.

(3) **Synergetic operating active systems for oxygen protection of bioactive and photoactive organic materials.** (Patent ap. EP 13 185 751.8 / 2013).

(4) **Paclitaxel-loaded polyphosphate nanoparticles: a potential strategy for bone cancer treatment.** Alexandrino, E.M.; Sandra Ritz, S.; Marsico, F.; Grit Baier, G.; Mailänder, V.; Landfester, K.; Wurm, F. *J. Mater. Chem. B* **2014**, *2*, 1298.

(5) **Selective Interfacial Olefin Cross Metathesis for the Preparation of Degradable Nanocapsules.** Malzahn, K.; Marsico, F.; Koynov, K.; Landfester, K.; Weiss, C.; Wurm, F. *ACS Macro Lett.* **2014**, *3*, 40.

(6) **Organophosphates as Protective Solvents for Long-Term Triplet Triplet Annihilation Upconversion in Oxygen-Saturated Environments.** *Submitted*

(7) **Hyperbranched Unsaturated Polyphosphates for Active-Passive Protection of Efficient Broadband Upconversion in Air.** Marsico, F.; *et. al. Submitted*

(8) **Hyperbranched Poly(phosphoester)s as Flame Retardants.** K Täuber, F Marsico, F Wurm, B. Schartel, *In preparation*

(9) **Reactive telechelic Polyphosphoesters.** Steinmann, M.; Becker, G.; Marsico, F.; Wurm, F. *In preparation*



Declaration

I hereby declare that I wrote the dissertation submitted without any unauthorized external assistance and used only sources acknowledged in the work. All textual passages which are appropriated verbatim or paraphrased from published and unpublished texts as well as all information obtained from oral sources are duly indicated and listed in accordance with bibliographical rules. In carrying out this research, I complied with the rules of standard scientific practice as formulated in the statutes of Johannes Gutenberg-University Mainz to insure standard scientific practice.

Marsico Filippo

Mainz, 1 April, 2014

Bibliography

- (1) (a) Westheimer, F.H. *Science*, **1987**,235, 1173 (b) Kamerlin, C. L.; Sharma, P.K.; Prasad, R.B.;Warshel, A. *Quarterly Reviews of Biophysics*, **2013**,46, 1-132. (c) Svava, J.; Weferling, N.; Hofmann, T. *Ullmanns Enc. Of Industrial Chemistry* **2000**, 21, 19.
- (2) Duncan, R. *Nat. Rev. Drug Discovery* **2003**, 2, 347.
- (3) Ikada, Y.; Tsuji, H. *Macromol. Rapid Commun.* **2000**, 21, 117.
- (4) Klosinski, P.; Penczek, S. *Macromolecules* **1983**, 16, 316.
- (5) Wang, Y. C.; Yuan, Y. Y.; Du, J. Z.; Yang, X. Z.; Wang, J. *Macromol. Biosci.* **2009**, 9, 1154.
- (6) Zhao, Z.; Wang, J.; Mao, H.-Q.; Leong, K. W. *Adv. Drug Delivery Rev.* **2003**, 55, 483.
- (7) Wang, J.; Mao, H. Q.; Leong, K. W. *J. Am. Chem. Soc.* **2001**, 123, 9480.
- (8) Liu, X.; Ni, P.; He, J.; Zhang, M., S. *Macromolecules* **2010**, 43, 4771.
- (9) Qiu, J. J.; Liu, C. M.; Hu, F.; Guo, X. D.; Zheng, Q. X. *J. Appl. Polym. Sci.* **2006**, 102, 3095.
- (10) Huang, S. W.; Wang, J.; Zhang, P. C.; Mao, H. Q.; Zhuo, R. X.; Leong, K. W. *Biomacromolecules* **2004**, 5, 306.
- (11) Wang, S.; Wan, A. C. A.; Xu, X.; Gao, S.; Mao, H. Q.; Leong, K. W.; Yu, H. *Biomaterials* **2001**, 22, 1157.
- (12) Pascual, B.; Vázquez, B.; Gurrachaga, M.; Goñi, I.; Ginebra, M. P.; Gil, F. J.; Planell, J. A.; Levenfeld, B.; Román, J. S.. *Biomaterials* **1996**, 17, 509.
- (13) Carnahan, M. A.; Middleton, C.; Kim, J.; Kim, T.; Grinstaff, M. W. *J. Am. Chem. Soc.* **2002**, 124, 5291.
- (14) Du, J.Z.; Chen, D.P.; Wang, Y.C.; Xiao, C.S.; Lu, Y.J.; Wang, J.; Zhang, G.Z. *Biomacromolecules* **2006**, 7, 1898.

-
- (15) Libiszowski, J.; Kałużynski, K.; Penczek, S. *J. Polym. Sci., Polym. Chem. Ed.* **1978**, *16*, 1275.
- (16) Kałużynski, K.; Libiszowski, J.; Penczek, S. *Makromol. Chem.* **1977**, *178*, 2943.
- (17) Lapienis, G.; Penczek, S. *Macromolecules* **1974**, *7*, 166.
- (18) Vogt, W.; Balasubramanian, S. *Makromol. Chem.* **1973**, *163*, 111.
- (19) Pretula, J.; Kaluzynski, K.; Wisniewski, B.; Szymanski, R.; Loontjens, T.; Penczek, S. *J. Polym. Sci., Part A: Polym. Chem.* **2008**, *46*, 830.
- (20) Penczek, S.; Pretula, J. *Macromolecules* **1993**, *26*, 2228.
- (21) Pretula, J.; Kaluzynski, K.; Szymanski, R.; Penczek, S. *Macromolecules* **1997**, *30*, 8172.
- (22) Wen, J.; Zhuo, R.X. *Macromol. Rapid Commun.* **1998**, *19*, 641.
- (23) Oussadi, K.; Montembault, V.; Belbachir, M.; Fontaine, L. *J. Appl. Polym. Sci.* **2011**, *122*, 891.
- (24) Xiao, C.S.; Wang, Y.C.; Du, J.Z.; Chen, X.S.; Wang, J. *Macromolecules* **2006**, *39*, 6825.
- (25) (a) Wang, Y.C.; Tang, L.Y.; Sun, T.M.; Li, C.H.; Xiong, M.H.; Wang, J. *Biomacromolecules* **2007**, *9*, 388. (b) Zhang, S.; Wang, H.; Shen, Y.; Zhang, F.; Seetho, K.; Zou, J.; Dove, A.P.; Wooley, K.L. *Macromolecules* **2013**, *46*, 5141.
- (26) (a) Banks, R.L.; Bailey, G.C. *Ind. Eng. Chem. Prod. Res. Dev.* **1964**, *3*, 170 (b) Mol, J.C.; *Journal of Molecular Catalysis A: Chemical* **2004**, *213*, 39.
- (27) (a) Trnka, T. M.; Grubbs, R. H. *Accounts Chem. Res.* **2001**, *34*, 18. (b) Grubbs, R. H., Olefin metathesis. *Tetrahedron* **2004**, *60*, 7117.
- (28) Connon, S. J.; Blechert, S. *Angew. Chem. Int. Ed.* **2003**, *42*, 1900.
- (29) Grubbs, R. H. *Handbook of Metathesis*; Wiley-VCH: Weinheim, Germany, **2003**.
- (30) Schrock, R. R.; Hoveyda, A. H. *Angew. Chem. Int. Ed.* **2003**, *42*, 4592.
- (31) Guidry, E. N.; Li, J.; Stoddart, J. F.; Grubbs, R. H. *J. Am. Chem. Soc.* **2007**, *129*, 8944.

-
- (32) Matson, J. B.; Grubbs, R. H. *J. Am. Chem. Soc.* **2008**, *130*, 6731
- (33) Ivin, K. J.; Mol, J. C. *Olefin Metathesis and Metathesis Polymerization*; Academic Press: San Diego, CA, **1997**.
- (34) Hilf, S.; Kilbinger, A. F. M. *Nat Chem* **2009**, *1*, 537.
- (35) (a) Zuech, E.A. ; Hughes, W.B. ; Kubicek, Kittleman, E.T. *J. Am. Chem. Soc.* **1970**, *92*, 528. (b) R. R. Schrock, J. S. Murdzek, G. C. Bazan, J. Robbins, M. DiMare and M. O'Regan, *J. Am. Chem. Soc.* **1990**, *112*, 3875. (c) Wagener, K. B.; Boncella, J. M.; Nel, J. G. *Macromolecules* **1991**, *24*, 2649.
- (36) Opper, K. L.; Wagener, K. B. *J. Polym. Sci., Part A: Polym. Chem.* **2011**, *49*, 821.
- (37) Boz, E.; Wagener, K. B.; Ghosal, A.; Fu, R.; Alamo, R. G. *Macromolecules* **2006**, *39*, 4437.
- (38) Hopkins, T. E.; Wagener, K. B. *Macromolecules* **2004**, *37*, 1180.
- (39) Matloka, P. P.; Wagener, K. B. *J. Mol. Catal. A: Chem.* **2006**, *257*, 89.
- (40) Fokou, P. A. ; Meier, M.A.R. *Macromol. Rapid Commun.* **2008**, *29*, 1620.
- (41) Biermann, U.; Metzger, J.O.; Meier, M.A.R. *Macromol. Chem. Phys.* **2010**, *211*, 854.
- (42) Opper, K. L.; Markova, D.; Klapper, M.; Müllen, K.; Wagener, K. B. *Macromolecules* **2010**, *43*, 3690.
- (43) Feast, W.J.; Cacialli, F.; Daik, R.H.; Herzog, E.; Heywood, B.R.; Hobson, L.; Megson, J.L.; Snowden, D. *Macromol. Symp.* **1999**, *143*, 81.
- (44) Feast, W.J.; Herzog, E.; Heywood, B.R.; Megson, J. L.; Williams, S.J. *NATO Sci. Ser. II Math.* **2002**, *56*, 69.
- (45) Marsico, F.; Wagner, M.; Landfester, K.; Wurm, F. *Macromolecules*, **2012**, *45*, 8511.
- (46) Tindall, D.; Pawlow, J. H.; Wagener, K. B. *Recent Advances in ADMET Chemistry. Topics in Organometallic Chemistry*, Fürstner, A. Ed. Springer: **1998**, *1*, 183.

-
- (47) (a) Wagener, K. B.; Brzezinska, K.; Anderson, J. D.; Younkin, T. R.; Steppe, K.; DeBoer, W. *Macromolecules* **1997**, *30*, 7363. (b) Nagarkar, A.A. ; Crochet, A. ; Fromm, K.M. ; Kilbinger, A.F.M. *Macromolecules* **2012**, *45*, 4447.
- (48) Nagarkar, A.A. ; Crochet, A. ; Fromm, K.M. ; Kilbinger, A.F.M. *Macromolecules* **2012**, *45*, 4447.
- (49) Fokou, P. A.; Meier, M. A. R. *Macromol. Rapid Commun.* **2008**, *29*, 1620.
- (50) Petkovska, V. I.; Hopkins, T. E.; Powell, D. H.; Wagener, K. B. *Macromolecules* **2005**, *38*, 5878.
- (51) Sworen, J. C.; Smith, J. A.; Wagener, K. B.; Baugh, L. S.; Rucker, S. P. *J. Am. Chem. Soc.* **2003**, *125*, 2228.
- (52) Wagener, K. B.; Nel, J. G.; Konzelman, J.; Boncella, J. M. *Macromolecules* **1990**, *23*, 5155.
- (53) Hilf, S.; Kilbinger, A. F. M. *Nat Chem* **2009**, *1*, 537.
- (54) Del Río, E.; Lligadas, G.; Ronda, J.C.; Galià, M.; Cadiz, V.; Meier, M.A.R. *Macromol. Chem. Phys.* **2011**, *212*, 1392.
- (55) Zhang, S.; Li, A.; Zou, J.; Lin, L. Y.; Wooley, K. L. *ACS Macro Lett.* **2012**, *1*, 328.
- (56) (a) Loudet, A.; Burgess, K. *Chem. Rev.* **2007**, *107*, 4891. (b) Kim, K.; Lee, M.; Park, H.; Kim, J.-H.; Kim, S.; Chung, H.; Choi, K.; Kim, I.-S.; Seong, B. L.; Kwon, I. C. *J. Am. Chem. Soc.* **2006**, *128*, 3490. (c) Banerjee, S.; König, B. *J. Am. Chem. Soc.* **2013**, *135* (8), 2967. (d) Callahan, J.; Kopeček, J. *Biomacromolecules* **2006**, *7*, 2347. (e) Beija, M.; Charreyre, M.-T.; Martinho, J. M. G. *Prog. Polym. Sci.* **2011**, *36*, 568.
- (57) (a) Isik, M.; Ozdemir, T.; Turan, I. S.; Kolemen, S.; Akkaya, E. U. *Org. Lett.* **2012**, *15*, 216; (b) Poirel, A.; De Nicola, A.; Ziessel, R. *Org. Lett.* **2012**, *14*, 5696. (c) Sunahara, H.; Urano, Y.; Kojima, H.; Nagano, T. *J. Am. Chem. Soc.* **2007**, *129*, 5597. (d) Baruah, M.; Qin, W. W.; Vallee, R.; Beljonne, D.; Rohand, T.; Dehaen, W.; Boens, N. *Org. Lett.* **2005**, *7*, 4377. (e) Yin, S. C.; Leen, V.; Van Snick, S.; Boens, N.; Dehaen, W. *Chem. Commun.* **2010**, *46*, 6329.
- (58) (a) Boens, N.; Leen, V.; Dehaen, W. *Chem. Soc. Rev.* **2012**, *41*, 1130. (b) Ulrich, G.; Ziessel, R.; Harriman, A. *Angew. Chem. Int. Ed.* **2008**, *47*, 1184.

-
- (59) Prusty, D. K.; Kwak, M.; Wildeman, J.; Herrmann, A. *Angew. Chem. Int. Ed.* **2012**, *51*, 11894.
- (60) (a) Zettl, H.; Häfner, W.; Böker, A.; Schmalz, H.; Lanzendörfer, M.; Müller, A. H. E.; Krausch, G. *Macromolecules* **2004**, *37*, 1917. (b) Zhou, P.; Chen, G.Q.; Hong, H.; Du, F.S.; Li, Z.C.; Li, F.M. *Macromolecules* **2000**, *33*, 1948. (c) York, A. W.; Scales, C. W.; Huang, F.; McCormick, C. L. *Biomacromolecules* **2007**, *8*, 2337. (d) Zhao, W.; Wang, Y.; Liu, X.; Cui, D. *Chem. Commun.* **2012**, 48, 4483.
- (61) (a) Benniston, A. C.; Copley, G.; Harriman, A.; Ryan, R. *J. Mater. Chem.* **2011**, *21*, 2601. (b) Nagai, A.; Miyake, J.; Kokado, K.; Nagata, Y.; Chujo, Y. *J. Am. Chem. Soc.* **2008**, *130*, 15276.
- (62) Iehl, J.; Nierengarten, J.-F.; Harriman, A.; Bura, T.; Ziessel, R. *J. Am. Chem. Soc.* **2011**, *134*, 988.
- (63) (a) Liras, M.; García-García, J. M.; Quijada-Garrido, I.; Gallardo, A.; París, R. *Macromolecules* **2011**, *44*, 3739. (b) Telitel, S.; Lalevée, J.; Blanchard, N.; Kavalli, T.; Tehfe, M.-A.; Schweizer, S.; Morlet-Savary, F.; Graff, B.; Fouassier, J.-P. *Macromolecules* **2012**, *45*, 6864.
- (64) (a) Mangold, S. L.; Carpenter, R. T.; Kiessling, L. L. *Org. Lett.* **2008**, *10*, 2997 (b) Roberts, K. S.; Sampson, N. S. *Org. Lett.* **2004**, *6*, 3253.
- (65) A. D. McNaught and A. Wilkinson, V. Gold, *The Compendium of Chemical Terminology, IUPAC*, **2012**.
- (66) G. Moad, D. H. Solomon, *The Chemistry of Radical Polymerisation*, 2nd Ed., *Elsevier*, **2006**, 9, 374,
- (67) C. A. Uraneck, H. L. Hsieh and O. G. Buck, *J. Polym. Sci., Part A: Polym. Chem.* **1960**, *46*, 535.
- (68) M. A. Tasdelen, M. U. Kahveci and Y. Yagci, *Prog. Polym. Sci.* **2011**, *36*, 455.
- (69) (a) Y. Yagci, O. Nuyken, V.-M. Graubner, in *Encyclopedia of Polymer Science and Technology*, ed. J. I. Kroschwitz, *John Wiley & Sons, Inc.*, New York, 3rd edn, **2005**, *12*, 57–130. (b) H. Mutlu, L. M. de Espinosaac, M. A. R. Meier, *Chem. Soc. Rev.* **2011**, *40*, 1404.
- (70) (a) Wurm, F.; Frey, H.; In: Matyjaszewski, K. and Möller, M. (eds.) *Polymer Science: A Comprehensive Reference*, **2012**, *6*, 177, Amsterdam: Elsevier BV. (b) Carlmark, A.; Hawker, C.; Hult, A.; Malkoch, M. *Chem. Soc. Rev.* **2009**, *38*, 352.

-
- (71)(a) Johansson, M.; Hult, A. *J. Coat. Technol.* **1995**, *67*, 35. (b) Lange, J.; Stenroos, E.; Johansson, M.; Malmström, E. *Polymer* **2001**, *42*, 7403.
- (72)(a) Gao, C.; Yan, D. *Prog. Polym. Sci.* **2004**, *29*, 183. (b) Flory, P. J. *J. Am. Chem. Soc.* **1952**, *74*, 2718.
- (73) Hawker, C. J.; Lee, R.; Fréchet, J. M. J. *J. Am. Chem. Soc.* **1991**, *113*, 4583.
- (74)(a) Emrick, T.; Chang, H.-T.; Fréchet, J. M. J. *Macromolecules* **1999**, *32*, 6380. (b) Yan, D. Y.; Gao, C. *Macromolecules* **2000**, *33*, 7693.
- (75) Kim, Y. H.; Webster, O. W. *Macromolecules* **1992**, *25*, 5561.
- (76) (a) Gorodetskaya, I. A.; Gorodetsky, A. A.; Vinogradova, E. V.; Grubbs, R. H. *Macromolecules* **2009**, *42*, 2895. (b) Gorodetskaya, I. A.; Choi, T.-L.; Grubbs, R. H. *J. Am. Chem. Soc.* **2007**, *129*, 12672.
- (77) Fokou, P. A.; Meier, M. A. R. *Macromol. Rapid Commun.* **2008**, *29*, 1620.
- (78)(a) del Río, E.; Lligadas, G.; Ronda, J. C.; Galià, M.; Cádiz, V.; Meier, M. A. R. *Macromol. Chem. Phys.* **2011**, *212*, 1392. (b) Biermann, U.; Metzger, J. O.; Meier, M. A. R. *Macromol. Chem. Phys.* **2010**, *211*, 854.
- (79) F. Auzel. *Chem. Rev.* **2004**, *104*, 139.
- (80) B. M. van der Ende, L. Aarts and A. Meijerink. *Phys. Chem. Phys.* **2009**, *11*, 11081.
- (81) (a) M. Haase and H. Schafer. *Angew. Chem., Int. Ed.* **2011**, *50*, 5808. (b) J. Z. Zhao, S. M. Ji and H. M. Guo, *RSC Adv*, **2011**, *1*, 937.
- (82) T. N. Singh-Rachford and F. N. Castellano, *Coord. Chem. Rev.* **2010**, *254*, 2560.
- (83) C. A. Parker and C. G. Hatchard. *Proc. Chem. Soc.*, London, 1962, 386.
- (84) (a) R. R. Islangulov, J. Lott, C. Weder and F. N. Castellano. *J. Am. Chem. Soc.* **2007**, *129*, 12652. (b) T. N. Singh-Rachford, J. Lott, C. Weder and F. N. Castellano. *J. Am. Chem. Soc.* **2009**, *131*, 12007.
- (85) (a) Schweitzer, C.; Schmidt, R. *Chem. Rev.* **2003**, *103*, 1685. (b) Allison, R.R.; Mota, H.C.; Bagnato, V.S. Sibata, C.H. *Photodiagn Photodyn.* **2008**, *5*, 19.

-
- (86) Islangulov, R. R., Lott, J. Weder, C., Castellano, F. N. *J. Am. Chem. Soc.* **2007**, *129*, 12652.
- (87) (a) Chen, H.-C.; Hung, C.-Y.; Wang, K.-H.; Chen, H.-L.; Fann, W. S.; Chien, F.-C.; Chen, P.; Chow, T. J.; Hsu, C.-P.; Sun, S.-S. *Chem. Commun.* **2009**, *27*, 4064. (b) Singh-Rachford, T. N.; Castellano, F. N. *J. Phys. Chem. Lett.* **2010**, *1*, 195. (c) Ji, S.; Wu, W.; Wu, W.; Guo, H.; Zhao, J. *Angew. Chem., Int. Ed.* **2011**, *50*, 1626. (d) Kim, J.-H.; Deng, F., Castellano, F. N.; Kim, J.-H. *Chem. Mater.* **2012**, *24*, 2250.
- (88) (a) W. Zou, C. Visser, J. A. Maduro, M. S. Pshenichnikov, and J. C. Hummelen, *Nature Photonics* **2012**, *6*, 560; (b) K. Börjesson, D. Dzebo, B. Albinsson, K. Moth-Poulsen, *J. Mater. Chem. A*, **2013**, *1*, 8521.
- (89) (a) R. R. Islangulov, J. Lott, C. Weder and F. N. Castellano, *J. Am. Chem. Soc.* **2007**, *129*, 12652. (b) T. N. Singh-Rachford, J. Lott, C. Weder and F. N. Castellano. *J. Am. Chem. Soc.* **2009**, *131*, 12007.
- (90) P. B. Merkel and J. P. Dinnocenzo. *J. Lumin.* **2009**, *129*, 303.
- (91) B. R. Crenshaw, C. Weder. *Adv. Mater.* **2005**, *17*, 1471.
- (92) (a) S. Balushev, V. Yakutkin, G. Wegner, B. Minch, T. Miteva, G. Nelles and A. Yasuda, *J. Appl. Phys.*, **2007**, *102*, 076103. (b) S. Balushev, V. Yakutkin, G. Wegner, B. Minch, T. Miteva, G. Nelles and A. Yasuda, *J. Appl. Phys.*, **2007**, *101*, 023101.
- (93) (a) G. Bergamini, P. Ceroni, M. Maestri, V. Balzani, S. K. Lee and F. Vogtle. *Photochem. Photobiol. Sci.* **2004**, *3*, 898. (b) G. Wegner, S. Balushev, F. Laquai and C. Y. Chi, *Macromol. Symp.* **2008**, *268*, 1.
- (94) (a) F. Laquai, Y. S. Park, J. J. Kim and T. Basche, *Macromol. Rapid Commun.* **2009**, *30*, 1203. (b) G. D. Scholes and G. Rumbles, *Nat. Mater.*, **2006**, *5*, 683.
- (95) J. D. Wuest. *Nat. Chem.* **2012**, *4*, 74.
- (96) (a) A. Hiltner, R. Y. F. Liu, Y. S. Hu and E. Baer, *J. Polym. Sci., Part B: Polym. Phys.* **2005**, *43*, 1047. (b) J. Lin, Shenogin, S.; Nazarenko, S. *Polymer* **2002**, *43*, 4733.
- (97) V. M. Litvinov, O. Persyn, V. Miri and J. M. Lefebvre *Macromolecules* **2010**, *43*, 7668.
- (98) N. C. Karayiannis, V. G. Mavrantzas and D. N. Theodorou *Macromolecules*, **2004**, *37*, 2978.
- (99) Shockley, W.; Queisser, H. J. *J. Appl. Phys.* **1961**, *32*, 510.

-
- (100) Trupke T.; Green M. A.; Würfel P. *J. Appl. Phys.* **2002**, *92*, 4117.
- (101) Pratt Jason, D.; Olson Brian, G.; Brandt Justin, P.; Hassan Mohammad, K.; Ratto Jo, A.; Wiggins Jeffrey, S.; Rawlins James, W.; Nazarenko, S. *In Polymer Degradation and Performance, ACS: 2009,1004*, pp. 17-30.
- (102) Di Mascio, P.; Kaiser, S.; Sies, H. *Archives of Biochemistry and Biophysics* **1989**, *274*, 532.
- (103) Cooksey, K., Oxygen Scavenging Packaging Systems. In *Encyclopedia of Polymer Science and Technology*, John Wiley & Sons, Inc.: **2002**.
- (104)(a) *Plastics Europe*, **2012**. (b) E. D. Weil, S. Levchik, *J. Fire Sci.* **2004**, *22*, 25-40. (c) S. V. Levchik, E. D. Weil, *J. Fire Sci.* **2006**, *24*, 137-151. (d) L. Chen, Y.-Z. Wang, *Polym. Adv. Technol.* **2010**, *21*, 1-26.
- (105) (a) G. Camino, L. Costa, M. P. Luda di Cortemiglia, *Polym. Degrad. Stab.* **1991**, *33*, 131. (b) S.-Y. Lu, I. Hamerton, *Prog. Polym. Sci.* **2002**, *27*, 1661.
- (106) Joseph DiGangi, Arlene Blum, Ake Bergman, Cynthia A. de Wit, Donald Lucas, David Mortimer, Arnold Schecter, Martin Scheringer, Susan D. Shaw, T. F. Webster, *Environ. Health Perspect.* **2010**, *118*, A516-A518.
- (107)(a) J. Green, *J. Fire Sci.* **1992**, *10*, 470-487. (b) S. Bourbigot, S. Duquesne, *J. Mater. Chem.* **2007**, *17*, 2283.
- (108) (a) C. Chivas, E. Guillaume, A. Sainrat, V. Barbosa, *Fire Safety Journal* **2009**, *44*, 801. (b) S. Kemmlin, O. Hahn, O. Jann, *Atmos. Environ.* **2003**, *37*, 5485.
- (109) H. M. Stapleton, S. Klosterhaus, A. Keller, P. L. Ferguson, S. van Bergen, E. Cooper, T. F. Webster, A. Blum, *Environ. Sci. Technol.* **2011**, *45*, 5323.
- (110) (a) A. P. Mouritz, A. G. Gibson, *Fire Properties of Polymer Composite Materials, Vol.143*, Springer, Dordrecht, Netherlands, **2006**. (b) C. A. Wilkie, M. A. McKinney, *Thermal Properties and Burning Behavior of the Most Important Plastics*, 3rd ed., Hanser Verlag, München, **2004**.
- (111) B. Schartel, *Materials* **2010**, *3*, 4710.

-
- (112) C. I. Lindsay, S. B. Hill, M. Hearn, G. Manton, N. Everall, A. Bunn, J. Heron, I. Fletcher, *Polym. Int.* **2000**, *49*, 1183.
- (113) U. Braun, A. I. Balabanovich, B. Schartel, U. Knoll, J. Artner, M. Ciesielski, M. Döring, R. Perez, J. K. W. Sandler, V. Altstädt, T. Hoffmann, D. Pospiech, *Polymer* **2006**, *47*, 8495.
- (114) D. Zhuo, A. Gu, G. Liang, J.-t. Hu, L. Yuan, X. Chen, *J. Mater. Chem.* **2011**, *21*, 6584.
- (115) J. Li, C. Ke, L. Xu, Y. Wang, *Polym. Degrad. Stab.* **2012**, *97*, 1107.
- (116) (a) X. Chen, C. Jiao, S. Li, J. Sun, *J. Polym. Res.* **2011**, *18*, 2229. (b) L. Zang, S. Wagner, M. Ciesielski, P. Müller, M. Döring, *Polym. Adv. Technol.* **2011**, *22*, 1182. (c) D. Zhang, H. Wu, T. Li, A. Zhang, Y. Peng, F. Jing, *Polym. Compos.* **2011**, *32*, 36. (d) Q. Wang, W. Shi, *Polym. Degrad. Stab.* **2006**, *91*, 1289. (e) H. Wang, Q. Wang, Z. Huang, W. Shi, *Polym. Degrad. Stab.* **2007**, *92*, 1788. (f) Z. Huang, W. Shi, *Polym. Degrad. Stab.* **2007**, *92*, 1193. (g) X. Chen, J. Zhuo, C. Jiao, *Polym. Degrad. Stab.* **2012**, *97*, 2143.
- (117) V. L. Keedy, *Oncotargets and Therapy*, **2012**, *5*, 153.
- (118) (a) J. T. Buijs and G. van der Pluijm, *Cancer Lett*, **2009**, *273*, 177-193. (b) G. A. Clines and T. A. Guise, *Expert Rev Mol Med*, **2008**, *10*, 1.
- (119) D. R. Clohisy and P. W. Mantyh, *Cancer*, **2003**, *97*, 866.
- (120) Posner, T. *Ber. Dtsch. Chem. Ges.* **1905**, *38*, 646.
- (121) Marvel, C. S.; Chambers, R. R. *J. Am. Chem. Soc.* **1948**, *70*, 993.
- (122) (a) Killops, K. L.; Campos, L. M.; Hawker, C. J. *J. Am. Chem. Soc.* **2008**, *130*, 5062. (b) Kade, M. J.; Burke, D. J.; Hawker, C. J. *J. Polym. Sci. Part A: Polym. Chem.* **2010**, *48*, 743.
- (123) Firdaus, M.; Montero de Espinosa, L.; Meier, M. A. R. *Macromolecules* **2011**, *44*, 7253.
- (124) Lorenz, K.; Frey, H.; Sthn, B.; Mlhaupt, R. *Macromolecules* **1997**, *30*, 6860.
- (125) H. C. Kolb, M. G. Finn and K. B. Sharpless, *Angew. Chem., Int. Ed.* **2001**, *40*, 2004.

-
- (126) (a) M. Li, P. De, S. R. Gondi and B. S. Sumerlin, *J. Polym. Sci., Part A: Polym. Chem.* **2008**, *46*, 5093. (b) C. R. Becer, R. Hoogenboom and U. S. Schubert, *Angew. Chem. Int. Ed.* **2009**, *48*, 4900.
- (127) (a) B. D. Fairbanks, T. F. Scott, C. J. Kloxin, K. S. Anseth and C. N. Bowman, *Macromolecules*, **2009**, *42*, 211. (b) J. W. Chan, H. Zhou, C. E. Hoyle and A. B. Lowe, *Chem. Mater.* **2009**, *21*, 1579.
- (128) H. Li, B. Yu, H. Matsushima, C. E. Hoyle and A. B. Lowe, *Macromolecules*, **2009**, *42*, 6537.
- (129) C. R. Becer, K. Babiuch, D. Pilz, S. Hornig, T. Heinze, M. Gottschaldt and U. S. Schubert, *Macromolecules*, **2009**, *42*, 2387.
- (130) B. M. Rosen, G. Lligadas, C. Hahn and V. Percec, *J. Polym. Sci., Part A: Polym. Chem.* **2009**, *47*, 3940.
- (131) J. Shin, H. Matsushima, J. W. Chan and C. E. Hoyle, *Macromolecules*, **2009**, *42*, 3294.
- (132) (a) J. A. Carioscia, J. W. Stansbury and C. N. Bowman, *Polymer*, **2007**, *48*, 1526. (b) N. B. Cramer, S. K. Reddy, A. K. O'Brien and C. N. Bowman, *Macromolecules*, **2003**, *36*, 7964. (c) V. S. Khire, D. S. W. Benoit, K. S. Anseth and C. N. Bowman, *J. Polym. Sci., Part A: Polym. Chem.* **2006**, *44*, 7027.
- (133) C. E. Hoyle, T. Y. Lee and T. Roper, *J. Polym. Sci., Part A: Polym. Chem.* **2004**, *42*, 5301.
- (134) J. W. Chan, B. Yu, C. E. Hoyle and A. B. Lowe, *Chem. Commun.* **2008**, 4959.
- (135) H. Kakwere and S. Perrier, *J. Am. Chem. Soc.* **2009**, *131*, 1889.
- (136) Voronkov, M.G. ; Deryagina, E. N. *Russ. Chem. Rev.* **1990**, *59*, 778.

